Site Specific Calibration of Laser Induced Breakdown Spectroscopy for Rapid Elemental Analysis of Gold Ore Drill Core Samples

Joseph R. W. Millington

School of Engineering
Master's Thesis
Otaniemi 26.10.2020

Supervisor
Prof. Jussi Leveinen

Advisors
Lasse Kangas
Ilkka Laine

TU Delft RWTH Aachen

Aalto University
School of Engineering

Aalto University, P.O. BOX 11000, 00076 Aalto
www.aalto.fi
Abstract of the Master's thesis

Author	**Joseph Millington**
Title:	**Site specific calibration of laser induced breakdown spectroscopy for rapid elemental analysis of gold ore drill core samples**
Degree Programme:	**European Mining Course (EMC)**
Major:	**Mining Engineering** **Code of Major: ENG3077**
Main Supervisor:	**Prof. Jussi Leveinen**
Advisors:	**Lasse Kangas and Ilkka Laine**
Date:	**26.10.2020** **Number of Pages: 86+8** **Language: English**

Abstract

Site-specific calibration of laser induced breakdown spectroscopy (LIBS) analysis can be achieved by presenting known geological sample data to update algorithms, therefore improving analysis of unknown samples post-calibration. The goal of this project is to optimise drill core analysis by LIBS for samples from Kittilä gold mine. In total 227 samples have been produced and analysed with a range of analytical techniques to build a comprehensive, site-specific reference library. The data from these analyses has been input into the reference library and utilised by algorithms for spectral peak identification during LIBS analysis of bulk drill core material.

The semi-quantitative and quantitative data of 40 Kittilä samples has been used as a comparison to ICP-AES data used by the mine. The Kittilä powders were used to produce 39 pellets, each representative of a section of drill core of which the ICP-AES and TXRF data was known. The pellets were scanned by LIBS and the data then compared to the known data. LIBS showed strong correlations (>0.75) with ICP-AES data for As, Cr, Cu, Fe, Mn and S, poor correlations were seen for Pb and Co, however these can be explained by issues related to ICP-AES. LIBS pellet data proved strongly competitive as 5/9 elements displayed stronger correlations between LIBS and ICP-AES than TXRF. Subsequently, the successful scanning of drill core boxes directly has proven that calibration can increase the speed with which the bulk material can be effectively analysed.

Keywords Laser Induced Breakdown Spectroscopy; LIBS; drill core; rapid elemental analysis; calibration; gold ore; mineral identification; sample preparation; XRD; TXRF.

Preface

This study has been completed as part of the wider LASO-LIBS project being undertaken in the School of Engineering at Aalto University. I would like to graciously thank my supervisor, Professor Jussi Leveinen, for providing me with the opportunity of being part of this innovative and exciting project. A special thank you goes to Lasse Kangas and to Ilkka Laine who have been pioneering the LASO-LIBS technology for some time and have always been available to assist me. Without Jussi, Lasse and Ilkka the LASO-LIBS project would not have got off the ground and for this they should be recognised. Furthermore, the support provided by the School of Engineering and the wider Aalto community has allowed me to thrive throughout my thesis, providing all the guidance and resources I required. I would also like to offer special thanks to the School of Chemical Engineering for the use of their labs and equipment.

I would like to extend my gratitude to my external advisors, Professor Mike Buxton of TU Delft and Professor Bernd Lottermoser of RWTH Aachen for their support and expertise whenever I have required it. The input of all EMC partner universities has been vital in my development and continues to support me during the transition period between studies and careers.

The LASO-LIBS project and this thesis relies on the use of real-life samples for testing. This thesis would not have been completed without samples provided by Agnico Eagle from the Kittilä gold mine. Core boxes amounting to 70 metres of half-cores, powdered samples of the corresponding half-cores and block ore samples have all been used during this thesis. As well as the physical samples, Kittilä mine provided their own confidential analysis results, allowing for comparisons to be made between LASO-LIBS data and results from conventional methods used by the mine. Without samples and analysis data this project would have taken far longer to gain the same volume of practical data.

This thesis was completed with the resources of Aalto University, the data of Kittilä mine and the combined knowledge of Jussi, Lasse and Ilkka along with others. However a special thank you has to go to my friends and family who have supported me throughout my time in Finland, through their friendship and love I have been able to overcome many issues of the period of completing this thesis and I hope they are proud of what I am achieving.

A final note aims to add weight to the gratitude that I feel for those I have already mentioned. This thesis had barely begun before quarantine, closures and lockdowns came into being; measures taken to combat the COVID-19 pandemic of 2020. With the global pandemic as a backdrop, the completion of this thesis represents the ability of students, professors, companies, friends and families to all come together to support one another during this unprecedented time. The closures and lockdowns have at times hindered the production of this thesis at times, however the resilience of those involved is testimony to the success of this ground-breaking project. It has been a privilege to be a part of its development.

Joseph Millington, 2020

Abbreviations

Analysis techniques and technologies		**As**	Arsenic	**Ga**	Billion years
AAS	Atomic Absorption Spectroscopy	**Au**	Gold	**Hz**	Hertz
AES	Atomic Emission Spectroscopy	**Bi**	Bismuth	**keV**	Kiloelectronvolt
APXS	Alpha Proton X-ray Spectroscopy	**Ca**	Calcium	**kg**	Kilogram
CMOS	Complementary metal oxide semiconductor	**Co**	Cobalt	**kHz**	Kilohertz
HSI	Hyperspectral Imaging	**Cr**	Chromium	**km**	Kilometre
ICP-AES/ ICP-OES	Inductively Coupled Plasma Atomic/ Optical Emission Spectroscopy	**Cu**	Copper	**km^2**	Square Kilometre
LASO-LIBS	Large Area Scanning Open-Source Laser Induced Breakdown Spectroscopy	**Fe**	Iron	**KSZ**	Kittilä Shear Zone
LIBS	Laser Induced Breakdown Spectroscopy	**HCL**	Hydrochloric Acid	**LLD**	Lower Limit of Detection
LIBS-LIF	Laser induced fluorescence LIBS	**HNO^3**	Nitric Acid	**m**	Metre
LIPS	Laser Induced Plasma Spectroscopy	**K**	Potassium	**m/s**	Metres per second
MA-LIBS	Microwave assisted	**Mn**	Manganese	**mg/kg**	Milligrams per kilogram
MASER	Microwave amplification by stimulated emission of radiation	**Na**	Sodium	**min^{-1}**	Revolutions per min
Mid-IR	Mid-Infrared	**Ni**	Nickel	**ml**	Millilitre
MLA	Mineral Liberation Analysis	**Os**	Osmium	**mm**	Millimetre
Nd:YAG	Neodymium-doped yttrium aluminium garnet	**Pb**	Lead	**Moz**	Million ounces
NIR	Near-Infrared	**PGMs**	Platinum group metals	**Mt**	Million tonnes
NIRS	Near-Infrared Spectroscopy	**S**	Sulphur	**nm**	Nanometre
QCL	Quantum Cascade Laser	**Sb**	Antimony	**oz**	Ounce
RE-LIBS	Resonance enhanced	**Se**	Selenium	**ppm**	Parts per million
SEM	Scanning Electron Microscopy	**Si**	Silicon	**s**	Seconds
TDP	Thin Disk Preparation	**Ta**	Tantalum	**s.d.**	Standard Deviation
TXRF	Total reflection X-ray Fluorescence	**Ti**	Titanium	**t**	Tonne
XRD	X-Ray Diffraction	**Th**	Thorium	**t/m^3**	Tonne per cubic metre
Institutions		**W**	Tungsten	**TDS**	Total dissolved solids
ARL	Army Research Laboratory	**Zn**	Zinc	**µg**	Microgram
CRCORE	Cooperative Research Council for optimising Resource Extraction	**General**		**µj**	Microjoule
LANL	Los Alamos National Laboratory	**€**	Euro	**µm**	Micrometre
NRC	National Research Council	**$**	US Dollar	**$µm^2$**	Square Micrometre
PWC	PricewaterhouseCoopers	**%**	Percentage	Percent	Ultra-Violet light
Elements and Chemicals		**CLGB**	Central Lapland Greenstone Belt	**W**	Watt
Ag	Silver	**cm**	Centimetre	**Wt%**	Weight percent
Al	Aluminium	**g**	Gram		
Ar	Argon	**g/t**	Grams per tonne		

Table of Contents

1 Introduction

The mining sector is changing. Times of high-volume, high-grade deposits are all but over and the industry faces a future of forever lowering ore grades in increasingly rural locations and at increasing stratigraphic depths. Governmental and organisational regulations, alongside rising social awareness have forced the mining industry to rethink (Harhira, et al., 2017). Time, money, commodity, market, environmental and social considerations cannot be overlooked; forcing the industry to innovate. Driving down costs, decreasing environmental impacts and increasing social acceptance are vital considerations for any modern-day mine; all while maintaining a strong profit to keep investors onside.

The mining industry is reliant on accurate and reliable information. Data controls the ability for a mine to make business-critical decisions effectively, decisions which can have a large impact on the company and all associates. Mineralogical data is of critical importance to all mining companies. Without understanding the orebody or the mineralogy in which a mine operates, operations and processing cannot be optimised. In 2012, the combined mining industry amassed costs of $220 billion (PricewaterhouseCoopers, 2018), paying $34.9 billion in exploration expenditure (Schodde, 2019), nearly 16%. 2012 represented a recent peak in exploration expenditure, PWC suggest that 2% of mining industry costs are in exploration, however that estimate is higher if the salaries, contractor and outside service costs are included (PricewaterhouseCoopers, 2018).

Currently there is a wide range of analytical techniques used globally, varying in cost, popularity and applicability to specific situations. However, there is no widely used cost-effective and rapid remote sensing device for instrumental mineral analysis which combines the benefits, while removing, or improving upon the drawbacks. The industry needs a device which can be mobile and easily operated, with little or no sample preparation. Furthermore, a device is required to operate in a field environment while providing reliable and accurate results consistently. Research is on-going in pursuit of a number of analytical techniques which are being considered as potential improvements, however, as of yet, the perfect analytical technique has not been found.

This thesis focusses on the potential of Laser Induced Breakdown Spectroscopy (LIBS), a widely used and well known elemental analysis technique. So far, LIBS has not made the transition to become a commonplace analytical technique within the mining industry like, for example XRF (X-ray Fluorescence). Despite the huge potential, the viability of LIBS in mining is still under investigation. This thesis goes some way to improving the understanding of the potential for LIBS in the analysis of drill core samples. Previous research has demonstrated the viability of the technique in theory, however a number of issues have also been raised and provided as an explanation for why LIBS has not yet become a feature of common mineralogical or elemental analysis in the mining industry.

1.1 Structure of this thesis

The following chapters begin with the aims of the LASO-LIBS project and this thesis, followed by evidence to support the need for rapid quantitative analysis within the mining industry. The thesis continues with comprehensive and wide-reaching literature study describing and explaining briefly the history of LIBS, how LIBS operates practically and the theory behind the technique. Within the background theory section of this thesis, advantages and disadvantages are discussed along with the current applications of LIBS across a wide variety of industries. Section 1.3, within the theory section focusses specifically on the content of this thesis and what research has been completed thus far; i.e. the use of LIBS for analysing drill cores and the use of LIBS in the analysis of gold ores. Accessible published literature is used to formulate a list of sample preparation methods which were considered to be used during the experimental phase of the thesis; the potential sample preparations are discussed in section 2.5. To conclude the theory section of the thesis, the current analytical practices within the mining industry are discussed in section 2.6, outlining the industrial comparisons for LIBS and considering techniques which may be used alongside LIBS. In order to outline current practices; methods including XRF, wet chemistry, neutron activation and hyperspectral imaging (HSI) are explained, their advantages and drawbacks noted, and some comparisons are drawn to LIBS.

Preceding the practical descriptions, the geology of the Kittilä mine and surrounding area will be detailed in section 2.7. The focus on the thesis has utilised powders and core samples from the Kittilä mine and therefore an understanding of the rock types is necessary. The practical research will be explained from section 3.0 in which the sample types and materials used will be commented upon. Following the sample descriptions, the experimental set-up used to obtain LIBS results will be explained. At this time images of the LASO-LIBS set-up cannot be shown as the project is undergoing commercialisation, further information and images will be released at a later date. The thesis will continue with section 3.2 regarding the creation of the reference sample library, discussing the use of TXRF and XRD combined with chemical analysis results to ensure the data input into the reference library is known to be accurate. Within section 3 shall be explanations of the sample preparation methods which were used during the experimental stage and explanations shall be provided for why specific methods were or were not chosen. The preparation methods applied to the mine samples will be used to calibrate, improve upon and check the repeatability or variations between the same sample in different phases. The reference library data will then be explained from section 3.3 along with the installation of the reference data into the LIBS algorithm.

The results are published in section 4.0, focussed on data collected from LIBS, TXRF, ICP-AES and XRD and comparisons are made between various techniques. Graphical and tabulated data will be presented within the results section and conclusions have been drawn and discussed in section 5.0. The conclusion section discusses the methodology with positives mentioned and improvements considered. Explanations for outliers and variations within the results are provided and defended where appropriate. Section 5.4 is a reflection on the project and a

situational overview are given. This thesis concludes with section 5.5 providing future research possibilities.

1.2 Aims of LASO-LIBS

Large Area Scanning Open-Source Laser Induced Breakdown Spectroscopy (LASO-LIBS) is a pioneering new technique which aims to deliver rapid, on-site, on-line analysis of drill core samples while encased within core boxes. This pioneering technology aims to reduce the time taken to manually analyse drill cores without increasing the need for time-consuming sample preparation as in the case of other analytical methods. While conventional LIBS technologies are used in elemental analyses, LASO-LIBS aims to analyse mineralogy of geological samples. To determine mineralogy a series of algorithms must be used which register and analyse the elemental composition of a measured area and effectively calculate the mineralogy. The algorithms require background data to draw information from when determining the correct mineralogy for a point. Improving the database improves the ability of the algorithms to accurately provide mineralogical results. To improve the database, a reliable data series must be presented with known values to aid the determination of minerals in unknown samples, allowing the algorithm to effectively compare an unknown datapoint with similar data presented previously.

This thesis focusses on determining the optimal method of developing and calibrating a reference library of data which can then be used in subsequent LIBS analyses of a specific sample set. The original reference library data set can be modified and updated to include additional site focussed data, decreasing data processing times and increasing accuracy. Once a reference collection of material has been completed and installed into the LASO-LIBS method, then mineralogical analysis of core boxes can be determined within a fraction of the time that manual analysis would take, with no prior sample preparation. LASO-LIBS aims to make mineralogical analysis as simple, rapid and cheap as possible to allow for increasing efficiency in orebody understanding during exploration, mining and restoration phases.

LASO-LIBS utilises existing, well understood LIBS technology, combined with a programmable movement system and data processing algorithm for mineral determination. The device will allow a drill core box to be scanned in a few minutes when measured in a 1 mm measurement-point grid. The point-grid resolution is not fixed, or limited, individual measurement points can be micrometres apart if desired by the user, however, the more measurement points, the more time is required. Hundreds of thousands of metres of drill core may be manually analysed for an individual mine site, LASO-LIBS could reduce time, reduce analytical bias and improve both reliability and accuracy of results, when compared to manual analysis. A key aim is to ensure that reliable results can be produced with no changes to current sample state; mining companies drill core boxes for analysis, it should be possible to directly analyse the cores in this state.

LASO-LIBS is designed to be portable; the aim being the production of a field-ready device which can be used in a multitude of environments including within a mining work shed, a mine

or a greenfield exploration setting. In order to achieve portability, the LASO-LIBS machine will weigh less than 20 kg and have dimensions which allow for easy one-man transportation over short distances without the need for assisting equipment such as vehicles or trolleys. Currently, ideas are being considered regarding the potential of making the device separate into easy-to-assemble pieces allowing all the constituents to be stored and transported more easily. Furthermore, there is the possibility to set up the device as a permanent fixture, potentially with conveyors to automatically feed a new drill core box into the device when required.

For the time-being, research and data are being collected to improve the current LASO-LIBS technique; including reference sample preparation, improving the algorithms for data processing to determine mineralogy from elemental compositions, component miniaturisation of the current set-up and the use of additional instruments to aid mineral determination - for example a camera. During this phase, many mining companies are involved, steering groups and regular meetings between stakeholders occur to aid the progression of the project to complete the main goal; producing a device which can easily be used throughout the mining industry.

1.3 Aims of this thesis

Site specific calibration of the LIBS algorithms has proven problematic. The development and deployment of the algorithms to unknown samples has created complexities which this thesis aims to simplify. The determination of a practical calibration technique which is cost and time efficient as well as effective could drive LIBS technology to become a major feature in drill core analysis.

Currently a machine learning algorithm artificial neural network is installed to produce imaging and quantitative analysis of samples. The set-up relies on a supervised algorithm which itself has a very high classification ability, however it is currently reliant upon an unsuitable and deficient geological reference library. Visible and UV wavelength light data are collected by 2 spectrometers, the data are then processed to produce the output result, the process however is unknown. The artificial neural network is initially subjective and may produce a wide range of outputs for the same sample type dependent upon the network set-up. Therefore, it is important to determine which of the algorithm set-ups produces results most representative of the analyte. Therefore, to determine the optimal algorithm parameters, there must be a range of known sample datasets to be compared with the algorithm output.

Reference samples were analysed using multiple long-standing and well understood laboratory analysis techniques for compositional understanding of mineralogical and elemental composition. The known samples were subsequently analysed through utilising LIBS and the retrieved data used to improve the reference library of data during processing.

1.4 Experimental sample preparation aims

Conventional LIBS technology is an elemental analysis technique with a wide range of

applications and is used within many industries. With the addition of algorithms, the mineralogy of samples can be determined, providing valuable information for mining companies. However, the algorithms must be capable of comparing unknown data-points with a recognisable data-set to allow for the presentation of mineralogical results established form elemental information.

For optimal analytical standards of LASO-LIBS to be achieved, algorithms must be provided with data of the highest accuracy and reliability possible. The 'training data' is collected, collated and uploaded to be used in the analysis of the desired, site-specific drill cores. All training data must be of the highest quality as the algorithm for LIBS produces results based on the database from which the information is drawn. If reference collection information is of poor-quality subsequent LIBS analysis will be equally unreliable. To ensure the quality of training data, samples are tested using multiple laboratory analysis techniques before analytical data is uploaded for use in LIBS.

Elemental reference samples were scanned using LASO-LIBS to provide pure elemental information to the algorithms. Elemental data will be supplemented with naturally formed mineralogical samples which have been previously analysed using XRD. Mineralogical samples will provide the algorithm with data to analyse multi-elemental as well as mono-elemental samples. As the exact elemental composition is known, the sample may be immediately scanned using LIBS and the data input into the algorithm since the data has been previously confirmed externally. The data produced from a known sample can be uploaded into the reference library and subsequently applied to analyse future unknown samples which display the same data point peaks. Increasing the volume of measured data is vital in order to build and develop a robust reference library to serve the analysis by LASO-LIBS. This thesis aims to accelerate and improve on the current development of the reference library and to produce a method of calibrating it to a specific site or material type.

The reference library of information provides a large amount of data for the LIBS analysis algorithms to accurately detect and determine sample mineralogy. However, it is also important to focus the algorithm through providing site-specific data which is as closely linked as possible to the unknown samples to be analysed. If a small selection of the unknown samples, or mineralogically analogous samples, have their exact compositions analysed through other means, the subsequent data can also be uploaded into the LIBS algorithms. Increased data volume within the algorithm allows for increased accuracy and reliability when analysing the unknown samples in bulk using LIBS.

Data from total reflection X-ray fluorescence (TXRF), inductively coupled plasma atomic emission spectroscopy (ICP-AES), LASO-LIBS and X-ray diffraction (XRD) will be combined to produce a series of known samples which can be used as calibration materials for the LASO-LIBS device. Kittilä mine have provided the project with halved drill cores for test scanning, the corresponding powdered half core and the ICP-AES (alternatively termed inductively coupled plasma-optical emission spectroscopy (ICP-OES) data sheet for each metre. This thesis analyses the Kittilä powder samples using alternative techniques to compare

with the mine data. Various methods will be used to convert the halved drill cores and their powdered sample counterparts into useful reference samples to be used for calibrating the LASO-LIBS device. The results of this thesis include comparisons between the compositional values for powdered samples and thin disks as determined by ICP-AES, LASO-LIBS and TXRF.

One key advantage of LIBS is the rapid speed of analysis; therefore, it is important that the site-specific calibration processes can also be completed rapidly. During these experiments, a series of sample preparation methods have been compared to determine their success in achieving suitable reliability and repeatability when analysed using LIBS. Sample preparation techniques outlined in section 2.5 represent a compilation of the known and potentially viable processes which may be useful to this thesis. All of the techniques have been considered based on their reliability, simplicity, cost-effectiveness and time efficiency; considerations regarding time, cost and equipment availability have been considered. Furthermore, the applicability of each technique to the samples involved is important, a number of LIBS sample preparations are not necessarily suitable, or ideal for use with ore samples. Considering all variables and limitations, the innovative thin disk preparation (TDP) combined with related analytical techniques are the principle areas of focus for experimentation.

1.5 The need for rapid quantitative analysis in mining

To assess potential ore deposits or improve understanding of an on-going operation, a typical mining company can drill tens to hundreds of thousands of metres of drill core sample on a yearly basis. Analysis generally requires each core to be split, leaving one half for an exploration geologist to manually assess and the corresponding half being passed on to an analytics laboratory (Bolger, 2000). Sections of the cores will be destroyed through grinding, milling and pulverisation during sample preparation processes for many of the analysis techniques. Laboratory based analysis of drill core samples often involves fire assay, wet chemistry (Harhira, et al., 2017) (Rifai, et al., 2017) or high precision, instrumental, multi-elemental analysis techniques such as XRD, XRF (Death, et al., 2008) and Hyperspectral Imaging (HSI) (Xue, 2020) and Near Infrared Spectroscopy (NIRS) (Rifai, et al., 2018).

A market study by Xue, 2020, states that according to exploration geologists interviewed, current field analytical instruments cannot provide enough reliable or detailed results. The precision instruments and techniques currently in use within the mining industry are laboratory-based devices which can seldom be moved, especially not into a field environment. The Xue 2020 study discovered that geologists require analytical devices which are portable, require little sample preparation and are effective in field environments (Xue, 2020). Currently, hand-held XRF devices are used by many geologists for field studies; XRF is the most commonly used surface analysis technique (Xue, 2020). A number of popular field analysis instruments have varying pitfalls including: poor accuracy, poor reliability, inability to operate efficiently in the field, the need for time-consuming sample preparation or a range of expensive, heavy or volatile consumables to ensure their functionality (Brand & Brand, 2014). These commonly used technologies are also limited by spectral ranges, spectral selectivity, and surface

requirements such as dust and moisture (Rifai, et al., 2018) which leads to low reliability, accuracy and reproducibility as suggested by Xue, 2020. Geologists are not only keen to understand the abundance of minerals within analyte samples but also mineral distribution within the sample i.e. as a mineral map (Khajehzadeh, 2018).

Laboratory testing processes are time consuming, labour intensive and expensive (Bolger, 2000). Results may take days, weeks or months to be reported back to the mining company, thus reducing a mine's ability to make rapid decisions, potentially delaying production decisions or highlighting issues which have previously been acted upon (Harhira, et al., 2017) (Rifai, et al., 2017), (Khajehzadeh, 2018). An on-site, reliable and rapid response technology would aid mining companies in reducing decision-making times and providing sufficient data to make decisions, therefore reducing financial losses. A technique to analyse mineralogical samples cannot only rely on being rapid but must also accurately detect elements in all concentrations, including trace elements (<1 wt%) which can be vital in mining operations (Harhira, et al., 2017), (Death, et al., 2009). Trace elements may be especially important to mining companies if they have the potential to drastically impact product price i.e. by-products (increase product value) or contaminants (decrease product value). Trace elements which are potentially toxic can also lead to increased environmental or processing costs. Furthermore, accuracy is becoming a more pressing issue as deposit grades decrease across the world, introducing finer and finer margins for error in cost analyses for companies.

In 2019, Agnico Eagle spent $11.8 million on drill cores including $8.2 million on further exploration of the main locality plus $2.6 million on exploration outside of the current site and on conversion drilling. A total of 34,400 metres of cores were drilled on the mine site, 8,000 metres of conversion drilling and 4,000 metres of exploration drilling along the Suurikuusikko, Kapsa and Hanhimaa Trends (Agnico Eagle, 2020). For Kittilä, a combined 46,400 metres of drilling per year is not excessive, for example, in 2009 exploration drilling totalled 105,886 metres (Agnico Eagle, 2010). Any reduction in cost of analysis per metre of drill core amounts to an immediate and considerable financial saving for any mining company. Comparing 2019 reserve and resource figures with those of 2015, it is clear to see the changing dynamic within the mining sector. It is not only the case for Kittilä, but also for a large majority of mines. In 2015, Agnico Eagle reported an average grade of 4.9 g/t in proven and probable reserves, compared to 2019 when the average grade dropped to 2.83 g/t for the same category (Agnico Eagle, 2019), (Wyche, et al., 2015).

Any price reduction in direct analytical cost of drill core analysis would result in noticeable financial benefits for mining companies. Indirect costs would be reduced if mineralogical analysis could be completed rapidly in the field; companies would not suffer losses or delays due to lingering drill core reports. The ability to make immediate decisions, based on immediate, reliable and accurate analysis provides a wide range of benefits for mining companies. Thus, explains the large investments and interest of the industry in on-line quantitative mineralogical analysis research (Harhira, et al., 2017).

While LIBS is fundamentally an elemental analysis technique, with sufficient data processing mineralogy can be determined. With a reliable laser based scanning analysis and complementary data processing set-up, there are many potential applications within the mining industry which could be aided by such a technique. LIBS presents an attractive alternative for elemental analysis and imaging as an on-site and on-line instrument capable of operating in the field (Rifai, et al., 2018). Xue, 2020, produced three service concepts which focus on the key issues posed by industry experts. The concepts are a drill core scanner for logging, a mine wall scanner for geological recording and a conveyor scanner for mill feed concentration analysis (Xue, 2020). The research and findings of this thesis will focus on the theoretical and practical aspects of a LIBS scanner for the use of mineralogical and elemental analysis of drill core samples.

2 Background

2.1 Background Theory of LIBS

In 1960 Sorokin and Stevenson achieved the production of a four-level lasing system using uranium-doped calcium fluoride crystals (Sorokin & Stevenson, 1960). A laser using neodymium and various hosts was introduced in 1961 which later evolved into the 1064 nm Nd:YAG laser, the most commonly used plasma-inducing laser today (Radziemski & Cremers, 2012). The following year, 1962, Brech and Cross observed a micro-emission of material using a ruby MASER (Brech & Cross, 1962) - this led to a race between scientists to discover a use for the newly found emission. Then in 1963 Debras-Guédon and Liodec (Debras-Guedon & Liodec, 1963) published the first spectrochemical analysis of surfaces using laser induced plasma. Now commonly termed Laser Induced Breakdown Spectroscopy (LIBS) – occasionally referred to as LIPS (Laser Induced Plasma Spectroscopy) – has become a widely used analytical tool with far-reaching, proven industrial applications in surface analytics.

LIBS is a type of atomic emission spectroscopy which uses a nanosecond, or shorter, duration, high-intensity and focussed laser pulse to atomise and excite samples (Harhira, et al., 2017). LIBS operates by ablating a small area of the surface of a sample in order to produce a microscopic plasma plume occurring when critical temperatures are reached (Dalm & Buxton, 2016). Critical temperatures vary between materials. Vaporisation occurs more slowly than energy deposition which causes an underlying region of material to reach the critical parameters before the surface does and so the surface explodes due to the pressure from below (Sun, et al., 2000) (Hou & Jones, 2000). During the early plasma stage, the ablated material dissociates into excited atoms and ions, the plasma which ensues emits atom specific wavelengths of light as photons as the excited ions or atoms return to their ground state (Jantzi, et al., 2016) (Sun, et al., 2000) (Brouard, et al., 2007). The emitted light can be analysed by a spectrometer and compared to standards or calibrated to determine and display the elemental composition of the region at which the laser was focussed (Cremers & Radziemski, 2013). The plasma also emits radiation throughout the ablation phase; however, the radiation contains no useful information regarding present species (Jantzi, et al., 2016). With a mechanically

controlled stage and specialised optics, the spatial layout of a sample surface can be mapped and this is useful to compare rich regions or regions with high impurities (Jantzi, et al., 2016).

LIBS is a minimally destructive technique with only mild damage occurring on the surface of a specimen, however very little heating occurs outside of the very small area that the laser is focussed upon (Pease, 2013) (Senesi, 2014). During experiments such as those completed by (Ho, 2012), it has been concluded that LIBS is not perceptively damaging if the correct laser pulse is selected for the sample in question. However, it is commonly mislabelled as a "non-destructive" technique, which whether damage is perceivable or not, LIBS is required to damage the surface of a sample, since without a plume of dissociated material, LIBS would not be able to analyse it (Ho, 2012).

Since LIBS is a surface analysis technique, a surface-to-bulk composition relationship must be assumed or demonstrated (Death, et al., 2008). There may be specific instances where a relationship between the surface being analysed and the bulk material will not exist; in these cases the results should be voided, and other analysis methods or preparations considered. Samples which are composed of homogeneous layers such as finely bedded ores or an ore with a fine film of contamination on the surface are suitable for depth profiling (Jantzi, et al., 2016) (Senesi, 2014). By focussing the laser and taking multiple readings in a single location by ablating the surface, each reading is effectively measuring the sample at increased depth. The same technique is used to remove the surface layer when there is known surface contamination or weathering of a sample. Depth profiling may produce ambiguous results, however, since ablated material of previously scanned spots may remain at the ablation crater edge, interfering with subsequent scans (Jantzi, et al., 2016) (O'Nagy, et al., 2014). In an instance where the surface is non-representative of the bulk, homogenisation and pelletization would provide more reliable results for general composition, or depth profiling can be considered, depending on the type of data the user requires. In heterogeneous samples a bulk scan can be performed by completing a raster scan of the specimen and averaging the results. Spatial variation can also be measured through scanning each point as an individual, rather than as part of the whole, and each point can display results per locality (Jantzi, et al., 2016).

2.1.1 Advantages of LIBS techniques

LIBS is capable of determining the elemental composition of any sample in any phase state; solid, liquid or gas, and can detect any known element - assuming that the laser has sufficient power to heat all elements to temperatures which allow for detection and also the sensitivity and wavelength range of the spectrometer is adequate (Jantzi, et al., 2016) (Brouard, et al., 2007) (Cremers & Radziemski, 2013) (Hou & Jones, 2000) (Andrade, et al., 2020). Unlike some analytical techniques, conductivity of a sample is not required for LIBS scanning (Luque Garcia & Luque de Castro, 2002). LIBS is particularly sensitive to light elements such as C, Be, H and Li, which are often difficult to detect with alternative instrumental geochemical analysis methods such as XRF (Senesi, 2014) (Harmon, et al., 2019). A number of the light elements, for example Li, are among the commodities required for the production of green

technologies, making them particularly important in the modern economy (Harmon, et al., 2019). Materials formed of very hard components, such as ceramics and superconductors, which are often difficult to dissolve or digest in order to complete chemical analyses may also be analysed with LIBS (Senesi, 2014), (Luque Garcia & Luque de Castro, 2002).

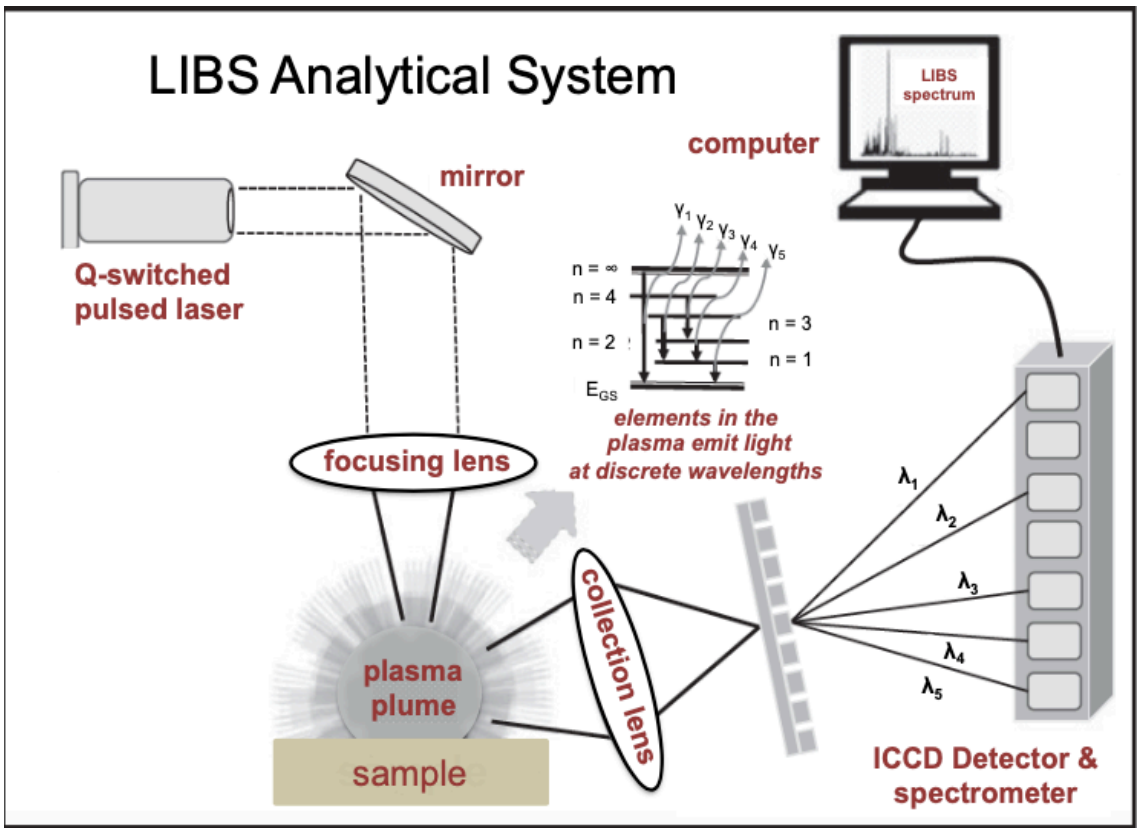

Figure 1: Taken from Harmon, et al. 2019. Schematic diagram of a conventional LIBS set-up including a laser, sample, detectors, spectrometers and computer for system control and data processing.

The key advantages of LIBS are; near real-time results, useful for high volume testing in large scale industrial settings (Sun, et al., 2000), (Han, et al., 2018); samples need only to be optically available, making micro-volumes (0.1 µg – 1 µg) of sample sufficient to determine results (Jantzi, et al., 2016), (Bolger, 2000), (Luque Garcia & Luque de Castro, 2002); LIBS is capable of remote operation making it useful in hazardous environments as a stand-off sensing technique (Sun, et al., 2000), (DeLucia, et al., 2009), (Fortes & Laserna, 2010) effective at distances exceeding 100 m (Harmon, et al., 2013); LIBS can also be conducted remotely in underwater environments (Senesi, 2014) (Radziemski & Cremers, 2012); generally no, or minimal, sample preparation is required (Sun, et al., 2000), (Ho, 2012), (Han, et al., 2018), (Hahn & Omenetto, 2010), (Fortes & Laserna, 2010), also reducing the potential for contamination (Luque Garcia & Luque de Castro, 2002); the methodology is relatively simple and does not require extensive levels of expertise; and the technology and operation of LIBS is priced attractively compared to many other analytical techniques (Jantzi, et al., 2016), (Han, et al., 2018), (Senesi, 2014), (Andrade, et al., 2020). Furthermore, the technique can be considered environmentally friendly as there is no waste, noise and no pollution produced

during analysis (Senesi, 2014) and no environment-damaging or scarce consumables are required for operation, e.g. liquid Nitrogen or helium.

Dependant on the LIBS arrangement, a conventional LIBS set-up is shown in figure 1, a spatial resolution of 1 - 100 μm^2 is possible. A comparable technique such as XRF irradiates 100,000 μm^2 of the sample surface, however different types of XRF can increase the spatial resolution to around 100 μm^2 (Rakovsky, et al., 2014) (Luque Garcia & Luque de Castro, 2002). A fine analysis point grid allows for analyses to be taken from individual grains or inclusions in geological samples and allows for the mapping of finely zoned or layered samples (Senesi, 2014). While a fine spatial resolution can be perceived as an unquestionable advantage however, the finer the measurement point grid distances, the higher resolution the analysis will provide, however a finer grid will take a longer time to measure. Therefore, in some situations a mine company may conclude that a coarser resolution proves favourable, for example in a heterogeneous geological sample where a coarser measurement grid may prove beneficial to rapidly understanding the overall sample mineralogy.

The flexibility of LIBS allows for analyses to be taken as requested, giving geologists the opportunity to understand the ore forming processes and therefore, understand the orebody. An individual spectrum can be obtained using the LIBS technique at a rate of 1,000 points per second, compared to only 1 - 10 points per second obtained by XRF allowing for individual measurement points to be analysed in below 1 second by LIBS but at least a few seconds for XRF (Xue, 2020), (Rakovsky, et al., 2014). When the single spectra analysis time is expanded to consider that of a drill core box, an entire drill core or a whole ore body, LIBS can save a large amount of analysis time for exploration geologists.

2.1.2 Drawbacks of LIBS techniques

A key drawback observed during the LASO-LIBS project, is the need to acquire a suitably robust suite of standard reference materials to develop the data reference library, as certified reference materials are difficult to apply to complex geological samples (Han, et al., 2018), (Hou & Jones, 2000). The difficulty in obtaining appropriate standard materials has led to the more frequent use of LIBS as a semi-quantitative technique most frequently (Luque Garcia & Luque de Castro, 2002). The accuracy of analysis on geological samples is influenced by matrix effects; hardness, density, surface texture and energy absorption can cause major interferences to the analysis (Pease, 2013), (Harmon, et al., 2019), (Harmon, et al., 2013), (Luque Garcia & Luque de Castro, 2002).

LIBS spectra are known to depend upon environmental, instrumental and sample conditions which leads to poor shot-to-shot reproducibility (Rinke-Kneapler & Sigman, 2014). Poor reproducibility may be due to many variations for example; pulse instability, plasma interaction, sample matrices and environmental changes leading to differing results at the same spot (Rinke-Kneapler & Sigman, 2014). LIBS also suffers from high lower limits of detection (LLDs) compared to alternative spectroscopic techniques which has led to the rise in the

research of double-pulse LIBS techniques. The double-pulse relies on the addition of an additional laser, however this increases the hardware configuration complexity. A range of additional signal enhancing modifications are being considered and research to improve the precision and sensitivity of LIBS, including; microwave-assisted (MA-LIBS), resonance-enhanced (RE-LIBS) and assisted by laser-induced fluorescence (LIBS-LIF) (Andrade, et al., 2020). Furthermore, problems are created by the presence of dust or moisture in the surrounding air which can settle onto the drill core surface. LIBS analyses micro volumes of ablated material from the sample surface, therefore surface contamination can negatively impact analysis accuracy and reliability. Procedural measures are required to avoid the collection of a dust or liquid film developing on the sample surface. Poor reproducibility may also be in part due to the nature of the pulse to sample interaction resulting in sample surface variation between 2 laser shots at identical localities.

It is also widely recognised that both chemical and physical effects play an important role in replicability, despite studies which attempting to prove either chemical or physical have a larger impact (Cremers & Radziemski, 2013). Material properties can have large effects on optical spectroscopy which cause over- or under-estimation of the true values being measured, especially in complex samples such as geological ores with many elements of interest. Overall, LIBS is a less sensitive analytical method when compared with conventional laboratory techniques such as Induced Coupled Plasma Atomic Emission Spectroscopy (ICP-AES) or Atomic Absorption Spectroscopy (AAS). LIBS data also tends to display poor precision, typically 5 – 10% depending upon the degree of heterogeneity, the matrix effects and the excitation properties of the laser (Luque Garcia & Luque de Castro, 2002). While LIBS can be effective at 100 m distance (Harmon, et al., 2013), the use of stand-off LIBS has been limited due to eye safety concerns and the potential for laser-spark ignition of certain sample types (Rinke-Kneapler & Sigman, 2014).

This thesis attempts to find a solution for reference material production through exploring various sample preparation methods and alternative analytical instruments, the results of which can be programmed into the LIBS data processing algorithm. Overcoming these issues is a key aim of the LASO-LIBS research project and its conclusions will go a long way towards proving the industrial applicability of this technique.

2.1.3 Applications of LIBS

Following on from the initial work done to explore the potential of LIBS, no practical uses were assigned to the theoretical concept for many years. From conception until 1975, approximately 100 publications regarding LIBS were submitted (Radziemski & Cremers, 2012), then LIBS based instruments began to appear in the 1980's. Early instruments were usually produced for a specific purpose by a specific laboratory and utilized without broader application, then by the 1990's commercial LIBS devices were available (Radziemski & Cremers, 2012). Currently, industrial applications vary and include; pharmaceutical, metallurgical, military, biological, geochemical and astronomical settings (Jantzi, et al., 2016),

(Bolger, 2000), (Pease, 2013), (Ho, 2012), (Wiens, et al., 2012), (DeLucia, et al., 2009) and has been proven effective, analysing a wide range of material types including; paint, rock, metals, glass and explosives (Jantzi, et al., 2016), (Bolger, 2000), (Ho, 2012). LIBS has been used in a wide range of other industries and research is continually being added to the library of potential applications. Over the past decade it has been clear to observe that published LIBS-based imaging studies have been increasing and further highlighting the potential of the technique (Fabre, 2020).

In the early 1990's, 2 of the earliest non-commercial LIBS devices were constructed for a buyer at the Los Alamos National Laboratory (LANL) and were used to analyse Be particles trapped in air filters to ensure that acceptable airborne Be limits were not surpassed (Radziemski & Cremers, 2012). In 1995, a suitcase-sized LIBS device was also developed at LANL for the intended purpose of lead detection in paints, the same device was then redesigned to monitor lead in soldered joints and for an application with the US Navy and other focussed tasks (Radziemski & Cremers, 2012). Research in the past one and half decades has focussed heavily on the miniaturisation of parts to allow the production of low power and portable machines which can be used in a wider range of industries and applications. Advances in the power and the size minimisation in lasers, optics, spectrometers and detectors make the development of a portable, field-ready LIBS instrument possible (Fortes & Laserna, 2010).

The applicability of LIBS in many industries is still ongoing as proven by the volume of research being continually published across a wide array of industrial settings. Nisar, et al., 2018 concluded that LIBS yielded precise and accurate results on Calcium tablets for the pharmaceutical industry, Tiwari, et al., 2019 stated that LIBS can be effective for analysing compositional variations including trace elements, active and inactive ingredients, and molecules contained in pharmaceuticals. Liu, et al., 2019 confirmed that LIBS when coupled with chemometrics can identify genetically modified maize and previously, Dixit, et al., 2018 confirmed that LIBS can image brine diffusion into beef. Aside from the food and pharmaceutical industries, Lopez-Claros, et al., 2018 successfully took measurements of a submerged shipwreck with no sample preparation besides the scraping away of barnacles or algae from the sample surface.

Further examples of LIBS viability across many industries include a US Army Research Laboratory (ARL) project (2000 - 2010) which used LIBS as a stand-off technique to aid in the detection of explosives and hazardous materials. The ARL determined that LIBS was one of very few techniques to detect hazardous or explosive signatures from a stand-off distance, but the technique still requires further refinement (DeLucia, et al., 2009). Research from other scientific areas also managed to prove the viability of LIBS. The Mars Science Laboratory took the first LIBS instrument to the surface of Mars in 2012 to provide inter-planetary remote sensing. A decision was made to install a LIBS onto the *Curiosity Rover* on the basis of perceived benefits when compared to the previously used Alpha-Proton X-ray Spectrometer (APXS) which was installed on the *Sojourner Rover* of 1997. As previous issues included the inability to brush away dust from the surface or for the APXS to take readings from un-weathered surfaces, it was concluded that the installation of a LIBS could circumvent these

issues (Wiens, et al., 2012). The LIBS device mounted on the *Curiosity Rover* can take readings with an accuracy of 10 - 15% at a distance of 7 m from a target (Radziemski & Cremers, 2012) although previous research has demonstrated that LIBS devices can accurately analyse a sample at distances exceeding 100 m (Harmon, et al., 2013) and has been proven effective at 180 m (Rohwetter, et al., 2005).

The valuable potential of LIBS which has been demonstrated through a wide range of published studies has been extensively applied to earth sciences and therefore mining (Fabre, 2020). LIBS is considered a quantitative geochemical analysis technique for ore samples including mineralogical and elemental compositions contained within ores. Most studies completed thus far have used pellets to determine elemental compositions of iron ore and studies to determine the effects of particle size on results (Harhira, et al., 2017), (Death, et al., 2009). The majority of LIBS use with mine samples has been for research only; but while there is much promise and interest, LIBS has not yet become a widely used analytical technique for the mining industry.

Quantitative analysis of ores in powder, pellet and whole rock forms have been studied and displayed promising results for a number of ore types including (Khajehzadeh, 2018), (Dalm & Buxton, 2016); iron ores (Sun, et al., 2000), (Death, et al., 2009), (Death, et al., 2008), (Grant, et al., 1991); Zn and Cu ores (Gondal, et al., 2007), (Porizka, et al., 2014); phosphate ores (Rosenwasser, et al., 2001), (Gaft, et al., 2007); uranium ores, nickel laterite (Death, et al., 2009) and coal (Gaft, et al., 2007). For many of the studied ore types it is still uncertain whether an on-line analysis system can detect ore quality defining elements with sufficient precision (Dalm & Buxton, 2016). Gaft, et al., 2007 showed how a LIBS sensor could be used as an on-line evaluation technique, however the study was limited only to coal and phosphate ores. As of April 2017, the Cooperative Research Centre for Optimising Resource Extraction (CRC ORE) and the National Research Council of Canada (NRC Canada) have collaborated to produce a proof of concept of a combined LIBS Mid-infrared (Mid-IR) Quantum Cascade Laser (QCL) analyser. Aiming to create an industrialised elemental and mineralogical analyser using advanced chemometrics, which is suitable for deployment in-pit, underground, for cross-belt scanning and on-line slurries (Wilkie & Blouin, 2017).

LIBS is an extremely versatile analysis technique and the volume of research still ongoing suggests that LIBS will continue to grow as a technology and will one day become a staple analytical tool across many industries. In 1975 when there were a total of 100 publications regarding LIBS, by 1995 this had grown to 600 and as of 2010 the figure stood at 5000. Furthermore, since 2000 there has been a biennial International LIBS Conference (Radziemski & Cremers, 2012) and so LIBS continues to grow in the scientific and industrial communities, it appears the growth will continue. Annually, further studies support the widespread use of LIBS technology, some technical issues remain, however they are continually being challenged.

2.1.4 LIBS for drill core and gold analysis

The goal of this thesis study is to research the potential of LIBS as an analytical technique for use extensively across the mining industry, research for this thesis is primarily based on experimental analysis of gold bearing drill cores from an orebody in Finnish Lapland. This section will summarise the literature focussing specifically on either LIBS analysis of gold bearing rocks and ores, or literature regarding the specific use of LIBS in the analysis of drill cores.

Analysis of Au bearing samples has presented difficulties during LIBS research, see studies by Haavisto., 2013 and Dalm and Buxton., 2016. The key issue with the analysis of gold ore is the range of entities within which Au may occur. Gold can be found as native, electrum and as an Au alloy but can also be *'invisible'* as gold tellurides, selenides and sulphides (Petruk, 2000). Gold commonly occurs with an assortment of specific gangue and ore minerals which are, some of which can cause problems during analysis or processing. The most common associated ore minerals include: pyrite, arsenopyrite, galena, sphalerite, chalcopyrite, magnetite, pyrrhotite and tetrahedrite-tennantite (Petruk, 2000) all of which are sulphide minerals besides magnetite which is an oxide. Common gangue minerals tend to be silicate or carbonate minerals including: quartz, muscovite, feldspars (K-feldspar, albite, microcline), tourmaline, carbonate minerals (ankerite, dolomite, calcite, rhodochrosite) and graphite (Petruk, 2000).

Processing problems can occur due to the presence of carbonate minerals, graphite, secondary copper minerals (malachite, covellite, chalcocite etc.) and iron sulphide minerals (bornite, enargite, pyrrhotite). Carbonaceous minerals and graphite can reabsorb gold during the leaching phase, in a process termed *'preg-robbing'* leading to the unavailability of gold for leaching. Pyrrhotite and secondary copper minerals are soluble in weak cyanide solutions which leads to the over-dilution of the solution, and so the solution is no longer able to dissolve the gold meaning pre-treatment steps must be put in place (Petruk, 2000). Mining companies have to understand their orebody, the minerals within and the materials which will be being processed. If the ore and gangue material is not understood then a mining company may face delays, reduced product quality, lower recoveries or increased waste.

Dalm and Buxton, 2016 studied epithermal Au/Ag ore using LIBS and reported a potential relationship between mineralogical alteration and Au/Ag content. Spectral peaks were observed which could represent Au or Ag, though no difference in peak intensity was witnessed between samples of various Au or Ag grades. It was determined not to be possible to observe Au and Ag by direct LIBS detection, although Na/Al peaks could be used to determine the economic or sub-economic nature of samples (Dalm & Buxton, 2016). Haavisto, Kauppinen, & Häkkänen, 2013 studied Au bearing drill cores and aimed to use LIBS in order to analyse drill cores without the need for removal from the drill core boxes and with no sample preparation. In research similar to that which this thesis relies upon, Haavisto, Kauppinen, & Häkkänen, 2013 also failed to directly measure Au, since the ore was refractory, Arsenic (As) was analysed and assumed to be the host of Au. It was found that defining elements of a drill

core can be analysed by LIBS effectively, producing results which correspond to those produced through laboratory assays. However, it was concluded that LIBS could not compete with Hyperspectral Imaging and can be considered useful as a calibration technique for high throughput instrumentation (Haavisto, et al., 2013). Dalm and Buxton, 2016 and Haavisto, Kauppinen, & Häkkänen, 2013 represent the two research papers which discuss the potential of LIBS in the potential analysis of refractory gold. This thesis is experimenting with refractory gold ores and hopes to add to the limited knowledge on using LIBS as an analytical technique in this field.

More recently, Rafai et al. 2017 studied quasi-homogenous Au bearing compressed fine powders of two size classifications; fine and granular. It was found that the fine grained samples proved to display less variance than their granular counterparts despite the quasi-uniformity of the samples. Rafai et al. 2017 concluded that the presented research sufficiently demonstrates the ability of LIBS to analyse Au directly in ppm ranges and provides proof of concept for an Au detecting quantitative analysis technique (Rifai, et al., 2017). Rafai et al., 2017, proposed the uneven spread of large Au grains through the samples (the nugget effect) as a potential explanation for the unexpected and unjustifiable variances witnessed (Rifai, et al., 2017). After the publishing of Rafai et al., 2017, the first of a set of companion papers (Diaz, et al., 2017) were published, followed by the second (Diaz, et al., 2018). The research focussed on the use of LIBS in the analysis of Au/Ag ores, acquiring samples from a Columbian mine and processing plant as well as producing laboratory surrogate samples also. Both native and refractory gold were present in the mine ore samples, meanwhile the surrogate samples were doped with Au bearing HCL solutions and Ag bearing HNO_3 (Diaz, et al., 2017). The samples were milled so 95% of material passed 140 mesh and pressed into pellets. It was determined that pellets able to withstand 5000 laser shots were successful in analysing gold to 1 ppm, however Au could not be analysed in any samples up to 9.5 ppm Au with only 100 shots (Diaz, et al., 2017).

Current literature on the use of LIBS in mining environments for geochemical and mineralogical analysis, are clear upon the potential, however many questions raised through research continue to hold the technology back. Rifai et al., 2017 raise questions around analysing Au independently of matrix effects and the effectiveness of utilising calibration curves produced of pressed powders for the analysis of solid rock samples. As a result, they suggested that the nugget effect impacts the study of gold ores. Harhira et al., 2017 echo this theory attributing the 45% variance measured between fire assay and LIBS analysis results to sample heterogeneity. Harhira, et al., 2017 also produced conclusions propounding Au concentration variation subject to Fe and Si concentrations, stating that Si-rich samples (<5% Fe) have lower detection limits (0.75 ppm) than Fe-rich (>13% Fe) samples (1.5 ppm). Diaz, et al., 2018 suggest further research in sample preparation, the use of standard materials, matrix effects, LIBS configurations and the use of multivariate algorithms. This thesis goes some way to adding to the library of LIBS research and aims to address a number of the questions which have been outlined.

2.2 LIBS sample preparation methods

Outlined in this section will be an overview of the potential sample preparation methods which have been considered for application within this project. Throughout this project, all sample types utilised have been in solid form and so liquid sample preparation techniques have not been discussed in detail. More detail on the sample preparation of liquid samples can be found in Jantzi, et al. 2016 and Andrade, Pereira-Filho and Amarasiriwardena 2020.

LIBS has developed a reputation for requiring no sample preparation; this is in part due to the wide range of specimens which might genuinely be suitable for immediate scanning. Homogenous samples such as glass, metals, paint and polymers are suitable for surface scanning (Jantzi, et al., 2016), (Bolger, 2000), (Ho, 2012). A focus on LIBS ability to operate without any sample preparation has taken the focus away from the benefits of modifying the samples to improve LIBS as an analytical method. A lack of consideration for sample preparation is one of the reasons that despite 50 years of proven viability and successful results, LIBS is not considered a mature technique (Jantzi, et al., 2016).

The possibility of scanning drill cores without preparation has been proven (Haavisto, et al., 2013), (Kuhn, et al., 2016) however, many calibration curves are required, one for each matrix, and thus standard univariate calibration techniques are currently not adequate (Harmon, et al., 2009). This thesis aims to reduce the complication of sample preparation to achieve the necessary data for site-specific calibration as simply as possible to allow for the accurate analysis of unprepared drill core samples.

The creation of calibration curves is commonly complex due to matrix effects which occur because of to the material properties. Matrix effects may be especially prevalent and difficult to handle in the case of geological samples due to their complexity both physically and chemically (Pease, 2013), (Harmon, et al., 2019), (Harmon, et al., 2013). Currently the standard approach to deal with matrix effects is the use of calibration curves (Harmon, et al., 2013) however since sample matrices can vary, different calibration curves are likely to be required for different mineral assemblages (Porizka, et al., 2014). A novel and new preparation technique will be outlined in this thesis which aims to improve the reliability of calibration curves while maintaining a relatively simplistic and time-efficient preparation process.

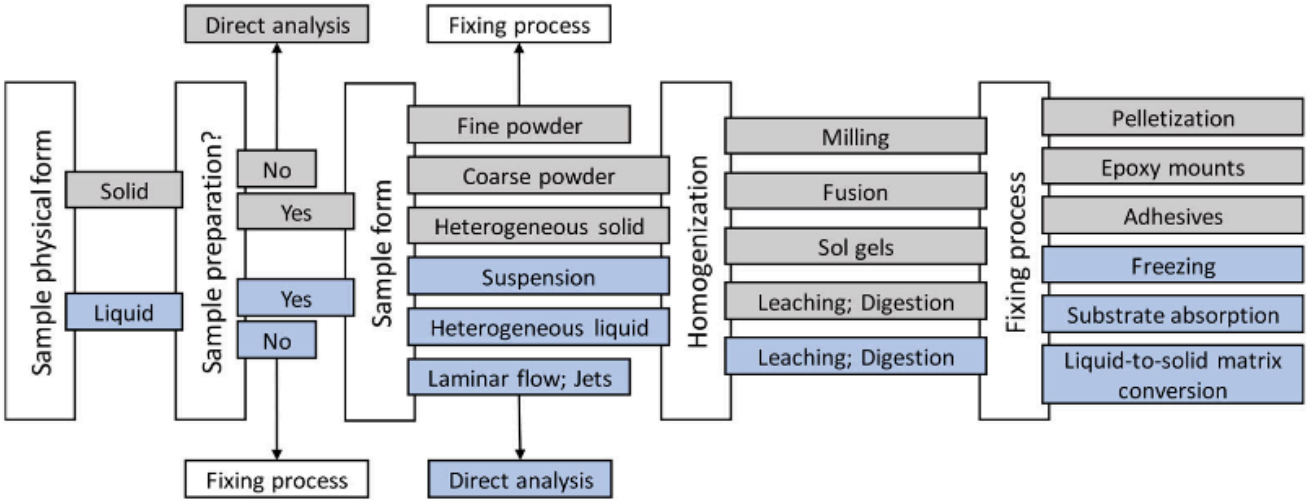

Figure 2: Taken from Andrade, et al., 2020. A flow chart of sample preparation techniques of solid and liquid samples.

Ideally matrices would be removed completely, however, research to find alternative means of matrix removal or reduction for the benefit of LIBS analysis has been thorough (Jantzi, et al., 2016), (Shi, et al., 2015), (Speranca, et al., 2018), (Pease, 2013), (Brouard, et al., 2007). Matrix removal is not always possible, however because the matrix materials may also be the material of interest also, so removing the matrix would also remove the focus of the investigation. In this instance, the matrices can be diluted. Dilution can be effective when the analyte concentration is sufficient to provide a suitably detectable signal after dilution has occurred. A good diluent will contribute as little matrix effect as possible and may have a secondary purpose in behaving as a binder (Jantzi, et al., 2016). In some cases, dilution may not be effective, so matrix-matched calibration standards can be used. Matrix effects can be reduced by the use of internal standards to normalise the analyte signals; thus the standards can improve the overall accuracy, precision and comparability of the results.

Often samples will need to be physically fixed and this can be for a number of reasons. Fixing can help maintain the integrity and reduce movement of the sample during LIBS which is especially important for powder samples. Different samples can be fixed in the same manner, for example in epoxy, to allow for easier testing since all the sample surfaces will be at the same vertical level. Furthermore, fixing increases the ease with which samples may be transported, handled and stored. There are a number of ways that samples can be fixed, for example; adhesives, epoxy mounting, pelletization, fusion and sol gels (Jantzi, et al., 2016). Figure 2 displays a decision flow chart for solid and liquid sample preparation options dependent upon the sample type and eventual purpose of the sample.

Milling of a sample can be beneficial for the purpose of homogenisation if a bulk sample analysis is required, and milling reduces the particle size therefore increasing surface area. The finer the particle size, the easier atomisation can occur in the plasma increasing uniformity and therefore precision (Jantzi, et al., 2016). During milling it is important to consider the surfaces

used, as wear of the mill drum or of the milling balls can result in contamination of the sample within. To combat equipment-originated contamination, the milling equipment should be made of a material which is known to be absent from the sample to be assessed. Therefore allowing for equipment material results to be removed from the final dataset.

2.2.1 Adhesives

The simplest form of sample fixing is with the use of adhesives. Sample preparation consists simply of spreading a thin layer of powdered sample onto the adhesive surface of ribbon, tape or a thin layer of glue (Jantzi, et al., 2016). Adhesives allow for the permanent or temporary fixation of a sample ensuring that no particle shifting occurs during analysis. Sun et al., 2000 determined no significant difference between the quality of analytical results from pelletised samples and loose powder fixed onto double sided adhesive tape. They reported that powder-on-tape is a promising, rapid sample preparation technique with fewer preparation steps required when compared to pelletization and therefore offers less opportunity for contamination (Sun, et al., 2000).

2.2.2 Pelletization

The most common preparation of solid samples for LIBS is the production of pellets from the milled sample through pelletization (Speranca, et al., 2018). Pelletization is the process by which loose, fine-grained powdered material is agglomerated using compression and occasionally requires a binding agent. Binding agents are only strictly necessary when a powdered material will not cohere as a solid pellet, even despite a very fine grain size being achieved; binding agents may also be used as diluents. Pelletization is a versatile method of fixing samples and it comes with many benefits which lead to the increased reliability and replicability of LIBS. There are some key advantages to pelletization; relative simplicity of the process, increased homogeneity compared to solid rock samples of the same dimensions, dust suppression, easier storage, simpler transportation and less lost material as dust. Especially in powder form, LIBS can displace the fine material which negatively affects the results, pressing the powder into pellets can reduce or stop the displacement by fixing the grains.

Pelletizing does have drawbacks however. During pellet production homogenisation cannot be guaranteed especially in the presence of binding agents where the ‘Brazil Nut Effect’ can be problematic (Shi, et al., 2015), and during milling it must be assured that no contamination has come from the mill tools (Speranca, et al., 2018). Additionally, problems can arise during the scan; the laser pulse can cause a shockwave which may dislodge loose pieces of the pellet leading crumbling and the emittance of fine powder into the air. This can impact the laser and therefore the results (Ho, 2012).

2.2.3 Epoxy mounting

Epoxy mounting of samples is a common preparation technique; samples can be fixed in resin to ensure stability and avoid displacement during scanning. It is commonly used to stabilise

and fix delicate samples which may otherwise separate or be dispersed by the LIBS laser. Samples of all forms and sizes can be mounted in epoxy which can also be produced in any desired shape. Adhesive mounts provide a similar function to epoxy mounts, but provide a simpler approach, by fixing a fine-grained specimen to adhesive tape the sample will remain in place (Jantzi, et al., 2016). Adhesive techniques have been proven to produce almost identical LIBS results when compared with those produced from pellets. However, it is important to consider the potential background emissions which could be produced from the tape itself (Jantzi, et al., 2016).

2.2.4 Fused glass disks

Fusion works by fusing a sample with a flux at very high temperatures to create glass disks. Through doing this the sample is thus diluted, homogenised and fixed. Disadvantages of fusion include the loss of volatile fusing agents and flux elements which can impact the results. Furthermore, heterogeneity can occur during cooling if heavier elements are allowed to settle (Jantzi, et al., 2016). Pease, 2013 focussed on a comparison between fused glass disk preparation and the more commonly used pelletisation. The study concludes that fused glass is a more efficient method when analysing bulk minerals and rocks when compared to the more commonly used pressed pellets (Pease, 2013). The disadvantages include the ability to avoid sample preparation, the requirement of specialised equipment and increased monetary cost.

2.2.5 Sol-gels

Sol-gels combine a colloidal solid particle suspension and a liquid comprised of water, co-solvent, a catalyst and either liquid metal or an alkoxide precursor which may or may not be heated. Brouard, et al., 2007 compared Silicon, Aluminium and Zirconium sol-gels in creating matrix calibrators to be used in LIBS. The aim of the study was to design an effective sample preparation method which was rapid, ensured good homogeneity in each analyte, offered strong repeatability and low optical background. The study concluded that the different sol-gel types were good candidates as materials to be used to determine tuneable solid calibration standards for LIBS. In particular the Aluminium based sol-gel presented a beneficial combination of; a low optical spectral background; high reproducibility due to reproducible sample ejection behaviours; and highly homogenous dispersion (Brouard, et al., 2007). It was concluded that sol-gels can offer simple and straightforward sample preparation which produces highly homogenous solid samples for analysis. As the sol-gel powders can remain stable over time, and a sol-gel can be produced quickly, the process can be used with the addition of an internal standard volume of powder to be used either as a calibration or correctional technique for a range of other samples (Brouard, et al., 2007).

2.2.6 Leaching and Digestion

Leaching and Digestion is another possibility, however there are many downsides; time-consuming, preparation requires laboratory grade equipment, acids and high temperatures, prone to contamination and prone to poor reproducibility (Jantzi, et al., 2016).

LIBS can also be used to analyse samples in the liquid state; however, there are many issues which can arise while scanning a liquid sample and so one method of dealing with these is to avoid the use of LIBS and select another analysis method (Jantzi, et al., 2016), (Speranca, et al., 2018). However, if LIBS is being used to analyse a liquid sample it is common that surface ripples, liquid splashing, surface heterogeneity, shorter plasma duration and poor reliability and replicability (Speranca, et al., 2018). Similar effects have been seen to occur in loose powders. There are a number of sample preparation techniques which can facilitate the analysis. With the theoretically simplest option is to freeze the liquid into a solid, other options include substrate absorption, liquid-to-solid matrix conversion and liquid-layer-on-solid matrix. The samples being considered for this study are all whole rock samples and so no attempt will be made to test liquid preparation methods.

2.2.7 Thin Disk Preparation

An innovative sample preparation technique has been researched for use during the LASO-LIBS project, a method believed to have not been considered or mentioned previously within the LIBS research community. Thin Disk Preparation (TDP) will allow a single batch of material to undergo a range of analyses to allow for direct comparability. A thin disk section can be cut and scanned using LIBS, the disk can then be pulverised and the powder can undergo a wide range of analyses including XRD, XRF, powder LIBS, pellet LIBS and a range of other laboratory tests if desired. More information regarding the concept and implementation of the pioneering TDP is presented in section 3.5.

2.3 Current analytical techniques in the mining industry

Should the industrial viability of LIBS be proven, the quantitative analysis will have to be compared to a number of techniques which are presently used extensively within the industry. Currently many mining companies utilise external laboratories for such analyses, though there are a number of companies who house their own laboratory on-site. Often financial constraints limit smaller companies to using external laboratories. LIBS could potentially allow mining companies to complete more analysis on-site and rely less on external analytical companies for mine-critical data. Therefore, it is critical that LIBS first proves its viability in comparison with the current competition.

2.3.1 X-ray Fluorescence

Portable X-ray Fluorescence (XRF) devices analyse the elemental concentrations of sample surfaces, currently they are the most commonly used surface analysis device. In many mining and geology related applications the operator may prefer to understand sample mineralogy, and so the elemental analysis data must be processed. XRF devices theoretically have the ability to detect elements with atomic numbers above 4 (Beryllium), however in practice issues arise when the atomic number is below 12 (Magnesium), including Carbon and Lithium which may have large implications during processing or for the understanding of the orebody.

X-ray Fluorescence (XRF) involves exposing a sample to X-rays, causing the emission of secondary X-rays from a material. Detectors measure the secondary X-ray fluorescence; the fluorescence output data is then processed and the intensity of the waves are used to determine the element and concentration. XRF devices have become a popular choice for elemental and chemical analysis of samples throughout the mining industry (Xue, 2020), (Rakovsky, et al., 2014) and their popularity is in part due to the availability of both laboratory and field-ready XRF devices. A laboratory XRF machine can weigh 1300 kg and can measure 1-10 points per second (Xue, 2020), (Rakovsky, et al., 2014). On-line systems based on XRF or neutron activation have been used in feed control, however these systems have a relatively low throughput and rigid geometrical requirements (Bolger, 2000) which is problematic in industrial applications.

Commonly, portable LIBS devices are compared with handheld XRF machines which are a strong competitor to the LIBS technique (Rakovsky, et al., 2014). Rather than considering the pair as competitors, it is known that combining XRF and LIBS can be effective. However, handheld XRF devices are known to have poor to very poor accuracy and wide concentration differences for certain elements when measured with different XRF devices (Brand & Brand, 2014). Therefore, processing this data to reveal mineral composition is unreliable. Furthermore, XRF devices are proven to deteriorate over time, gradually displaying lower elemental concentrations, especially for elements with lower atomic numbers; Al and Si are the worst affected (Brand & Brand, 2014). Degradation of concentration readings can occur after as little as two months when the same sample is tested, using the same portable XRF device and under the same conditions.

2.3.2 X-ray diffraction (XRD)

XRD is a powerful, non-destructive analytical method for the determination of the atomic and molecular structure of crystalline substances. A sample is bombarded with X-rays generated in a cathode ray tube and accelerated using a voltage. Electrons in the sample absorb a portion of the energy and as excitation occurs inner shell electrons are dislodged and produce a characteristic X-ray spectra. The spectra produced are detected and reveal the crystalline phases present in the sample material, therefore identifying chemical composition information. Information can also be extracted regarding the average particle size, structures, phase ratios, crystallinity, stress and crystal defects. Like LIBS, the identification of phases is directly linked to the comparison of detected spectra to that of reference library data.

2.3.3 Near-Infrared Spectroscopy and Hyperspectral Imaging

Near Infrared Spectroscopy (NIRS) is becoming especially important in the latter stages of exploration as a technology to quickly and precisely map mineral deposits. One benefit to NIR is that it penetrates samples more deeply than mid-infrared radiation, however because of this, NIRS is a less sensitive technique compared to many. NIRS detects and analyses the NIR reflected from an irradiated sample, within the NIR region (700 – 2500 nm) (Harhira, et al.,

2017). Like LIBS, NIRS is a non-destructive and rapid technique which is useful in analysing bulk materials with little or no sample preparation. NIR Spectroscopy is used in the mining industry to analyse alteration minerals, since usually NIRS active minerals are formed by hydrothermal alteration (Dalm, et al., 2014). Conclusions regarding metal grades in ore bodies can be deciphered from the results of an NIR scan, it has been concluded that a negative correlation exists between the presence of NIR active minerals and copper grade (Dalm, et al., 2014). However, NIR Spectroscopy can only identify minerals which produce NIR active molecules and therefore this limits the technology to a specific niche within the mining industry.

Hyperspectral Imaging (HSI) was originally designed as a remote sensing technique and combined the advantages of NIR, rapid and non-destructive, with the possibility of analysing spatial relationships through imaging technology (Caporaso, et al., 2018). HSI has grown in popularity over the past three decades as the technology has evolved to become a reliable analytic tool for use in many applications including food processing, agriculture, eye care, astronomy and mineralogy. HSI involves the capture of multidimensional digital images; such images are in the form of ultraviolet or far infrared bands (Picon, et al., 2009). Hyperspectral imaging systems acquire images with millions of pixels and hundreds of narrow contiguous bands which can then be analysed, the information contained within HSI represents three dimensional data containing spatial distributions of material components (Caporaso, et al., 2018), (Ran, et al., 2017). Each pixel of the image is defined by different captured spectral components which form a vector (Picon, et al., 2009). The hyperspectral vector contains the colour information and chemical composition of the scanned materials. Imaging spectroscopy then determines material composition through the identification of spectral characteristics related to chemical bonds which can then be compared and analysed via a variety of different methods (Warner, et al., 2009). Ideally, for mineralogical identification, hyperspectral imaging systems should cover the visible to near infrared and shortwave infrared to thermal infrared spectral wavelengths (Warner, et al., 2009).

Since an entire spectrum is taken per pixel during HSI, no prior geological understanding of the sample in question is required, and post-processing allows for the entire spectrum data to be analysed. As a remote sensing technique HSI allows for detection from large distances, with analysis having been performed on HSI images from aircraft and satellites. In comparison with the aims of this thesis, HSI can scan a drill core box in 15 – 60 seconds, which is quicker than the LIBS device which can measure 1,000 points per second (Xue, 2020), making a drill core box scan approximately 5 minutes in at low resolution. However, in this instant, post-processing of the images may be highly time consuming to decide upon the optimal setup of conventional features and the optimal parameter values for specific datasets which may have different physical or visual properties (Ran, et al., 2017). The complexity of determining optimal parameters may limit the success of HSI; this is one reason why constructing a successful and more speedy calibration for LIBS could lead to an increase in popularity and usage. Furthermore, HSI equipment costs between €500,000 and €1,000,000 due to the number of components including high processing PCs, sensitive detectors and large storage requirements for spectral bands and metadata which are collected with each image (Xue, 2020).

2.3.4 Fire Assay

Fire Assay is one of the most commonly used analysis methods in precious metal mining and has been used for thousands of years to determine concentrations of precious metals within their ores. Gold, silver, PGMs, scraps/secondary metals are the most common materials which undergo fire assay analysis. Fire assay is generally more time-consuming but more reliable and accurate than instrumental analytical methods in most cases (TheIPMI, 2015). Sample preparation begins with milling, thoroughly mixing the fine powder with dry powder chemicals - this is then followed by crucible fusion which begins the collection stage. The collection step produces a glass like slag through a complex series of reactions and leads to the formation of a precious metal-bearing alloy, commonly Pb. Often other metals and compounds are sometimes required as collectors for PGMs during fire assay. The lead alloy is then separated and the lead removed through cupellation leaving behind a precious metal bead which can be weighed. The precious metal bead can then be further analysed using instrumental methods (TheIPMI, 2015).

The key issues with fire assay include the time-consuming sample preparation steps, the potential complexity of the reactions and the addition and removal of various metals. It should be noted that analysis of the solutions and compounds is often required for confirmation alongside the fire assay results anyhow. LIBS is aiming to complete an analysis with similar reliability and accuracy as fire assay, but in much shorter time scales and in environments outside the laboratory.

2.3.5 Wet Chemistry methods

Wet chemistry analysis are commonly used for the measurements of minerals in higher concentrations (>5%). In the higher concentration range wet chemistry displays superior precision and accuracy when compared to instrumental methods. Samples must undergo a number of preparation steps and must be either liquid to begin with or if not dissolved in solution. The addition of various chemicals allows for selective separation of elements in the liquid state.

2.3.5.1 Gravitational analysis by precipitation

Gravimetric analysis by precipitation is the most commonly used wet chemistry method for analysing precious metals. Initially a sample is dissolved in solution, then a specific chemical or set of chemicals is added to the solution depending upon which minerals and elements are present in the sample. Precipitation of compounds will occur as specific reactions take place within the combined sample and reactant solution. The precipitate is then filtered, washed, dried and weighed to give an accurate value for precious metal content by comparing the metal weight to the total original sample weight. Gravimetric analysis can require multiple steps to separate various elements in complex samples, and therefore many mines may prefer alternative methods. However, gravimetric analysis is chosen over instrumental analysis for precious metal percentages over 5% when absolutely accuracy is required, however the trade-

off is often time and money (TheIPMI, 2015).

2.3.5.2 Titration

Another form of wet chemistry is titration, which involves the addition of liquid reagent, the titrant, of known chemical concentration to the analyte of unknown concentration. The titrant and analyte react, a colour change occurs, at which point no more titrant is added. The total volume of titrant added by the time of the colour change is termed the 'titration volume' and is used to determine the total precious metal content within the analyte solution.

Both titration and gravimetric analysis by precipitation are relatively time consuming processes and both require chemicals which may either be harmful, expensive or present storage difficulties. Mining companies often use external companies to complete wet chemistry analysis, however this comes at an increased cost and can potentially delay production should analysis take some time (Harhira, et al., 2017), (Rifai, et al., 2017), (Khajehzadeh, 2018). As discussed in section 1.5, the increased cost and potential delay or inaccurate assumptions made during production necessitates a rapid on-line, on-site analytical technique, such as LIBS.

2.3.6 Atomic Spectroscopy

Atomic spectroscopy techniques can be separated into two fields, absorption and emission. During absorption techniques, specific wavelengths of light are absorbed and in emission techniques the analyte emits light. In both cases the spectra can be analysed to determine elemental compositions. During absorption, atoms are excited to higher energy levels whereas during emission, electrons are moved to lower energy levels.

2.3.6.1 Atomic Absorption Spectroscopy (AAS)

AAS uses the variation in optical light absorption by free atoms to determine elemental composition. A radiation source is required and can be a hollow-cathode lamp, electrode-less discharge lamp, vapour discharge lamp or a high-intensity hollow-cathode lamp (Van Loon, 1980). An atomisation system is also required to convert a solid or liquid analyte into free ground-state atoms. No atomising systems appear to challenge the flame as the most generally useful atomiser for use in AAS, despite the flame being the least understood component of atomic absorption equipment (Van Loon, 1980). As light is passed through the flame containing a small amount of analyte, the flame absorbs a certain portion of the light spectra - the unabsorbed spectra are unique to corresponding materials. The intensity of the peak produced is equivalent to the relative abundance of the specific material within the sample. Through data processing the peaks and intensities can be compared to the peaks produced from a set of known standard samples to ascertain the sample chemistry (TheIPMI, 2015).

AAS requires the sample to be in solution which for the analysis of gold, for example, can be difficult due to the corrosive acids which are required. Analysis also requires multiple steps of addition of various acids, evaporation, dissolution and separation. The detection limits for AAS

analysis of gold are 1 ppm. Furthermore, AAS cannot detect all elements. Approximately 70 elements are detectable via this method, but there are issues with key elements such as sulphur, fluorine, nitrogen, phosphorous or carbon and if present in concentrations over a certain threshold, special treatment is required before analysis (Van Loon, 1980). AAS is commonly used throughout the mining industry and is effective when the correct procedures are followed and when the technique is employed appropriately. However, it is important to consider other analytical techniques alongside AAS.

2.3.6.2 Atomic Emission Spectroscopy (AES)

AES analyses the wavelength of light emitted by a sample during excitation, therefore, LIBS falls into this category. Excitation occurs through either the presence of a flame, inductively coupled plasma (ICP) or spark and arc, in the case of LIBS, the excitation source is a laser pulse. The atoms transfer between an excited state and return to their ground state, during which time light is emitted as photons. The light spectra produced by each material is unique and therefore can be measured, compared and an elemental composition determined.

ICP-AES is a commonly used analytical technique within the AES group; ICP-AES uses a plasma flame, which can reach temperatures between 6,000- and 10,000-degrees kelvin, which is controlled by a plasma coil (TheIPMI, 2015). A sample can enter a flame as a gas, as a sprayed solution or as a solid. The heat from the flame creates free atoms, the ICP excites the atoms which emit electromagnetic radiation unique to the present element. ICP-AES allows for multi-elemental analysis, low interference, high reproducibility and has excellent limit detections. Spark and arc are methods used for metal analysis in conductive solid samples, if the sample is not naturally conductive then graphite is added. An electric arc or spark is passed through the sample which excites the atom and causes light to be emitted which can be analysed using a monochromator.

Atomic emission techniques tend to be expensive both in capital cost and operating cost. The potential for multiple emission lines and spectral interferences, and so, samples have to be carefully prepared as a solution. LIBS however offers the potential for both lowered costs and lower interferences and therefore potentially offering a more beneficial technique.

2.4 Kittilä Introduction

2.4.1 Geology of Kittilä

The Suurikuusikko gold deposit is the largest of many epigenetic gold deposits located within the Paleoproterozoic Central Lapland Greenstone Belt (CLGB); a part of the Karelian craton, which itself is a section of the Ferroscandian Shield (Wyche, et al., 2015). Hanski and Huhma 2005 comment on the controversial nature of many findings when determining the precise age of many CLGB formations and therefore the conclusions drawn when considering inter-relations internally and externally to the CLGB stratigraphy (Hanski & Huhma, 2005). Further contradictions have been made as Lehtonen, et al., 1998 considers the Salla group to be the eastern-most section of the CLGB while Nironen, et al., 2002 consider the same group to be

the northern extent of the Kuusamo belt. Two 2015 studies, Wyche, et al., 2015 and Niiranen, et al., 2015 have contradicted the separate nature of the CLGB and the Kuusamo belt by suggesting that they are combined into one entity. The stratigraphy of the CLGB remains an open topic of discussion with different research providing different successions and varying lateral extents. The region is poorly exposed and so exploration and research data has mostly been provided by geotechnical and geochemical data, leaving ample room for a range of interpretations to be drawn. Direct observation is limited to diamond drilling and trenches which commonly only allow for direct observation to occur to the first few hundred metres depth (Niiranen, 2015).

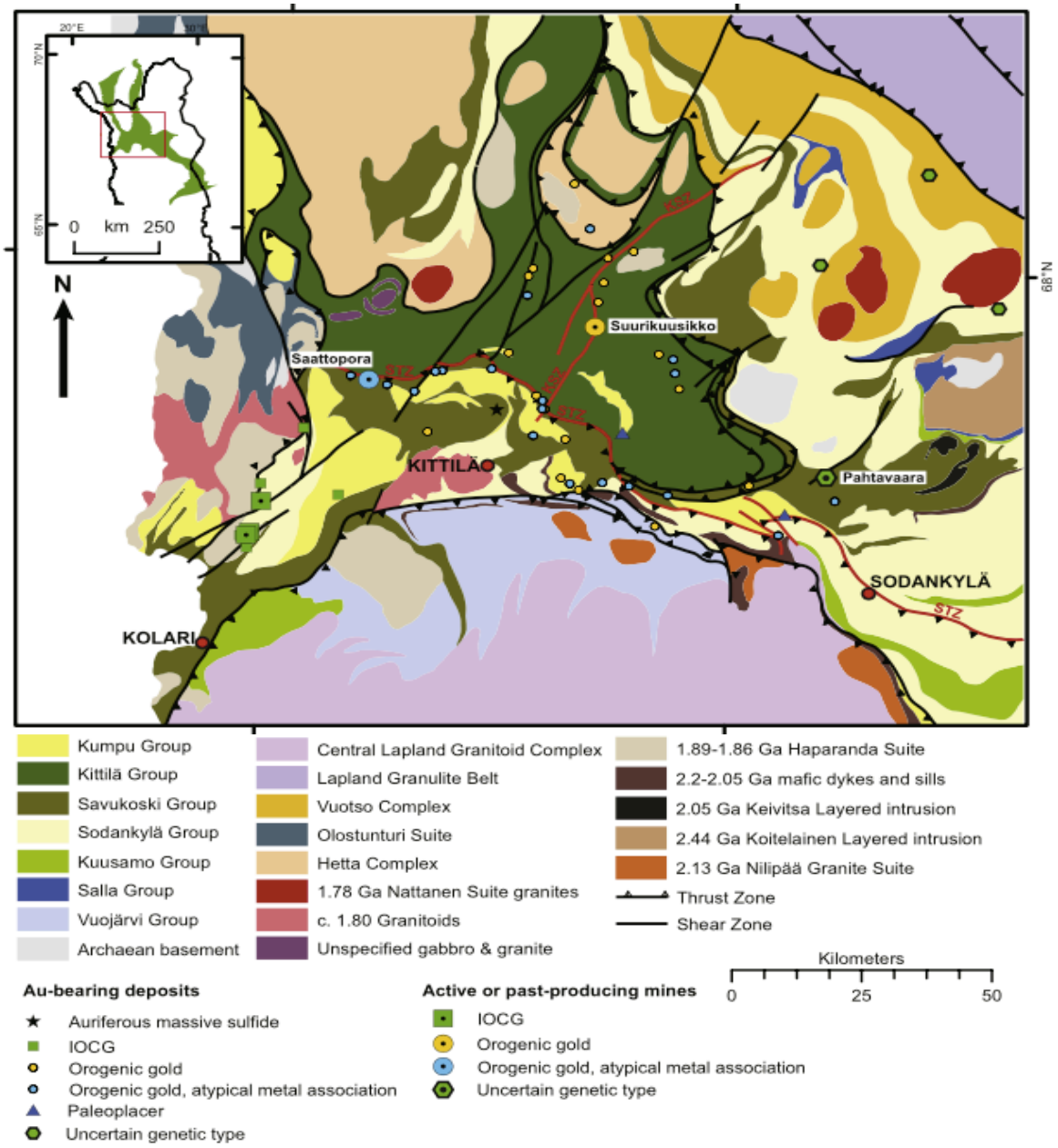

Figure 3: Taken from Wyche, et al., 2015. Regional geological map of central Lapland with the locations of deposits and mines within the region. The localities of the seven lithological groups are shown. KSZ = Kiistala shear zone, STZ = Sirkka thrust zone.

The supracrustal stratigraphy is most commonly subdivided into a set of either five or seven key units which overlie the Archaean basement. The five groups in order from oldest to youngest, the unit groups are: Salla, Onkamo, Sodankylä, Savukoski, Kittilä and the most recent, the Kumpu group which can then be divided into the Lainio and Kumpu groups (Lehtonen, et al., 1998), (Hanski & Huhma, 2005). Wyche, et al., 2015 and Niiranen, et al., 2015 split the stratigraphy into seven units, with the addition of the Vuojärvi group and the Kuusamo group between the Salla and Sodankylä groups and the omission of the Onkamo group all together. The regional geological map produced by Wyche, et al., 2015 is shown in figure 3, including the location of the study area and extent of the CLGB.

The succession represents a major marine regression dominated by poly-folded metamorphic rocks including schists, tuffites, phyllites, and mafic and ultramafic metavolcanics which have undergone three major deformation phases (Boliden, 2018). The CLGB formed as a result of multistage rifting between 2.44 and 2.0 Ga, followed by multiphase compressive and metamorphic events caused by the Svecofennian orogeny between 1.91 and 1.79 Ga. The CLGB can be divided into two units, the Karelian (2.44 – 2.0 Ga) metamorphosed volcaniclastic sequence and the Svecofennian sequence (1.89 – 1.77 Ga) of metasediments which are bound by various igneous intrusion complexes (Niiranen, et al., 2015). Following the rifting, compressing and metamorphosing stages, intrusive granites and migmatites occurred in an igneous phase causing extensive contact metamorphism and then creation of more metamorphic bodies 1.8 Ga (Niiranen, et al., 2015).

The Salla group comprise metamorphosed intermediate and felsic volcanic rocks, ranging from basaltic andesite to rhyolite with a silica content remaining mostly between 54 – 70% (Hanski & Huhma, 2005). The Salla group shares tectonic contacts with all bordering units including the Vuojärvi group of schists and gneisses, of which little is known (Niiranen, et al., 2015), (Lehtonen, et al., 1998). Both the Vuojärvi and the Salla groups are overlain by the laterally extensive but discontinuous Onkamo group. The Onkamo group lithologies are comprised of predominantly subaerial amygdaloidal mafic to intermediate volcanics and breccias (Hanski & Huhma, 2005). In some localities the Onkamo group is formed of submarine deposited continental and oceanic island arc ultramafic basalts and tuffs and subaerial which in some areas are deposited directly onto the Archean basement (Lehtonen, et al., 1998), (Hanski & Huhma, 2005). Lehtonen, et al., 1998 express some ambiguity of potential depositional environments for the Onkamo and the expansivity, it appears that the topic is still up for debate with subsequent papers being confidently opposing of others in the succeeding years.

The Salla and Onkamo groups represent a seismically active period with extensive rifting and vulcanism. A quieter period followed as the thick epiclastic sedimentary Sodankylä group of quartzites, meta-arkoses and minor mafic metavolcanics were deposited during basin extension (Wyche, et al., 2015), (Niiranen, et al., 2015), (Lehtonen, et al., 1998). Sedimentary structures observed within the Sodankylä group suggest various depositional environments in each sub-unit of the group with formations providing evidence of deposition within a shallow basin. Sedimentary structure including cross bedding, graded bedding herringbone structures and mud cracks all suggest that the environment was impacted by tidal waves and areas which were

subaerially exposed for periods (Lehtonen, et al., 1998), (Nikula, 1988). The Onkamo and Sodankylä groups were deposited between 2.2 – 2.44 Ga; at the commencement of Onkamo deposition (2.44 Ga) (Wyche, et al., 2015) the Koitaleinen layered intrusion penetrated the stratigraphy which indicates a period of regional extension and plate thinning.

In the period 2.05 – 2.2 Ga, the deposition of Savukoski metasediments occurred, including: phyllite, graphite- and sulphide-bearing schists, metatuffites (Niiranen, et al., 2015), (Hanski & Huhma, 2005). No hiatus has been observed suggesting a gradual increase in volcanic activity filling the deepening basin with tholeiitic lavas and tuffites (Wyche, et al., 2015), (Niiranen, et al., 2015), (Lehtonen, et al., 1998). The deposition of the Savukoski unit was coupled with the east – west trending intrusion of mafic sills and dykes in 2.2 Ga followed by mafic to felsic dyke intrusion 2.1 Ga (Niiranen, et al., 2015), also within the deposition period was the intrusion of the Kevitsa layered intrusion 2.05 Ga and the 2.13 Ga Rantavaara gabbros (Lehtonen, et al., 1998). The stratigraphically highest rocks in the Savukoski are komatiitic and picritic metavolcanics which represent a further period of rifting within the basin, before the deposition of the Kittilä group 2.02 Ga (Wyche, et al., 2015). The stratigraphically highest unit is the Kumpu, deposited since 1.89 Ga, defined by immature sedimentary and volcanic clastic rocks deposited during a period of continental collision (Wyche, et al., 2015).

The Koitaleinen and Kevitsa layered intrusions, as well as the mafic sills and dykes represent repeated rifting within the depositional basin. Syn-extensional magmatism occurred in multiple phases during the rifting periods, three granitoid units represent different phases of the regional extension the; (a) 2.13 felsic Nilipää suite; (b) the most voluminous intrusive rocks in the region, the 1.91 – 1.86 Ga calcalkaline felsic to mafic Haparanda suite and; (c) the 1.79 – 1.77 Ga Nattanen granites. The Nilipää suite was intruded during the initial extensional phase, the Haparanda suits represents syn- and late collisional intrusives and the youngest intrusions (Nilipää) are post-collisional (Wyche, et al., 2015).

2.4.2 Kittilä group geology

The Kittilä group is observed as a succession of shallow to deep marine meta-sedimentary rocks and tholeiitic metavolcanics with cross-cutting felsic porphyry dykes deposited around 2.02 Ga (Wyche, et al., 2015), (Niiranen, et al., 2015), (Lehtonen, et al., 1998). Though the metavolcanic rocks of the Kittilä group are thought to be genetically unrelated, and there are carbonate and banded-iron formation lithologies present (Hanski & Huhma, 2005). As one of the largest mafic metavolcanic accumulations in the Ferroscandian Shield, the folded volcanic pile can reach 6 km in vertical section and covers 2600 km^2 (Lehtonen, et al., 1998), (Hanski & Huhma, 2005). The Kittilä group represents a period of increased syn- and/or post-extensional volcanic activity in the area with two major magmatic stages (Lehtonen, et al., 1998). The Kittilä group has also been termed the Kittilä terrane due to the characterisation of the stratigraphy to be of ophiolitic and oceanic origin. Hanski, et al., 1997 interpreted the north trending Nuttio serpentine belt, located to the east of the Kittilä group, as ophiolite fragments. The metavolcanic rocks of the Kittilä group were further interpreted and have since been researched and supported (Niiranen, et al., 2015), (Lehtonen, et al., 1998), (Hanski & Huhma,

2005), (Niiranen, 2015), to be an allochronous unit which is in part of oceanic origin and are penecontemporaneous with the 2 Ga thrusted ophiolite (Hanski, et al., 1997). An unconformable tectonic contact with enclosed serpentine lenses separates the Kittilä group from Savukoski and Sodankylä groups below (Niiranen, et al., 2015), potentially implying a collisional event including micro-continents or an island-arc (Lehtonen, et al., 1998).

The Kittilä group is comprised of four units, from oldest to youngest they are the Kautoselkä, Porkonen, Vesmajärvi and the Pyhäjärvi formations (Wyche, et al., 2015), (Lehtonen, et al., 1998). A small sample set of the Kittilä formations has been magnetically analysed and the retrieved data has been used and extrapolated to determine the lateral extent of each formation (Wyche, et al., 2015). The oldest, Kautoselkä, group is defined by iron-rich tholeiitic amygdaloidal lavas, tuffs and tuffites erupted in a submarine environment (Lehtonen, et al., 1998), (Hanski & Huhma, 2005) interpreted as the mafic formation with increased magnetic responses (Wyche, et al., 2015). The Kautoselkä group also exhibits evidence of a sub-continental lithospheric mantle source or the crustal contamination of a depleted mantle (Hanski & Huhma, 2005). The Porkonen formation hosts the banded-iron formations as well as oxides and carbonates, the formation is known to have mixed packages of conductive and magnetic rocks (Wyche, et al., 2015). The Vesmajärvi formation consists of submarine deposited tholeiitic metavolcanic rocks including pillow lavas, pillow breccias and hyaloclastites with associated gabbroic sills and co-genetic dykes (Hanski & Huhma, 2005). Geochemical analysis of the tholeiites indicate a depleted mantle source with no crustal contamination (Hanski & Huhma, 2005), (Wyche, et al., 2015). Magnetic signals from the Vesmajärvi formation are weaker than those from the Kautoselkä formation and so can be easily distinguished through aeromagnetic survey (Wyche, et al., 2015). The youngest Kittilä formation is the Pyhäjärvi which is dominated by sedimentary schists and sericite quartzites (Lehtonen, et al., 1998), (Niiranen, 2015).

2.4.3 Suurikuusikko area and ore deposit

The world class Suurikuusikko gold deposit is found within the Kittilä stratigraphic unit, the deposit is found centrally within the Kittilä unit, approximately 15 km south-southeast of the thickest section. The stratigraphy dips moderately to the northeast but exhibits open folding, the dip increases as the proximity to the Kiistala shear zone (KSZ) increases (Wyche, et al., 2015). The KSZ, also known as the KiTZ (Kiistala Thrust Zone) is the deposit hosting structure. The KSZ hosts a structural framework which allowed for the formation of sizeable hydrothermal regions to become Au-enriched (Niiranen, 2015). The estimated dip/dip direction is 80/090 and while the dip direction varies moderately along the length, the dip remains constantly steep (Wyche, et al., 2015). The deposit rock also varies and contains pillow lavas, volcaniclastic breccias, thick mafic lava packages and a heterogeneous package between lava-dominated stratigraphy which has been deformed and altered. Volcaniclastics, intermediate to felsic rocks, graphitic sedimentary intercalations with chert, mafic rocks, sulphide-rich sediments and argillite claystones are found within the heterogeneous unit (Wyche, et al., 2015). Uneconomic appearances of increased gold concentration occur along stratigraphic contacts as shoots from the central deposit where alteration and fluid flow has transported and

redeposited minor gold traces as fine layers within the unmineralised mafic lavas (Wyche, et al., 2015).

The gold is hosted within mineralised portions of the deposit body. The mineralised rocks have been formed through pervasive albite alteration and quartz-carbonate veining through the introduction of hydrothermal fluids. Heavy fracturing has formed breccias which have a hydrothermal quartz-carbonate matrix (Wyche, et al., 2015). Further examples of mineralised rock within the deposit include a range of reworked minerals including carbon within schists and volcaniclastic sediments. However, sedimentary units rarely host more than minimal mineralisation and later stage sheared rocks remain fractured and have not been healed through this process (Wyche, et al., 2015).

2.4.4 Kittilä Gold Mine

Gold was originally discovered in a road cutting 4 km south-southwest of Suurikuusikko during an exploration study by the Geological Survey of Finland (GTK) in 1986 (Wyche, et al., 2015). The mine is located 860 km north of Helsinki, 320 km north of Oulu and 150 km north of the Arctic Circle. Agnico Eagle have owned and run the 237 km^2 Kittilä mine site which encapsulates 25 km of the gold-bearing Suurikuusikko Trend, since the purchase in 2005 (Agnico Eagle, 2020). Mining began with an open pit in 2009 and underground mining commenced the following year using open stoping and delayed backfill. Now Kittilä is the largest primary gold producer in Europe (Agnico Eagle, 2020).

The Suurikuusikko gold deposit boasts proven and probable reserves totalling 21.6 Mt of ore with an average grade of 2.83 g/t Au, amounting to 4.5 Moz of gold. In addition to this there are 18.2 Moz of gold with an average grade of 1.32 g/t in measured and indicated resources (Agnico Eagle, 2019). Annual production is growing due to an expansion plan which began in 2018, In 2018 production was 188,979 oz of gold, then in 2019 204,165 oz and in 2020 it is expected that 215,000 oz will be produced (Agnico Eagle, 2020). The gold is refractory, being hosted within arsenopyrite and pyrite, and associated with carbonate-albite-sulphide alteration, some of the gold may be present as extremely fine free gold grains in pyrite (Agnico Eagle, 2020), (Wyche, et al., 2015). The majority of the gold is found within the structure of arsenopyrite (73.2%), with 22.7% occurring in pyrite and 4.1% is present as free gold which tends to occur in the outer, eroded and oxidised edges of the minerals (Kojonen & Johanson, 1999). Thus far, mining work has focussed on a 4.5 km stretch of the Suurikuusikko Trend which hosts the six zones of the reserves and resources, they are: Etela, Ketola, Roura, Rimpi, Sisar and Suuri zones (Agnico Eagle, 2020).

Due to the arsenopyrite hosting of gold, some issues may be faced during processing and tailings disposal, to aid the processing of the refractory ore an autoclave (pressure oxidation circuit) is used. Currently 5,000 tonnes of ore per day are fed through the processing plant, the is processed by: crushing and grinding, floatation, pressure oxidation and carbon-in-leach circuits (Agnico Eagle, 2020). Agnico Eagle expect to maintain an 86% gold recovery over the 17-year life span of the mine, and through a processing plant expansion it is expected that

annual throughput will increase from 1.6 million tonnes to 2.0 million tonnes per year (Agnico Eagle, 2020).

Exploration also continues to occur across the mine site, focussing on extending the current Rimpi and Roura zones. There is also budget set aside to explore the potential of the Sisar Top Zone and the Rimpi Deep to forge a new mining horizon. Money has been identified to pay for exploration drilling outside of the mining licence area to assess any potential need to extend the licence area in the near future (Agnico Eagle, 2020). Due to the volume of exploration drilling which takes place each year within the Kittilä mine site, it is crucial that an efficient and rapid mineralogical analysis technique can be devised which is both time and cost-effective for the benefit of the mining company.

3 Methods and Materials

3.1 LIBS prototype set-up

In this section the equipment and materials used to complete each analysis are discussed and explained. The methodologies used throughout the experimental phases are outlined, any preliminary testing and modifications to procedures are mentioned and justified. The current LASO-LIBS prototype resides in a laboratory at Aalto University. The prototype, and any future device, is reliant on 4 components; a high repetition rate laser source, 2 broadband (UV to NIR) spectrometers an auto-focus system and high performance linear actuators.

A computer-controlled measurement head moves the LIBS scanning equipment over the samples which lie below, the carrier can be programmed to run a movement programme automatically. The prototype casing dimensions are 120 x 70 x 40 cm, sufficiently sized to house a drill core box, the LIBS measurement head is housed in a 10 x 10 x 20 cm capsule and moves along runners connected to the outer frame. A conventional power source provides sufficient power for the device, and so no special modifications are required. Currently the device is in a commercialisation phase and so no images can be presented, technical details will be released at a later date.

Samples of all geometries can be measured using the automated set-up. Once a measurement area is written the carrier will follow the programme, while simultaneously the LIBS equipment follows a separate measurement programme. The LIBS equipment can be programmed to produce laser shots at varying time or distance intervals and to fire multiple laser shots in a single spot, depending upon the desire of the user. The carrier can move up to 0.5 m/s, allowing for rapid scanning of a drill core box, the programme can also be slowed down to produce highly-detailed scans of smaller samples. The carrier can be slowed to a pace more suitable for the scanning of a pelletised sample with a diameter of 10 mm or smaller. The autofocus system installed in the current set-up allows for a wider range of sample geometries to be analysed without concerns about surface roughness and allows for whole rocks to be analysed without the need for levelling, slicing or pulverising.

The laser induced plasma which is critical in LIBS analysis is produced by a high-performance Q-switched diode pumped laser. The design of the laser is compatible with LIBS measurements and provides high pulse repetition rates, short pulse durations and high pulse to pulse stability, therefore making it well suited.

Two spectrometers are used in this set-up to ensure the possibility of all elements being measured. Each spectrometer contains two important parts, the first is the spectrograph, an optical system where light is split, the second part is the detector which measures wavelength signal intensities. Both spectrometers within the set-up use complementary metal oxide semiconductor (CMOS) detectors to monitor and record signals. Both spectrometers being used are designed specifically for use in plasma measurements and LIBS applications. Utilising CMOS linear image sensors, one spectrometer measures UV light within the 200 – 400 nm band, the second spectrometer measures visible light between 350 nm and 950 nm. The 50 nm overlapping spectral range between the two spectrometers is useful to make comparisons between measurement points within that area. Each spectrometer is capable of 218,000 counts/μW per ms integration time and the 4096 pixels produce a resolution of <0.2 nm (Avantes, 2020).

The LIBS device is set-up with an auto-focus system which allows for the direct analysis of whole rock samples and samples with uneven surfaces ranging up to 70 mm difference between the physically highest and lowest points. This offers a great advantage in saved time and therefore increased throughput when compared to analytical techniques such as Scanning Electron Microscopy (SEM). SEM sample preparation requires samples to be ground and polished until the sample surface is flat and without scratches when viewed under an optical microscope.

3.2 Reference library development

Building the initial reference collection has included the analysis of 67 mineralogical reference samples (see table 1) which have undergone XRD, TXRF and LIBS analysis. The composition of each has been determined and the data has been presented to the algorithms for analysis in further scans. XRD analysis for mineralogical samples was completed off-site by an Stenman Minerals who analysed the <20 μm mineral powders using synchrotron X-ray Diffraction (XRD) and Rietveld analysis. The same analysis method will be applied to the Kittilä powder and thin disk samples later in the project. All LIBS and TXRF analyses were completed at Aalto University laboratories located in the Civil Engineering building using a PicoTax multi-elemental total reflection X-ray fluorescence (TXRF) spectrometer.

Reference collection information draws from standard samples of both elements and minerals which have been analysed previously. The algorithm can be focussed with the addition of data determined from site-specific samples to the reference collection. With the addition of focussed information specific to the exact samples to be scanned en masse, the quality of the LIBS analysis can be improved.

3.3 Mineralogical samples

Table 1: List of mineralogical samples analysed by XRD, LIBS and TXRF with the pure-form chemical formula.

Mineral	Formula	Mineral	Formula	Mineral	Formula
Adularia	$K_4Al_4Si_{12}O_{32}$	Galena	PbS	Quartz (x5)	SiO_2
Aegirine (x2)	$NaFeSi_2O_6$	Gypsum	$CaSO_4 \cdot 2H_2O$	Sapphirine	$(Mg,Al)_8(Al,Si)_6O_{20}$
Albite	$NaAlSi_3O_8$	Hematite	Fe_2O_3	Scapolite (x2)	$Ca_4(Al_2Si_2O_8)_3(CO_3,SO_4)$
Almandine	$Fe_3Al_2Si_3O_{12}$	Hornblende	$(Ca,Na)_{2-3}(Mg,Fe,Al)_5(Al,Si)_8O_{22}(OH,F)_2$	Sphene	$CaTiSiO_5$
Andalusite	Al_2SiO_5	Hydroxyapatite	$Ca_5(PO_4)_3(OH)$	Spodumene	$LiAl(SiO_3)_2$
Arsenopyrite	$FeAs_2$	Hypersthene	$(Mg,Fe)SiO_3$	Staurolite	$(Fe,Mg)_2Al_9Si_4O_{23}(OH)$
Augite	$(Ca,Na)(Mg,Fe,Al,Ti)(Si,Al)_2O_6$	Ilmenite	$FeTiO_3$	Stibnite	Sb_2S_3
Baryte (x2)	$BaSO_4$	Kyanite (x2)	Al_2SiO_5	Sulphur	S
Beryl	$Be_3Al_2Si_6O_{18}$	Lepidolite	$K(Li,Al)_3(Al,Si,Rb)_4O_{10}(F,OH)_2$	Talc	$Mg_3Si_4O_{10}(OH)_2$
Bismuth	Bi	Magnesite	$MgCO_3$	Mn-Tantalite	$MnTa_2O_6$
Chlorite	$(Mg,Fe)_3(Si,Al)_4O_{10}(OH)_2 \cdot (Mg,Fe)_3(OH)_6$	Magnetite	Fe_3O_4	Topaz	$Al_2SiO_4(F,OH)_2$
Clinopyroxene	$(Mg,Fe,Al,Ti)(Ca,Na,Fe,Mg)(Si,Al)_2O_6$	Microcline (x3)	$K(AlSi_3O_8)$	Tourmaline	$(Ca,K,Na,)(Al,Fe,Li,Mg,Mn)_3(Al,Cr,Fe,V)_6(BO3)_3(Si,Al,B)6O_{18}(OH,F)_4$
Columbite	$(Fe,Mn)Nb_2O_6$	Monazite	$(Ce,La,Nd,Th)PO_4$	Tourmaline Schorl	$NaFe_3Al_6(BO_3)_3Si_6O_{18}(OH)_4$
Cordierite (x2)	$(Mg,Fe)_2Al_4Si_5O_{18}$	Muscovite	$KAl_2(Si_3AlO_{10})(OH)_2$	Tremolite	$Ca_2(Mg_{4.5}Fe_{0.5})Si_8O_2(OH)_2$
Cr-Diopside	$MgCaSi_2O_6$	Olivine	$(Mg,Fe)_2SiO_4$	Wollastonite	$CaSiO_3$
Epidote	$Ca_2(Al_2,Fe)(SiO_4)(Si_2O_7)O(OH)$	Orthoclase	$KAlSi_3O_8$	Zircon	$Zr(SiO_4)$
Fluorapatite (x2)	$Ca_5(PO_4)_3F$	Phlogopite	$KMg_3AlSi_3O_{10}(F,OH)_2$		
Fluorite	CaF_2	Plagioclase (x2)	$NaAlSi_3O_8$-$CaAl_2Si_2O_8$	Total	67

In addition to the mineralogical samples, 37 certified standard elemental samples were obtained and analysed using the LIBS device. Since the exact composition of the 'pure' (>99%) elemental samples is known previously, the data collected from LIBS should display only the single element as being present. The data collected from the minerals and standard samples are then stored in the reference library and can be utilised by the algorithm. The LIBS elemental data can be used in subsequent scans allowing LIBS analysis to more accurately detect the specific elements in unknown samples.

3.4 New sample preparation method – Thin Disk Preparation

In this section a pioneering new sample preparation technique is outlined, utilising thin disks of sample material which were then prepared and analysed. Currently unknown in the field of LIBS sample preparation is the Thin Disk Preparation (TDP) approach for the production of reliable and site-specific calibration data to aid LIBS data processing. At the time of writing, it is believed that no published research papers have discussed the potential of using thin disk preparation to aid the development of reference libraries for LIBS. This study represents the first usage and initial method explanation. The theory behind TDP is outlined in section 2.2.7. The experimental methodology used to achieve the results published in this thesis shall be described in section 3.4.1.

TDP allows a single sample to be analysed in multiple states (see figure 4) allowing for the direct comparison between various sample preparation techniques using identical material. TDP also combines whole rock analysis with pellet and powder LIBS analysis to allow for calibrations, error margins and analytical precision. Pelletization is a frequently employed technique throughout the industry and has been used during this study. Through a series of analyses and simple sample preparation methods undertaken with exact identical sample material, resulting data can be input into the LIBS data analysis system for site-specific calibration. Avoiding contamination is critical to establish that the sample material is identical to that analysed in the previous stage, making data comparison simple and effective. During the work for this thesis, the thin disk material also underwent XRD analysis to further improve the accuracy and reliability of results further.

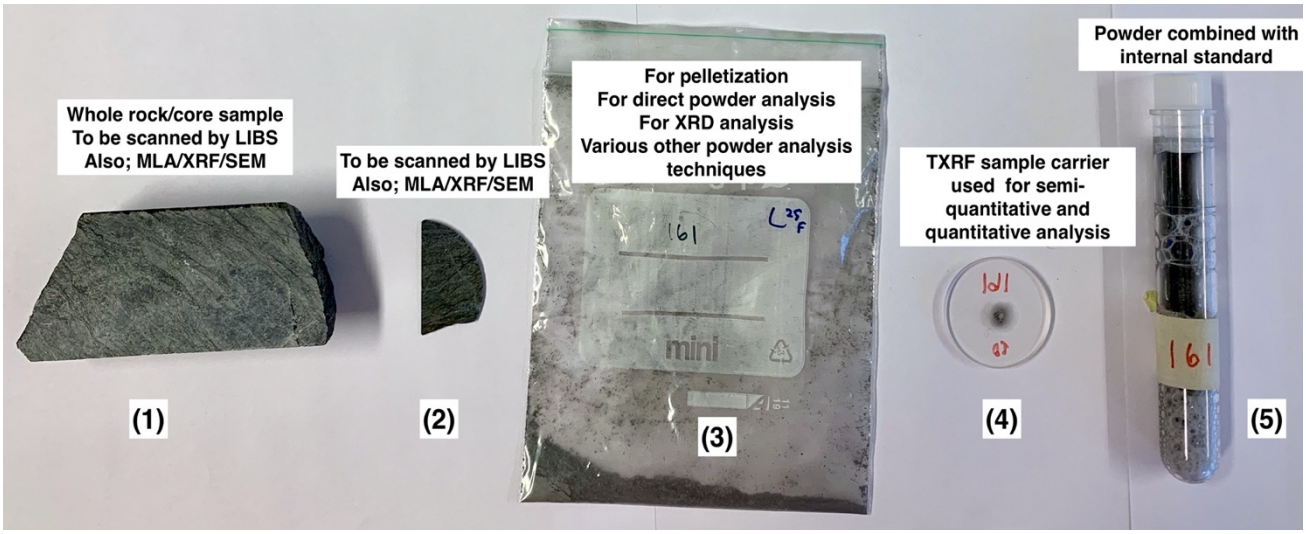

Figure 4: : The sample life of a single thin disk. Left to Right; (1) Core rock, (2) Thin Disk, (3) Powdered thin disk, (4) Semi-quantitative analysis by TXRF, (5) Solution of sample and internal standard for quantitative analysis by TXRF.

Whether a desired analyte is whole rock, or in pellet or powdered form, LIBS will be able to successfully analyse the elemental and mineralogical compositions using the data collected from the calibration steps achieved using TDP. Using both powdered and pelletised samples

allows the original sample to be analysed homogeneously, producing data regarding the overall average mineralogy and elemental composition. Thin disk analysis will also produce data regarding the spatial relationships of elements and minerals within the original heterogeneous sample, allowing mineral maps to be created using the data and providing useful insight. The ability to analyse mineralogical spatial relationships is especially important in samples which are particularly heterogeneous. Spatial data is vital for understanding sample types, for example those which may contain large inclusions or banding, for example in layers of paint or in coarse grained rock samples. Furthermore, surface mapping is important for ores in which gold may appear as nuggets, therefore affecting the average mineralogy despite only being found in small, high grade sample areas.

TDP begins with the coring of a comparable sample to those which are the desired analyte and in the case of mining, this is likely to be an ore rock from a similar location. If necessary, material from the desired analyte can be used to produce the thin disks if there is a sufficient quantity of sample material. The core material is cut finely and then a grinder is used to thin the core disks until a thickness where individual grains or fine geological structures can be identified from both sides. The optimal thickness of each disk is related to the grain size of the sample in question, the larger the grain size, the thicker the disk can be while maintaining suitable resemblance on either side. When the surfaces of each side of the disk become indistinguishable, the disk can be analysed using LIBS on each side creating two datasets containing spatial and compositional data. Data from each disk face should be analogous so that the datasets can be combined to create an average composition for the entire disk. In the case of the Kittilä disks, an average thickness of 0.5 – 1 mm was achieved. However, in the case of the Kittilä samples, thickness was constrained by certain geological features such as finely bedded, highly brittle, graphite layers which typically sheared as a host-disk became thinner. Therefore, it was necessary to prepare disks to a slightly thicker dimension than initially desired.

Thin disks underwent LIBS analysis as a sliced section and were subsequently pulverised for analysis by XRD, as a powder and as a pressed pellet relatively simply and cheaply. If desired, it would also be possible to add a multitude of alternative analyses at various stages of the thin disk lifespan. Following the scanning of the thin disks, if one side of the disk is polished then the sample can proceed to Mineral Liberation Analysis (MLA) if desired. MLA would provide useful data on the sample grain size, mineral associations (liberations and locking), particle density and shape factors as well as providing another useful comparative measure of composition. A polished thin disk section would also be appropriate for Scanning Electron Microscopy (SEM) which can provide data on the elemental composition and spatial relationships of the sample surface also. Upon the completion of all desired intermediate steps using the thin disks, the samples can be milled and undergo powdered analysis using adhesives, and then pelletization, both of which are described earlier in this section.

Following the completion of a number of intermediate alternative analyses, the data collected can be input into the LIBS algorithms. The samples selected must be representative and contain all facies present so that data can be collected on all elements within the sample. The data is

then used to increase the reference library leading to improved accuracy and reliability when a LIBS scan is completed on the bulk material.

3.4.1 Implementation of thin disk preparation

For this study, chemical data from the Kittilä laboratory which corresponds to the core-halves was analysed. Therefore, a relatively clear idea of the composition of each core is known, from this data, a selection of 40 samples were selected. The Kittilä core boxes totalled 71.1 m, 40 samples is the equivalent to one per every 1.78 m of core, so it was concluded that it would be more beneficial to individually select samples on their potential data-providing benefit, rather than on a predetermined distance interval. Determination factors included the relative abundance (high or low) of key ore minerals, the presence (or lack of) specific elements and the overall combination of elements present in each sample. Samples showing both high and low abundances of certain elements were selected, along with samples containing noteworthy element combinations as well as a mix of intermediate samples which may not have proven extraordinary in any other way besides their normality. Sample selection aimed to provide the widest range of sample types, minerals and elements to be analysed.

Once the sample set had been decided, the sample preparation began. Initially the cores were cut as finely as possible using a conventional worktop circular saw, commonly it is only possible to cut slices around 5 mm thick. The disks then required further thinning, which was done by grinding the disk using a worktop metallographic grinding and polishing machine and a coarse grained (125 μm) grinding plate. As previously explained in section 3.1, the LIBS set-up used for these experiments is fitted with an effective auto-focus system which allows for the analysis of samples with uneven surfaces. Thus, when grinding the surface, a rough grinding disk of 125 μm grit is acceptable as scratches and minor surface defects can be analysed nonetheless, no time-consuming polishing is required. The use of coarser grinding plates may present issues when attempting to reduce the thickness of a disk to below 1 mm as the friction and shear forces are more likely to lead to breakages. The thin disk samples were ground until individual grains or geological structures could be observed on both sides of the disk. In the case of the Kittilä drill core samples, the disks exhibited an appropriate thickness at between 0.5 – 1 mm. Difficulties can occur when the disks become thinner than 0.5 mm and splitting may occur.

It is important during the production of the thin disks that the sides of the sample are as analogous as can be achieved, depending upon the sample grain size. The sample dimensions may change as both sides of the sample may be equally representative at different thicknesses. Finally, the disks were cleaned in an ultrasonic bath at 50 degrees, to ensure that no dust particles from the grinding stage remained on the surface, as loose dust particles could affect the LIBS measurements; after cleaning, the samples were allowed to dry in air.

The thin disks were subsequently analysed by LIBS on both sides; assuming the sample has been prepared correctly and each side appears a mirror of the other, the data should reflect the

similarity. The data from each side can be combined to form a single, average, dataset of the composition and spatial relationships present in specific samples. Before LIBS scanning begins, photographs were taken of both sides of each disk (an example shown in the appendix) to allow for such comparisons to be made.

If a single sample were to undergo thin disk preparation, pulverisation and pelletization, the process would take approximately 120 minutes. However, if samples are produced in batches then less time is required and up to 10 samples can be produced and analysed through all three preparation and analysis stages. Approximately 30 samples had to be analysed in all three sample states for a suitable calibration to be completed. It is predicated that if a team of 3 people were working on preparations then a 30 sample calibration should take less than one day. Following this, analysis began on the core boxes and the desired data was collected.

3.5 Pulverisation of samples

A number of analysis methods require samples to be in powder form, commonly with specific requirements on particle size. Thin disk and the Kittilä powders were milled for analysis by XRD and TXRF analysis, the powders were also milled for pressing into pellets and for direct powder analysis. For all samples pulverised during the time of this study, a McCrone Micronising Mill (see figure 5) was used to produce a particle size below 20 µm. A sample with a maximum particle size of 20 µm is suitably prepared for direct powder analysis by LIBS, TXRF and XRD analysis; additionally, fine sample particle size allows for improved reliability in pellet production compared to coarser powders.

Figure 5: McCrone Micronizing Mill, polypropylene jar and grinding stone selection, including agate which were used to pulverise thin disk and powder samples in preparation for XRD analysis. Image taken from The McCrone Group, 2020.

The McCrone mill is specifically designed for producing XRD suitable fine powders, providing even particle size distribution in short grinding times without impacting the crystal lattice or chemically degrading sample material. The 100 W mill at 60 Hz can run at 1,500 min^{-1}, rapidly reducing sample particle size to the low micron range. In all of the sample preparation methods described in this thesis, the McCrone mill was operated at full speed (1500 min^{-1}). The McCrone mill grinds up to 5 ml of sample in a 125 ml polypropylene jar and utilises 48 cylindrical grinding stones. For this thesis, agate grinding stones were used which have a hardness of 7 on Moh's scale and was proven sufficient for the desired purpose. The jar is

produced of moulded polypropylene due to the chemical resistance properties; polypropylene is inert to most alcohols, non-polar hydrocarbons and does not react readily with dilute bases or acids. The motion of the grinding stones produces planar shearing and linear contact forces, increasing efficiency compared to the random contact blows occurring in a conventional ball mill, resulting in sample pulverisation in a relatively short time.

3.5.1.1 **Milling methodology**

Use of the McCrone mill is very simple. Firstly, the grinding jar is filled with the 48 agate grinding elements using a purpose designed spacer to ensure the correct alignment; eight elements per layer in six layers. The sample is then loaded. 6 grams of sample was chosen to ensure that the threshold 5 ml limit was not exceeded and also, as the Kittilä samples have an average density of approximately 2.9 t/m3, 6 g of material is equivalent to approximately 2 ml which is the optimal mill load according to the user manual. The sample must be gently shaken to make sure no material rests on the surface of the top-layer grinding stones before the lid is screwed on tightly. The filled grinding jar is placed into the mill, a speed and a time are selected, and the grinding cycle may then begin. At completion of the milling cycle, the grinding jar is removed and emptied onto a single-use worktop cover, the grinding stones are removed by a single-use gloved hand and placed into a cleaning beaker. The ground sample can then be collected and poured into a pre-labelled sample bag.

Cleaning the grinding jar and grinding stones is the most time-consuming step; the cleaning methodology remained constant and followed the instructions provided in the user manual. Between each milling stage, whenever there is a material change, the grinding elements and the sample jar must be cleaned to maintain a non-bias and uncontaminated environment for all subsequent samples to be milled. Due to the nature of XRD analysis, nanoscopic contamination between samples can be detected and therefore it is important that all possible measures are taken to reduce the possibility of any contamination occurring.

To achieve minimal contamination, after each mill cycle the grinding stones are removed, bathed in alcohol, cleaned in an ultrasonic bath for 3 minutes and subsequently rinsed in de-ionised water. The grinding jar, once emptied, must be manually washed with water and scrubbing brushes to remove all accessible particles. Manual cleaning is followed by filling the grinding jar with a dilute base cleaning solution and placing it into the mill to run for 30 seconds each time, this process will have to be completed at least twice, and if after the second round the jar is not sufficiently clean then another round is necessary. Between rounds, the base cleaning solution is washed out with water, after the second (or final) round, the grinding jar is rinsed with de-ionised water. On some occasions the grinding jars required three or more rounds with the cleaning fluid before being cleaned sufficiently. Finally, the washed grinding stones are dried and placed back into the dried grinding jar, then 0.1 ml of the new sample is loaded into the jar. With the top screwed on, the grinding jar is placed back into the mill and run for 1 minute before being removed, opened and the contents being discarded. The next sample is then ready to be fully loaded into the grinding jar and run on the next cycle. In total, each sample requires approximately 20 minutes to produce, including cleaning measures.

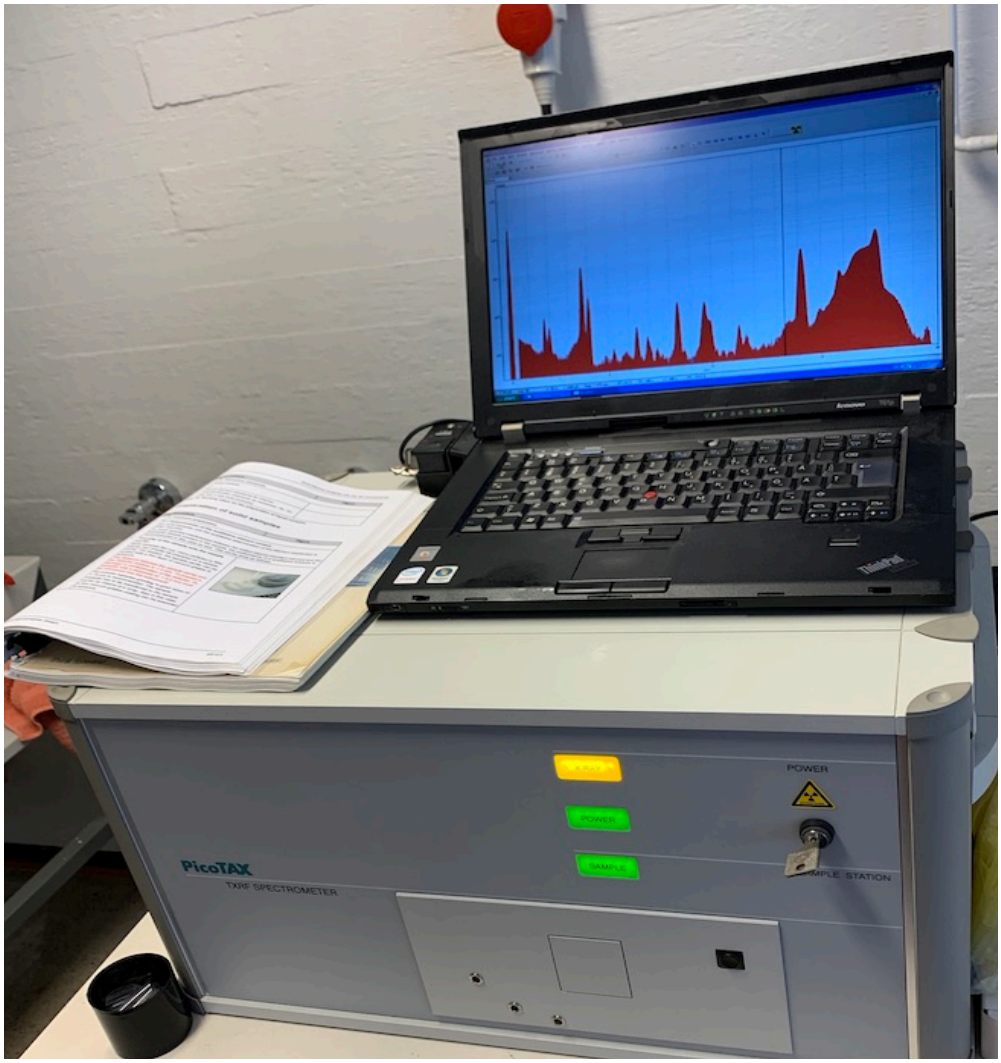

Figure 6: The Bruker PicoTax multi-elemental total reflection X-ray fluorescence device and associated PC for system control and data processing used for analysis of mineralogical, Kittilä powder and thin disk powder samples.

3.6 TXRF and XRD preparation

3.6.1 TXRF analysis method

Total Reflection X-ray Fluorescence (TXRF) was used to determine exact elemental compositions of mineralogical samples which had previously undergone XRD mineralogical analysis, as shown in table 1. TXRF was also used to determine the elemental compositions of 40 thin disk powder samples and their corresponding Kittilä powder sample. TXRF operates as a versatile trace element detector unit suited for a wide range of sample types but particularly liquids, powdered and micro samples. Preparation for the TXRF removes the issues associated with matrix effects such as absorption or secondary excitation which is important for effective analysis (Stosnach, 2005). The TXRF data was compared alongside the XRD data for the mineralogical samples and subsequently underwent LIBS analysis to allow for direct analytical comparisons to be made between the data produced in each test. The thin disk samples had

been previously analysed by LIBS while in as a whole rock thin section sample. Kittilä powder samples had also been previously analysed using LIBS in pellet form. Thin disk powders used during TXRF analysis were ground from the same thin disk, which was analysed by LIBS, while the Kittilä powders used for TXRF were sourced from the same sample bag as the pellets – however, the material was not identical. A benchtop Bruker PicoTax multi-elemental TXRF spectrometer was used to conduct XRF analyses and data was reported using S2 PicoFox software.

Before TXRF analysis can be initiated, solid samples require a grain size of <75 μm which was achieved in a mill as part of the preparation for XRD-ready samples. The Kittilä powders and thin disk samples were milled separately while the mineralogical powder samples had been previously analysed with XRD and so were milled to <20 μm. Once the size constraint has been met, any sample type can be analysed using the PicoTax, shown in figure 6. Before analysis commenced, an analysis cycle was run with no sample present and a second cycle was run with a blank sample carrier to determine what the background spectra displays to allow for comparisons and corrections to be used if required.

3.6.2 Semi-quantitative analysis

Before quantitative analysis can be completed using TXRF, semi-quantitative analyses are required in order to conclude an acceptable reference standard. 67 mineralogical samples previously analysed using XRD were also analysed semi-quantitatively using TXRF. Additionally, 40 samples of milled thin disks and the 40 corresponding Kittilä powders were also analysed. For the completion of semi-quantitative analysis using the PicoTax, approximately 30 μg of the powdered samples were loaded using a Q-tip onto an acrylic sample carrier. The powder material was fixed in place using a thin film of vacuum grease and any loose particles were removed using an air duster. The sample carrier was then ready to be placed into the sample cassette and locked into the device.

The TXRF analysis is set-up and run using S2 PicoFox software produced by Bruker and operated through a PC connected to the device. During the experiment, each analysis ran for 300 seconds and the resulting spectra were analysed, at which point a reference standard was chosen for the ensuing quantitative analysis. The standard solutions considered were Bismuth (Bi) and Selenium (Se) due to their generally low abundance in geological materials. The semi-quantitative analyses were used to determine which of Bi or Se were most appropriate for use during subsequent quantitative analyses. The most important considerations when selecting a standard solution are that the element is found in sufficiently low abundance and to ensure that the spectral peak of the standard element is not overlapping or interfering with any elemental peaks within the desired analyte.

Contamination is an important consideration at all stages of sample preparation and especially for TXRF in which micro-volumes of sample are used and trace elements to the ppb range can be detected. Even nano-particle contaminant may be detected and presented in the analytical spectra produced by the spectrometer. To reduce the likelihood of any contamination arising

during the experiment a number of practical measures were put into place. Each sample was analysed on a single-use acrylic sample carrier and loaded on using an individual Q-tip as suggested by the PicoTax user manual.

Spectra were made for an unloaded sample carrier and for a carrier with a thin layer of vacuum grease to determine the base-state upon which the samples are being measured. It was shown that the molybdenum excitation tube is visualised as a large peak on the resulting spectra, meaning Molybdenum cannot be analysed using this method due to the high background values registered.

3.6.3 Quantitative analysis

The aim of quantitative analysis by TXRF was to determine the concentration of sample-containing elements for comparison with XRD or ICP-AES data which could then be input into the LIBS algorithm. For validation of the TXRF device, 10 mineralogical samples were analysed to determine the effectiveness of the device. The 10 mineralogical samples were selected to aid in the validation of the Kittilä sample TXRF data. Since the mineralogical samples had been previously analysed by XRD an easy comparison could be made to determine potential issues or biases. The selected mineralogical samples included arsenopyrite, quartz, iron-containing minerals and bismuth, all of which are important in quantitative analysis of the Kittilä samples. The remaining mineral samples can be analysed using TXRF and compared to the corresponding XRD data when deemed necessary for future analysis of rock types may containing different elements.

Subsequently the 40 thin disk and Kittilä powder samples were analysed. The concentration of 11 elements were analysed to allow for direct comparison with the ICP-AES data provided by the mine the elements were; S, Cr, Mn, Fe, Ni, Cu, Zn, Pb, Au, As and Sb. ICP-AES provided data for concentrations of Ag and Mo, however these data were not considered during this study. The TXRF device relies on a molybdenum excitation anode which naturally produces a large spectral peak, making the quantitative analysis of Mo very difficult. The spectral peak of Ag appears in the same location as Ar which is found naturally in the air during the analysis process and so the software often identifies the large Ar peak as Ag, producing very inconsistent and unreliable results.

The addition of an internal standard solution to sample material allows for direct quantification of elemental composition within the analyte. In order to introduce the internal standard homogeneously throughout the sample, the preparation method differs to that explained in section 3.7.3. A solution must be formed containing a known mass of analyte and a known volume of internal standard. The mass and volume values are required by the software to allow for qualitative elemental concentrations to be calculated. A precision scale with the capability of measuring 0.1 mg and mechanical pipettes with 0.01 µl precision were used to ensure the highest levels of data could be input into the software. A laboratory vortex sample shaker was used to suitably homogenise samples before pipette extraction.

Initially, 25 - 45 µg of the powdered sample was precisely weighed, transferred into a test tube and the weight (to 0.1 µg) was recorded. The solid powder sample was subsequently suspended in 2.5 ml of 1% Triton^{TM} X100 solution as recommended by Bruker, the PicoTax TXRF machine manufacturer. The pre-defined reference solution, with an externally determined concentration, was pipetted into the solution as the internal standard. A mechanical pipette was used to ensure an exact volume of internal standard was used which is vital for the software to analyse spectra and produce concentration data. Thorough homogenisation is necessary to ensure the powder material is suitably and uniformly spread throughout the sample, this was achieved using the Janke and Kunkel IKA-Labortechnick VF2 vortex sample shaker. Quickly proceeding thorough homogenisation, 10 µl of the sample-laden suspension was pipetted onto a single use acrylic sample carrier. The period between homogenisation and sample transfer should be as short as possible to reduce the opportunity for particles to settle. The loaded sample carrier is then placed in an oven until the liquid has evaporated, leaving behind the sample material with the reference standard.

The sample laden carriers were left in an oven for 40 minutes at 60 degrees to allow for total drying of the solution on the sample carriers, following this, TXRF analysis could begin. As with semi-quantitative analysis, quantitative analysis was run for 300 seconds. In reference to the methodology, the analysis remains the same as previously outlined in section 3.7.3. During quantitative analysis additional information is required by the software to allow for accurate analysis of the spectra. The software requires information regarding the reference sample including the element used, the concentration of the solution and the exact volume. Reference sample values are used alongside the measured mass of unknown sample within the solution, allowing for the accurate determination of sample composition. By comparing the data of the analysed elemental peaks to the data of the reference element peak allows for quantitative data whilst taking into account the concentration, counting error and detection limit.

To ensure the reliability of TXRF quantifiable analysis, 10 mineralogical samples were analysed. TXRF results for the mineral samples were compared to XRD data to validate future data produced for unknown samples. Following validation, the Kittilä powder samples were analysed to allow for direct comparisons with the corresponding ICP-AES mine data. Following the data comparison of ICP-AES and TXRF the thin disk samples were analysed by TXRF also.

3.6.4 Producing XRD-ready samples

Initially it was planned that synchrotron XRD would be used and the results collected during this study. However the XRD analysis will be completed at a later time during the project due to delays. XRD utilises 'white' synchrotron X-rays produced across a wide array of energy levels, opposed to a monochromatic XRD which utilises only a single wavelength. From the synchrotron beam a single wavelength can be isolated to create a monochromatic beam, reducing the intensity of the beam overall. However the intensity of the 'white' beam is so powerful that this does not cause a problem. XRD requires samples to be in the low micron range to ensure effective analysis. In order to benefit the most from the XRD analysis it is

important to consider the sample preparation methods which have been employed in this study. XRD results produced using the samples prepared as part of this thesis will be published as part of the LASO-LIBS project report but will not be included within this thesis.

A total of 120 samples were prepared to be analysed by synchrotron powdered XRD requiring samples with a particle size in the low micron range. One sample per metre of core was reduced from <100 µm powder samples, produced for use in chemical analyses, to a particle size of <20 µm. An additional 40 samples were produced from thin disks cut from the half-cores which have previously been through LIBS analysis and this is discussed in section 3.7.2.

For the preparation of the Kittilä <100 µm chemical analysis powders, the same method was applied to all 80 samples to ensure continuity and comparability. Firstly, the most appropriate grinding time for the samples needed to be determined. A selection of 5 samples were chosen to include multiple rock types and different stratigraphic levels of the drill cores to ensure suitable variety. A selection of samples were chosen to be tested for grinding times of 3 and 5 minutes, with 3 additional samples which were analysed to determine the original particle sizes of the drill core powders. Samples FIKID508128/155/187 all represent Massive Mafic Lava (MML) formations which dominates 70.15 m of the 71.10 m drill core sample set being studied. Sample FIKID508163 represents a segment of the 0.25 m Banded Iron Formation (BIF) unit. The final sample, FIKID508170 is considered within the MML lithological unit however it is visually distinctive when compared with the remaining samples - FIKID508170 also contains the lowest levels of Arsenic (As) throughout the entire core length. The selected samples were separately milled using the McCrone mill as described, the resulting powders for each of the 5 samples subsequently underwent particle size analysis. The results of the grinding tests are shown in tables 2 and 3 in section 4.1.

For particle size analysis, a Beckerman Coulter LS13320 laser diffraction particle size analyser was used to determine the exact sample size range. Initially the machine had to be cleaned and calibrated to ensure that all of the results produced were reliable and accurate. Cleaning the device consists of filling the sample holder with 15 ml of specialised garnet abrasive and running a clean cycle, taking only a few minutes. Calibration involves running a routine particle size analysis cycle using a standard sample of a known particle size as a comparison. In this case 15 ml of 35 µm garnet powder was used as a calibration standard. This produced results within the expected range for the machine and so analysis on the unknown samples could commence. One downside to using the particle size analyser is that each sample run analyser is lost and therefore not every sample can be analysed individually. It has to be assumed that the results achieved by the selected samples are representative and so all succeeding samples were ground on a 5 minute cycle.

3.6.4.1 Milling thin disks

Powdered samples are vital for the effectiveness of the thin disk preparation method as the resulting pulverised disk material is then used in a number of subsequent analyses. In this study, the thin disk powders will go on to be analysed by XRD and pressed into pellets to be analysed

by LIBS. Thin disk preparation allows for analytical flexibility since when the disk is pulverised the resulting powder can undergo multiple analyses, so long as the techniques chosen do not contaminate, destroy or modify the powder.

The thin disks cannot be immediately milled using the McCrone mill as the maximum material feed size is 0.5 mm. Therefore, following LIBS analysis the thin disks must undergo a pre-crushing stage before they can be milled; pre-crushing is completed using an agate pestle and mortar to grind the thin disks into a powder. The coarse powder can then proceed to milling to reduce the <0.5 mm sample in order to attain a particle size consistently below 20 μm.

3.6.4.2 Determination of milling time

Before the milling of all samples can be undertaken, the most appropriate milling time must first be defined. In order to determine this, 5 additional thin disks were produced from representative areas of the core, due to material management and time considerations only a small number of additional thin disks were produced. The powder of each pre-crushed thin disk was loaded into the grinding jar and milling took place as explained in 3.6.1.1. On this occasion, the mill was run for 10 minutes, allowing sufficient time for coarse powder to be ground into a suitably fine powder. The ground product was then analysed in the particle size analyser as previously outlined in 3.6.

After 10 minutes of milling, particle size analysis revealed that the ground thin disks were all reduced to a particle size 99% below 20 μm and mean particle sizes of below 5 μm which is acceptable for analysis using XRD. Considering the particle size analysis results, it was concluded that the 40 thin disk samples would be ground for 10 minutes in order to achieve XRD-ready powder.

Uniformity is important for the direct LIBS analysis of powder. This is because the material in all grains should be equally optically available to avoid any bias towards certain minerals which may pulverise into finer powders more readily. As the material is already appropriately milled, sample preparation for the powder analysis is simple, requires little set-up and the subsequent analysis process requires few consumables.

3.7 Pellet preparation

Pelletization is a simple step requiring only a laboratory hydraulic pellet press, a precision scale and the pre-prepared powdered sample along with a few easily obtainable consumables. The methodology aims to maintain simplicity while successfully achieving stable pellet production in the least time at the lowest cost.

Before deciding upon a definitive set of procedures, a number of preliminary experiments were conducted with a range of sample weight, sample grain size, pressing time and pressure to

understand how each variable impacts the pellet quality. Pellets of 3 g, 2.4 g, 2.1 g, 1.5 g, 1.4 g, 1.3 g, 1 g and 0.8 g were all tested, some samples were ground to <20 μm before pressing. Pressing times were varied from 5 minutes through to 10 minutes and pressures ranging between 10 tonnes and 15 tonnes were also tested. Pelletization success varied between each test and outliers occurred occasionally, however generally trends could be recognised in pellet quality. Pellets produced of finer grained material bonded more robustly, generally creating increasingly stable pellets compared to coarser grained pellets. Similar results occurred with increasing pressure and with increasing pressing time, as expected.

Figure 7: A Specac 15T manual bench-top pellet press and associated die set used to produce pellets for LIBS scanning. Image taken from (Specac, 2020).

Each method presented issues, some of which challenged the main directive. The study found that increasing pressing time or reducing particle size leads to the increase in the preparation time for each sample, therefore throughput decreases. The general consensus is that a mineral ore may require up to 40 tonnes (Specac, 2017), (Specac, 2017) of sustained pressing force to produce a stable pellet. During this study the set-up did not allow for this to be tested. There remains the potential to further increase pressing pressure which deserves additional research, but the set-up utilised in this study was only capable of a maximum of 15 tonnes. Through the completion of varying tests, a preferred methodology was defined which aims to balance pellet stability and usefulness with time and throughput considerations.

3.7.1 Pelletization methodology

Pelletization production is relatively simple and can be completed quickly if the sample is already suitable. Initially, the unloaded die sleeve and one divider are weighed, then 1 g of the powdered sample is loaded into the die sleeve, on top of the first divider. The second divider is placed on top of the sample, with efforts made to flatten the sample inside through gentle shaking and pressing. To complete the die set, the plunger rod is inserted into the top of the set so that the flat side is in contact with the top divider. The die set can then be placed into the press, a predetermined pressing force can be loaded and maintained for a consistent amount of time. When the time has elapsed, the pellet can be removed from the press and analysed

immediately. In the thesis experiments a Specac 15.011 manual worktop hydraulic pellet press, shown in figure 7, was used and a pellet die set with a 15 tonne pressure limit for 10 minutes.

Following the removal of the pellet from the die set it is important that all equipment is cleaned appropriately to remove any possibility of contamination between samples or external contaminants. In order to guarantee the minimum possible contamination of each pellet, multiple methods were introduced. During pellet production and sample handling, single use gloves were worn, single use sample scoops and single use work surface coverings were used and changed each time a new sample was being handled. The die set was cleaned for 3 minutes in an ultrasonic bath while bathed in ethanol to ensure effective decontamination. All potentially contaminated surfaces were also cleaned regularly with ethanol.

One pellet per metre of drill core powder were produced from Kittilä mine ore samples and ground to <100 μm for chemical analysis, totalling 80 pellets. It was determined that the production of a stable pellet was mostly successful using the <100 μm powder without the need for further, time consuming, particle size reduction. With the Kittilä samples it was concluded that the most efficient pellet pressing arrangement was a pressing force of 15 tonnes for 5 minutes. Exactly 1 gram of powdered sample was used to produce each pellet with the resulting dimensions of 16 mm diameter and approximately 2 – 2.5 mm thick depending upon sample density. The resulting pellets were relatively fragile and on occasion pellets split, there was sufficient surface to be analysed, even in the broken pellets. This method is proved to be mostly successful at producing LIBS-ready single-use samples.

Using this method, one pellet takes between 15 and 20 minutes to produce, from the weighing of the die set until the cleaning has been completed and the next sample is ready to be compressed. This allows for one laboratory technician to produce approximately 25 samples per day assuming all pellets remain whole. Throughput can be increased with; a greater number of personnel to assist with cleaning, weighing and documenting; an additional die set to allow for pre-loading of sample material while another pellet is being pressed; and potentially by using a press with a higher maximum load to produce similar results with less pressing time.

In addition to the 79 pellets made from the original Kittilä chemical analysis samples, 40 further pellets were produced using the powdered material from the thin disks. The thin disk material was pre-milled to below 20 μm and therefore compresses to form a more stable pellet when prepared according to the same parameters as utilised with the <100 μm powders. The 40 thin disk pellets were subsequently analysed using LIBS and the results can be compared to the original thin disk. Reliabilities and correction values were determined allowing for calibration to be achieved. The calibrated sample data was input into the analytical algorithm so that analysis could begin on the desired, unknown, samples.

On one occasion, sample FIKID508157, it was not possible to produce a stable pellet after 10 attempts. Various pressures and times were used however none of the resulting pellets were sufficiently stable for analysis. Considering the ICP-AES and TXRF data, there is no compositional reasoning behind the inability to form a pellet. In this instant, a press with a

higher pressure potential or a binding agent could be used.

Table 2: Particle size analysis results for Kittilä powder samples at various milling time intervals. In total, 8 samples were measured to determine the original grain size of the provided Kittilä powders. 5 of the analysed samples went on to be analysed under different grinding conditions (180 and 360 seconds). The mean particle and d_{90} values for each analysis are given. MML = Massive Mafic Lava. BIF = Banded Iron Formation.

Sample ID	Grinding Time	Mean Particle Size	d_{90} value (μm)	Comments
FIKID508128	0	12.01	47.07	MML
	180	6.61	15.58	
	300	5.42	12.98	
FIKID508155	0	12.43	48.15	MML
	180	9.27	17.51	
	300	5.40	13.45	
FIKID508163	0	11.90	46.25	BIF
	180	5.82	14.05	
	300	5.14	12.01	
FIKID508170	0	59.18	170.20	Visually distinctive
	180	15.77	55.71	
	300	11.61	46.29	
FIKID508187	0	12.24	48.89	BIF
	180	5.90	13.59	
	300	5.43	13.91	
FIKID508121	0	14.74	55.21	
FIKID508151	0	12.35	50.28	
FIKID508197	0	12.24	49.45	

4 Results

4.1 Particle size analysis results

Using the Beckerman Coulter LS13320 laser diffraction particle size analyser, particle size analysis revealed that 3 of the 5 samples were suitably ground after a 3 minute cycle; composed entirely of particles below 20 μm. However, after 3 minutes, sample FIKID508170 maintained a range of particle size peaks of over 20 μm and up to 100 μm despite having a mean particle size of 15.77 μm. Similarly, but less extreme, samples FIKID508128 and FIKID508155 showed small peaks around 40 μm despite the mean particle size being 6.614 μm and 9.273 μm and the d_{90} values being 15.58 and 17.51 μm respectively. Though samples FIKID508128/155/170 all displayed mean particle size values below 20 μm (shown in table 2), particles remained which were above the desired size. Therefore a new sample was made for each with a grinding time of 5 minutes.

Results for each 5 minute grinding time displayed suitable particle sizes for XRD analysis. Sample FIKID508170 maintained the highest mean particle size of 11.61 μm while the

remaining four samples had a mean particle size ranging from 5.142 – 5.430 μm representing a very narrow particle size range. Sample FIKID508170 presented an anomaly as even after 5 minutes of grinding the d_{90} value still exceeded 20 μm and the mean particle size did not fall within the narrow range as observed with the other four test samples. Particle size analysis on the original FIKID508170 powder provided by Kittilä revealed that it was considerably coarser than the other 7 original test samples, as is shown in table 2. While the majority of samples display an initial d_{90} particle size of between 46 μm and 51 μm which represents a very narrow range, FIKID508170 initially has a d_{90} value of 170.20 μm.

Table 3: Results of thin disk particle analysis after 10 minutes milling at 1500 min-1 in the McCrone Mill.

Test	Mean grain size (μm)	d_{90} grain size
1	4.61	11.17
2	4.42	10.76
3	3.09	6.61
4	4.45	11.09
5	4.54	11.14

The thin disks were initially crushed using a pestle and mortar to a grain size below 0.5 mm. As the pre-milling grain size was larger than that of the Kittilä powder samples, an increased amount of time was required to sufficiently pulverise the samples. 5 tests were completed and the results proved highly successful in producing XRD-ready samples, all with a mean grain size below 5 μm. The results in table 3 show that the mean grain size provides a comfortable buffer before the samples would be unacceptable for XRD, therefore all subsequent samples were ground for 10 minutes. Grain size testing using the size analyser is a destructive technique and so any analysed material is lost. Therefore only 5 samples were selected and assumed to be representative of the entire sample population.

4.2 TXRF Results

4.2.1 Preliminary TXRF findings

Upon TXRF analysis of the unloaded machine as well as the machine loaded with a blank carrier, a number of spectral peaks were noticed. Figure 8 shows the spectra produced during the analysis of a blank sample carrier, the largest peak seen at 17.4 keV is attributed to Molybdenum and another minor peak is seen at 2.9 keV which belongs to Argon (air). Molybdenum is seen in such concentration as it is the material used in the machine anode and because of this, Molybdenum concentration cannot be accurately measured using the PicoTax. Furthermore, the lower energetic slope of the Mo peak at 17.4 keV is created by both Compton- and Rayleigh scattering. The consistent presence of Argon proved problematic during the analysis of the thin disk and Kittilä powder samples. Comparisons between ICP-AES analysis and TXRF for Ag was not possible due to the proximity of the Ag and Ar peaks in the spectra.

The interaction between the 2 peaks caused both elements to be affected and produced varied and inaccurate concentration data for the presence of Ag.

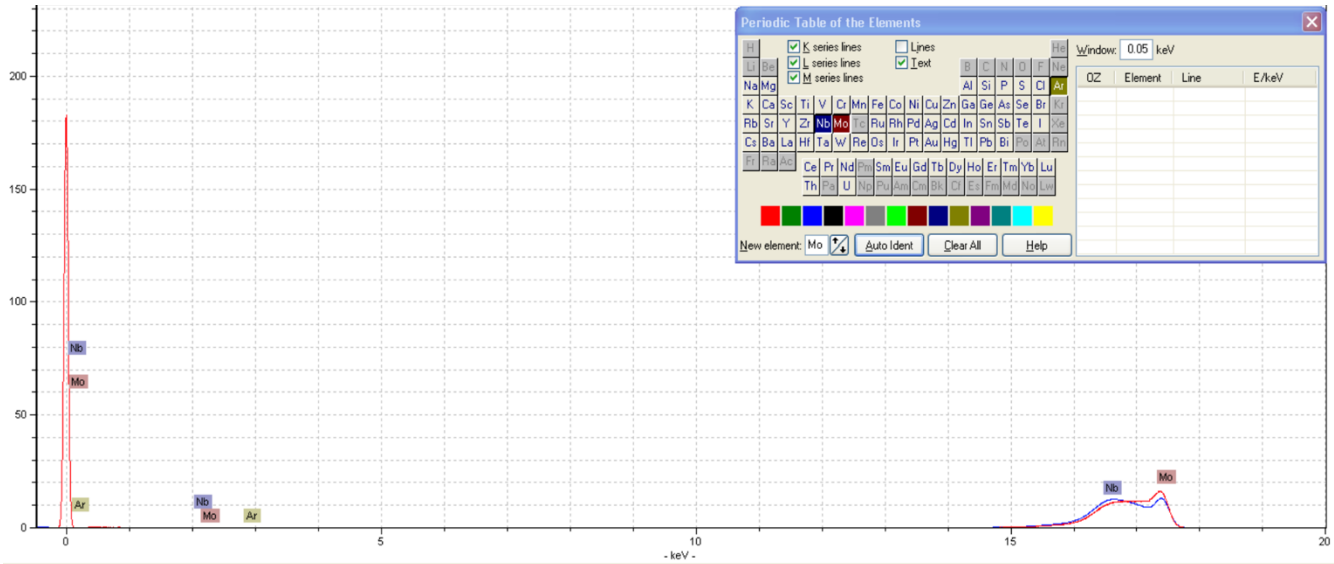

Figure 8: The spectrum produced when analysing a blank sample carrier, utilising the software 'Auto Ident' function which has identified Mo, Ar and Nb.

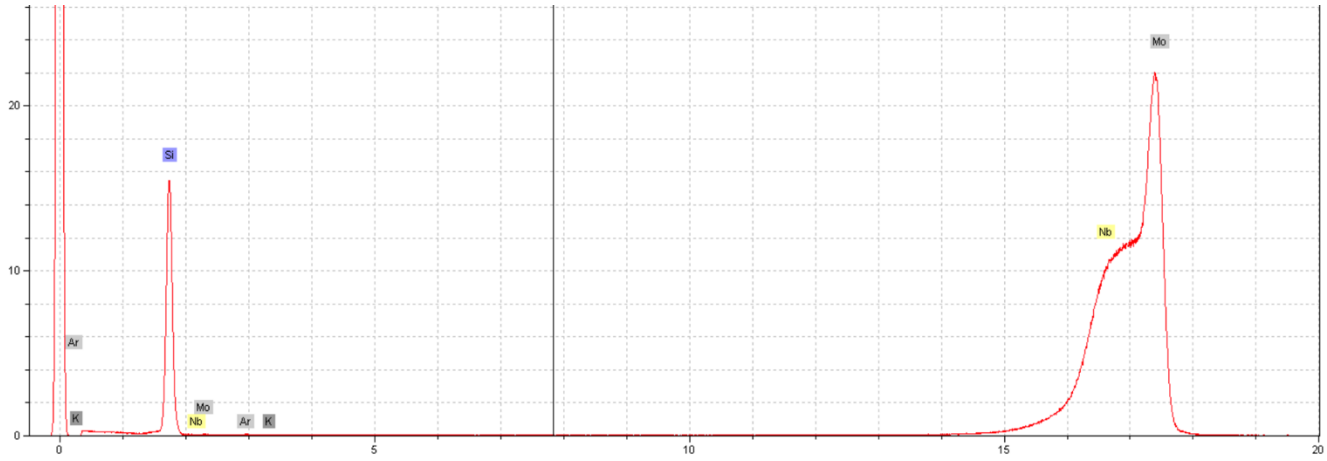

Figure 9: The spectrum produced after analysis of a sample carrier with vacuum grease which was used to fix powder samples during semi-quantitative analysis.

Figure 9 shows a spectra with the addition of vacuum grease, therefore providing a base spectra for semi-quantitative analyses. The silicon based vacuum grease produces a clear Si peak as well as minor K peaks, likely present due to carrier surface or grease contamination. Once a background spectra for the sample carrier and the vacuum grease was produced to confirm that there is no inexplicable contamination which may impact the results of the subsequent analyses, semi-quantitative analysis could begin.

Table 4: Semi-quantitative TXRF results for 67 mineralogical samples and the determination of the most appropriate mono-elemental standard solution to be used for quantitative analysis. Analysed on an acrylic sample carrier using vacuum grease to bind the <5µm mineralogical samples

Mineral Sample	Code	Standard	Mineral Sample	Code	Standard	Mineral Sample	Code	Standard
Adularia	E11	Bi	Galena	E27	Se	Quartz	12	Bi
Aegirine	11	Bi	Gypsum	42	Se	Quartz (Rose)	E31	Bi
Aegirine	44	Bi	Hematite	37	Bi	Quartz (Smoky)	E26	Bi
Albite	E39	Bi	Hornblende	E29	Bi	Quartz (Smoky)	E34	Bi
Almandine	26	Bi	Hydroxyapatite	35	Bi	Quartz (White)	E24	Bi
Apatite	35	Bi	Hypersthene	E7	Bi	Sapphirine	29	Bi
Andalusite	32	Bi	Ilmenite	E14	Bi	Scapolite	28	Se
Arsenopyrite	24	Se	Kaolinite	9	Se	Scapolite	36	Bi
Augite	21	Bi	Kyanite	E20	Bi	Sphene	45	Bi
Baryte	43	Se	Kyanite	14	Bi	Spodumene	19	Bi
Baryte	E23	Se	Lepidolite	31	Se	Staurolite	30b	Bi
Beryl	22	Bi	Magnesite	E47	Bi	Stibnite	X3	Bi
Bismuth	2	Se	Magnetite	20	Se	Sulphur	X2	Bi
Chlorite	4	Bi	Microcline	23	Bi	Talc	38	Se
Clinopyroxene	25	Bi/Y	Microcline	E6	Bi	Mn-Tantalite	3	Bi
Columbite	15	Bi	Microcline	E16	Bi	Topaz	27	Bi
Cordierite	16	Bi	Monazite	8	Se	Tourma Elbaite	33	Bi
Cordierite	E15	Bi	Muscovite	E22	Bi	Tourma Schorl	34	Bi
Cr-Diopside	5	Bi	Olivine	6	Bi	Tremolite	18	Bi
Epidote	13	Bi	Orthoclase	7	Bi	Wollastonite	30a	Bi
Fluorapatite	41	Bi	Phlogopite	E46	Bi	Zircon	17	Bi
Fluorapatite	X4	Bi	Plagioclase	E2	Bi	Total Se =	13	
Fluorite	39	Se	Plagioclase	X1	Bi	Total Bi =	54	

4.2.2 Semi-quantitative TXRF analysis

A total of 67 mineralogical samples, previously analysed by XRD, were analysed by TXRF. Table 4 displays each sample and the reference standard to be used during quantitative analysis. In 32 of the 67 semi-quantitative analyses, both Se and Bi values registered below the background level, therefore allowing either to be used for the subsequent quantitative analyses in their respective cases. In cases where both values were found to be below the background there was commonly a value which was clearly preferable when compared to the alternative, for example; Cordierite sample 16, the Bi value compared to the background was 1/7578 and the Se ratio 7260/8665, in this situation, Bi is chosen as the reference sample. In cases where both Bi and Se ratios were extremely low the ratio value is still considered and so the reference element with a lower ratio would be used, for example; Talc sample 38 displayed ratios of Bi 1/3376 and Se 1/3960, in this case Se was chosen. Spectral peak positioning was also

considered for all samples, ensuring that the potential reference standard elemental peak is not produced in a similar area to another elemental peak within the specific sample. If 2 elemental peaks are located too closely, the quantitative data may be affected, for example, Arsenopyrite 24 which registered lower values for Bi than Se. However it is likely that the Bi peak was impacted by the large As peak in the same region, therefore, Se was chosen as the most appropriate standard.

In the case of 34 of the remaining 35 mineral samples there was either Bi or Se detected within the sample and so the non-present element was chosen. Some examples saw the appearance of at least one of the potential standard elements; Microcline 23 produced results of net/background Bi 1/8412 and Se 27,245/8938, therefore in this case, Bi was selected as the reference solution in quantitative analysis. In one instance Clinopyroxene 25, both Bi and Se values were detected as being present. For sample 25, Bi was determined to be the most suitable standard since the corresponding spectral peak interfered to less of an extent when compared to Se. In the future, sample 25 could be more accurately quantitatively analysed using Yttrium since the peak is isolated and the element is not present in the sample.

Figure 10 shows the semi-quantitative analyses spectrum for a sample of Bi, displaying a clear peak around 10.8 keV and another large peak at 13.0 keV denoting Thorium (Th). Thorium is a decay product of Bi and therefore can be expected in large concentrations within a natural mineralogical sample of Bi. In this instance the selected reference standard to be used in quantitative analysis was Se as the addition of a Bi solution would distort and invalidate the results. The same methodology and analysis was completed on all mineralogical samples, the results of which are shown in table 4.

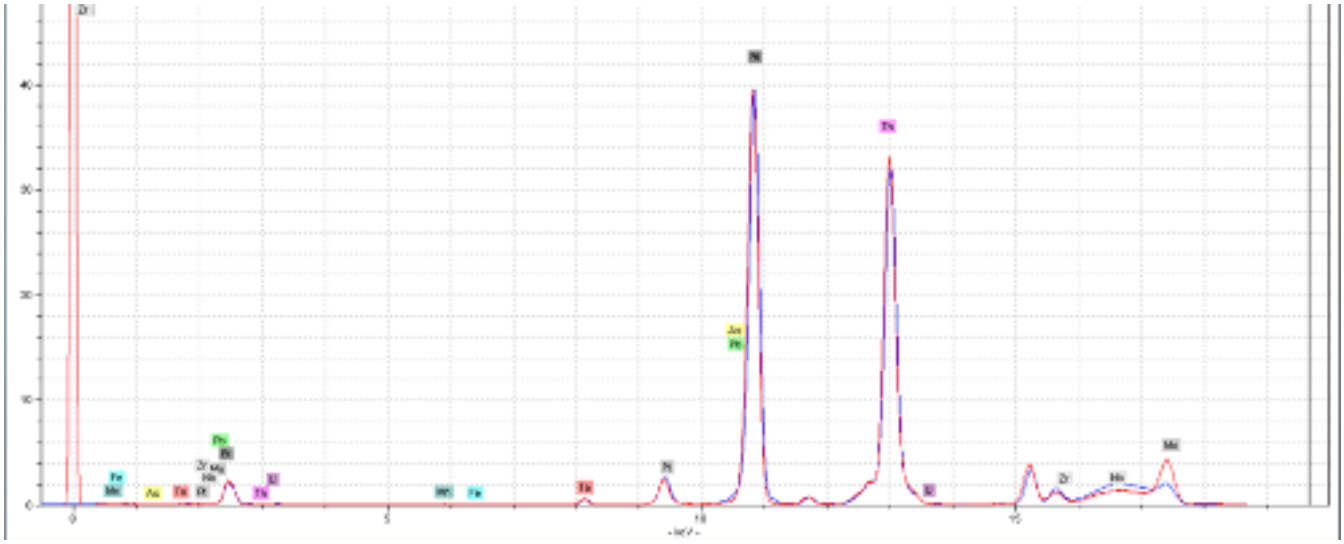

Figure 10: The spectrum produced after semi-quantitative analysis of a Bi mineralogical sample, as expected, a large peak at 10.8 keV was produced and Se had to be chosen for the internal standard in quantitative analysis.

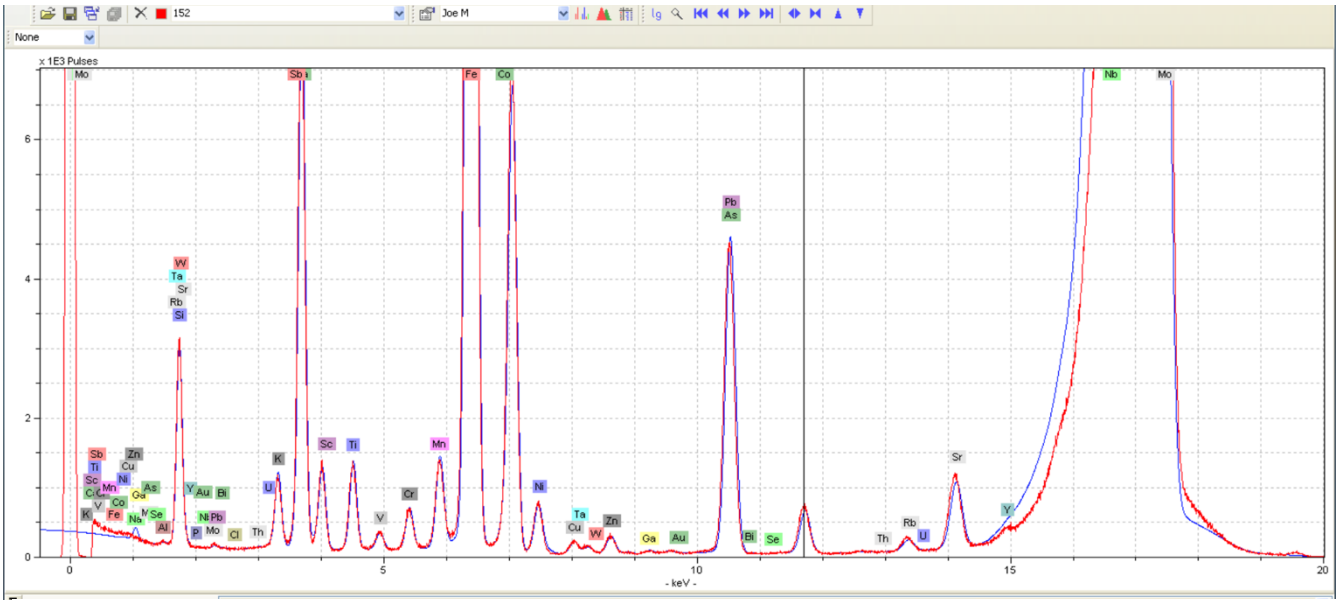

Figure 11:The spectrum produced after semi-quantitative analysis of Kittilä powder sample FIKID508152, displaying the proximity of the Bi spectral region to the higher energy flank of the Pb/As peak at 10.5079.

4.2.3 Quantitative TXRF analysis

In addition to the mineralogical samples, semi-quantitative analysis of 12 Kittilä powders was completed. The semi-quantitative analysis revealed that the Bi spectral peak is located in too close proximity to the large Pb/As peak. As shown in Figure 11, the Bi spectral peak lies on the downslope of the Pb/As peak making Bi an unsuitable reference element. When analysing the 12 Kittilä powder samples, the Bi peak is observed between 10.7310 and 10.8390 E/keV while Pb is between 10.4490 – 10.5510 E/keV and As between 10.5079 – 10.5434. The Se spectral peak begins at 11.1837 presenting a larger region of difference and therefore reducing the possibility of influence on the sample data from the reference element. Therefore, all Kittilä powders and thin disk samples were quantitatively analysed using Se as the reference element.

Table 5: The quantitative TXRF analysis of 10 selected mineralogical samples and compared with XRD data. The data was used to validate the use of TXRF for further analysis on the Kittilä samples. Syn = Synthetic.

	XRD Results			TXRF Results		
Sample name	Minerals present	Mineral composition	%	Standard	Elements	%
C3P001_24 loellingite	Loellingite	FeAs2	85	Se	As	68.032%
	Quartz	SiO2	1		Fe	30.886%
	Albite	Na (Al Si3 O8)	13		Si	0.536%
	Bismuth	Bi	1		S	0.335%
	Pyrrhotite	Fe1.05 S0.95	1		Ca	0.128%
					Bi	0.082%
A2P001_2 bismuth.txt	Bismuth, syn	Bi	82	Se	Bi	97.756%
	Bismutite	Bi2 (C O3) O2	3		Ta	1.675%
	Tellurobismuthite,	Bi2 Te3	3		Mn	0.204%
	Osmium, syn	Os	4		Te	0.138%

	Molybdenite-2H	Mo S2	8		Ca	0.132%
					Fe	0.095%
E8P001_39 fluorite.txt	Fluorite, syn	Ca F2	100	Se	Ca	99.952%
	Quartz	Si O2	-		Co	0.023%
					Fe	0.015%
C8P001_37 hematite.txt	Hematite, syn	Fe2 O3	92	Bi	Fe	99.045%
	Qusongite, syn	W C	8		Ca	0.621%
	Chalcopyrite	Cu Fe S2	-		S	0.147%
					Ti	0.111%
					V	0.073%
					Cu	0.004%
B11POO1_magnesite 8769.txt	Magnesite	Mg (C O3)	97	Bi	Mg	97.507%
	Quartz	Si O2	3		Si	1.312%
	Qusongite, syn	W C	-		Ca	1.065%
C6P001_20 magnetite.txt	Magnetite, syn	Fe3 O4	-	Se	Fe	95.633%
	Hematite, syn	Fe2 O3	-		V	3.157%
					Mn	1.076%
					Zn	0.135%
A12P001_quartz (rose).txt	Quartz	Si O2	100	Bi	Si	99.687%
	Qusongite, syn	W C	-			
A13P001_sulphur.txt	Sulfur, syn	S8	100	Bi	S	99.365%
B1P001_3_Mn tantalite.txt	Tantalite-(Mn),	Mn (Nb0.5 Ta0.5) 2	100	Bi	Ta	84.301%
					Mn	15.135%
					Ca	0.287%
					Ti	0.270%
					Nb	Present
E4P001_17 zircon.txt	Zircon	Zr (Si O4)	100	Bi	Si	94.731%
	Qusongite, syn	W C	-		Zr	Present

Comparisons between the TXRF elemental results and the XRD mineralogical results proved the viability of TXRF for use with the Kittilä samples. Figure 12 shows the spectrum and report produced by quantitative analysis of a Bi mineralogical sample which was prepared with Se as an internal standard. 33.5 mg of Bi sample was combined in solution with 10 µg of Se standard solution. The report reveals that the Bi sample consists of 851.9 g/kg of Bi and when combined with the other calculated concentrations, Bi represents 97.76% of the sample.

After the validation of the TXRF technique using the mineralogical samples, 40 Kittilä powder samples were measured using the same methodology. Figure 13 shows the quantitative analysis results for Kittilä powder FIKID508159 and displaying the appropriateness of Se as an internal standard element. The Se peak at 11.2 keV is suitably isolated from the adjacent peaks and therefore the introduced volume of Se is not likely to have had an impact on the determined concentrations of the surrounding elements.

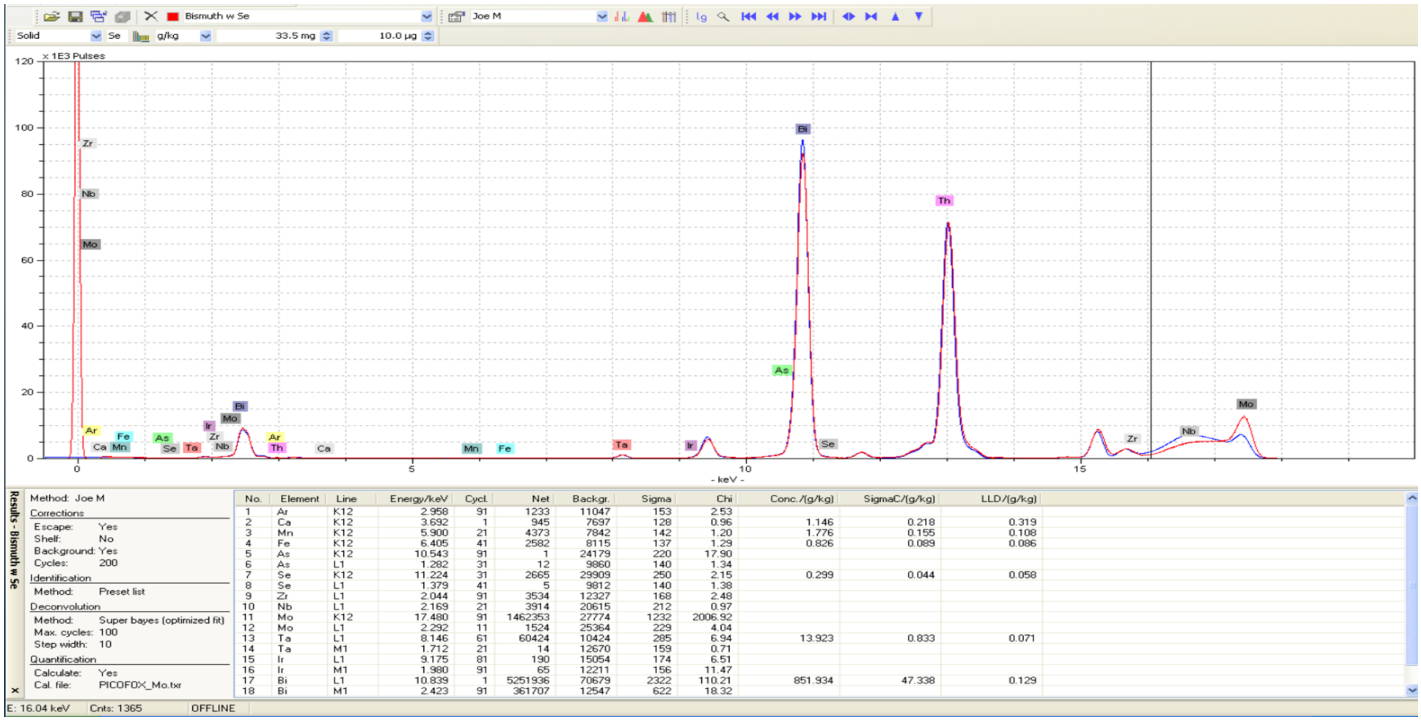

Figure 12: The spectrum and associated report produced by quantitative analysis using TXRF for a Bi mineralogical sample.

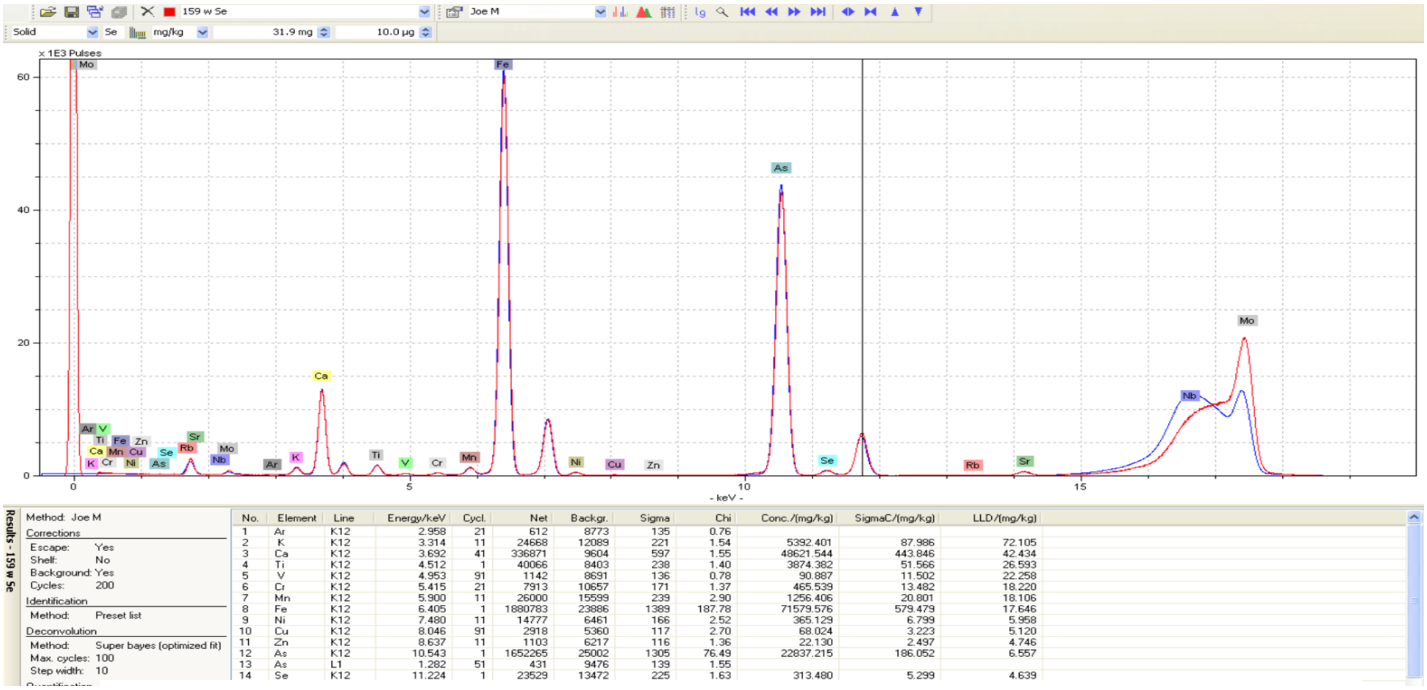

Figure 13: Produced spectrum and report after quantitative analysis of Kittilä powder FIKID508159 with Se used as an internal standard.

4.3 TXRF and ICP-AES

Table 6 shows the results and comparison between TXRF and ICP-AES data for 41 Kittilä samples. The figures were produced by quantitative TXRF analysis at Aalto University and the ICP-AES data provided by the mine. Conclusions and discussions surrounding these results are provided in section 5.0. In total, 14 elements have been considered across the 2 analytical techniques. However, due to interferences with TXRF analysis only 11 elements have been directly compared.

Table 6: Tabular comparative display of 40 samples analysed using ICP-AES and TXRF. Three samples have been analysed twice by ICP-AES for repeatability purposes. Each sample was analysed for 14 elements during ICP-AES, 10 elements were analysed during TXRF as concentrations of Mo, Ag, Co and Sb could not be reliably determined.

Sample ID		mg/kg	mg/kg	mg/kg	mg/kg	mg/kg	mg/kg	mg/kg	mg/kg	mg/kg	mg/kg	mg/kg	mg/kg	mg/kg	mg/kg
Sample ID	**Analysis**	**S**	**Cr**	**Mn**	**Fe**	**Co**	**Ni**	**Cu**	**Zn**	**As**	**Mo**	**Ag**	**Sb**	**Au**	**Pb**
FIKID508121	ICP-AES	37,455	35	1,616	60,162	16	77	88	28	3,204	6	1	36	1.18	21
	TXRF	20,823	97	2,962	94,530	0	85	87	31	6,149	N/A	N/A	0	0.00	51
FIKID508123	ICP-AES	17,478	14	2,462	82,363	40	82	146	37	265	<2	2	31	0.09	16
	TXRF	7,431	65	2,274	86,388	0	52	95	25	199	N/A	N/A	411	0.00	24
FIKID508124	ICP-AES	3,468	13	2,725	89,836	40	63	85	42	190	<2	<1	<20	0.02	<10
	TXRF	2,430	33	3,610	140,211	0	52	89	50	244	N/A	N/A	0	0.00	70
FIKID508126	ICP-AES	2,813	18	2,007	65,438	39	78	98	27	174	<2	1	<20	0.03	<10
	TXRF	979	147	2,748	102,406	0	87	116	27	217	N/A	N/A	0	0.00	55
FIKID508128	ICP-AES	15,914	18	2,084	61,721	34	74	91	29	3,108	<2	1	21	1.01	12
	TXRF	7,579	169	3,128	112,551	0	112	91	31	7,324	N/A	N/A	0	0.00	41
FIKID508130	ICP-AES	34,063	76	1,712	83,136	40	168	314	121	9,492	8	1	139	5.59	14
	TXRF	17,547	259	1,721	89,526	0	175	362	107	9,676	N/A	N/A	204	6.67	51
FIKID508131	ICP-AES	7,880	79	3,191	71,351	53	441	97	30	838	<2	5	59	0.17	10
	TXRF	1,990	526	2,546	69,850	0	368	42	19	728	N/A	N/A	0	0.00	47
FIKID508136	ICP-AES	1,118	13	1,508	58,022	34	59	91	26	153	<2	<1	28	0.02	<10
	TXRF	1,009	140	2,586	118,398	0	108	122	46	306	N/A	N/A	0	0.00	48
FIKID508138	ICP-AES	3,028	13	1,459	63,462	37	58	104	28	135	<2	<1	<20	0.03	<10
	TXRF	2,152	101	1,867	99,056	0	58	238	31	166	N/A	N/A	0	0.00	60
FIKID508142	ICP-AES	2,495	17	1,309	65,195	38	75	100	34	186	<2	<1	<20	0.05	<10
	TXRF	1,073	186	2,598	147,069	0	142	187	35	352	N/A	N/A	0	0.00	100
FIKID508145	ICP-AES	42,771	61	1,372	70,379	41	288	103	55	7,129	2	1	79	8.22	<10
FIKID508145(2)	ICP-AES	42,620	61	1,363	70,461	41	289	98	56	6,977	<2	2	72	8.18	<10
	TXRF	16,255	473	1,610	95,573	0	298	109	51	10,002	N/A	N/A	0	7.00	56
FIKID508146	ICP-AES	35,501	47	1,262	59,320	34	188	106	63	8,733	2	<1	85	6.59	<10
	TXRF	6,422	131	563	39,989	0	100	37	27	8,890	N/A	N/A	399	6.00	23
FIKID508147	ICP-AES	27,740	98	1,567	62,407	49	455	103	65	4,667	2	2	89	3.90	<10
	TXRF	11,574	722	1,501	71,362	0	423	94	61	4,556	N/A	N/A	0	3.33	37
FIKID508149	ICP-AES	58,685	36	1,292	77,345	36	186	75	39	9,402	4	1	55	7.25	10
	TXRF	19,033	193	1,208	91,494	0	146	53	22	15,341	N/A	N/A	0	16.00	72
FIKID508150	ICP-AES	31,483	75	1,684	83,208	40	164	280	143	7,982	7	1	127	4.37	13
	TXRF	8,260	145	931	56,375	0	83	161	73	5,096	N/A	N/A	0	6.00	46
FIKID508152	ICP-AES	12,364	95	1,815	55,101	55	532	111	79	1,672	<2	1	29	0.76	<10
	TXRF	10,624	1,641	3,425	118,141	0	974	165	102	4,144	N/A	N/A	0	0.00	40

FIKID508157	ICP-AES	53,010	42	1,758	78,367	36	199	74	28	12,184	<2	2	37	6.78	11
	TXRF	15,233	334	1,980	77,336	0	164	44	18	11,797	N/A	N/A	0	7.37	41
FIKID508158	ICP-OES	29,928	80	1,363	55,164	42	418	55	22	13,778	<2	<1	37	6.78	<10
	TXRF	6,678	338	955	47,834	0	294	27	10	17,799	N/A	N/A	0	6.46	9
FIKID508159	ICP-AES	22,983	69	1,181	46,237	32	351	53	22	12,255	3	<1	36	5.84	<10
	TXRF	9,623	398	1,075	61,249	0	305	55	16	19,533	N/A	N/A	0	0.00	22
FIKID508160	ICP-AES	33,898	74	1,709	84,511	40	167	312	117	9,517	8	<1	138	5.53	14
	TXRF	16,574	295	1,829	104,975	0	129	223	135	11,713	N/A	N/A	0	11.00	49
FIKID508161	ICP-AES	39,266	22	1,632	69,392	36	79	85	26	6,457	3	1	38	2.80	10
	TXRF	11,854	61	1,692	68,568	0	57	60	21	4,731	N/A	N/A		6.86	39
FIKID508162	ICP-AES	26,290	43	291	29,456	3	54	32	25	1,760	8	1	<20	2.84	<10
	TXRF	8,249	44	289	28,013	0	34	27	18	2,987	N/A	N/A	0	0.00	0
FIKID508163	ICP-AES	206,111	44	262	197,246	32	240	254	53	618	21	4	139	1.27	119
	TXRF	96,924	95	157	249,120	0	203	405	71	1,211	N/A	N/A	0	0.00	275
FIKID508164	ICP-AES	32,307	19	1,839	77,972	39	93	143	70	1,176	4	<1	31	0.21	<10
	TXRF	19,205	97	2,992	153,397	0	127	180	68	3,089	N/A	N/A	0	0.00	138
FIKID508166	ICP-AES	42,408	15	1,858	106,952	39	84	110	64	3,775	2	1	41	0.57	17
	TXRF	18,084	35	2,939	178,750	0	135	225	39	5,480	N/A	N/A	0	4.00	171
FIKID508167	ICP-AES	34,284	23	1,896	70,567	32	75	118	48	19,206	<2	2	53	1.69	<10
	TXRF	6,726	100	1,613	63,602	0	44	63	33	15,755	N/A	N/A	0	13.00	32
FIKID508168	ICP-AES	139,969	18	1,415	154,218	31	155	285	50	8,837	10	3	99	1.91	58
	TXRF	56,907	98	1,705	207,324	0	153	365	53	16,028	N/A	N/A		16.00	243
FIKID508169	ICP-AES	41,884	22	1,332	65,240	36	67	82	72	9,906	<2	1	33	6.34	<10
	TXRF	18,474	111	1,694	107,006	0	102	124	97	18,833	N/A	N/A	0	0.00	50
FIKID508172	ICP-AES	58,395	68	2,001	96,501	38	205	172	69	2,040	5	<1	41	2.65	21
FIKID508172(2)	ICP-AES	56,876	68	1,979	93,875	38	204	166	67	1,967	3	1	40	2.74	11
	TXRF	28,860	422	2,394	152,733	0	207	222	85	7,730	N/A	N/A	0	6.06	70
FIKID508173	ICP-AES	12,148	103	2,072	67,505	51	328	140	46	892	<2	<1	31	0.42	<10
	TXRF	5,141	718	3,057	111,311	0	403	117	71	1,109	N/A	N/A	0	0.00	50
FIKID508177	ICP-AES	29,873	17	1,424	58,891	36	65	86	24	3,805	<2	<1	26	3.15	<10
	TXRF	5,885	81	864	47,358	0	59	43	13	3,311	N/A	N/A	0	0.00	15
FIKID508180	ICP-AES	29,364	69	1,552	76,816	37	150	258	132	7,399	7	1	110	4.39	17
	TXRF	17,448	385	2,762	144,529	0	193	540	110	13,098	N/A	N/A	0	14.66	91
FIKID508181	ICP-AES	77,376	22	1,146	103,099	43	89	114	53	4,404	3	<1	47	3.50	10
	TXRF	27,051	74	1,122	129,627	0	67	91	69	7,852	N/A	N/A	0	0.00	62
FIKID508183	ICP-AES	35,159	24	1,128	70,494	38	68	99	51	4,518	<2	<1	25	4.64	<10
	TXRF	14,674	172	2,167	155,263	0	111	113	15	12,865	N/A	N/A	0	9.25	82
FIKID508185	ICP-AES	5,394	20	1,521	57,854	38	77	106	26	1,182	<2	<1	<20	0.74	<10
	TXRF	1,726	125	1543	68,234	0	86	85	25	1274	N/A	N/A	0	1.19	25
FIKID508187	ICP-AES	17,627	12	1,751	78,017	39	68	135	25	3,600	<2	<1	28	4.26	<10
	TXRF	6,267	107	2,093	101,022	0	54	128	16	3,662	N/A	N/A	0	0.00	32
FIKID508191	ICP-AES	16,951	106	1,644	64,912	51	413	76	40	3,279	<2	1	48	2.18	<10
	TXRF	5,090	475	1,537	71,810	0	346	52	33	4,378	N/A	N/A	0	0.00	29
FIKID508193	ICP-AES	1,528	81	1,848	63,442	52	430	82	34	670	<2	<1	82	0.05	<10
	TXRF	560	2,103	3,696	149,281	0	736	120	67	1,207	N/A	N/A	0	0.00	100
FIKID508194	ICP-AES	3,127	97	2,197	66,066	57	492	78	33	668	<2	1	133	0.07	<10
	TXRF	1,816	1,531	3,281	126,982	0	795	98	57	1,126	N/A	N/A	0	0.00	97

FIKID508195	ICP-AES	3,462	103	2,080	68,889	56	522	75	34	740	<2	<1	101	0.05	<10
FIKID508195(2)	ICP-AES	3,610	106	2,181	72,024	59	543	78	35	761	<2	1	112	0.07	<10
	TXRF	2,398	1,130	2,783	114,113	0	623	70	46	988	N/A	N/A	0	0.00	36
FIKID508200	ICP-AES	23,817	90	1,741	81,846	42	178	182	135	3,955	4	<1	90	1.76	<10
	TXRF	14,306	368	2,532	129,333	0	232	207	151	5,563	N/A	N/A	0	1.80	88

The average values across the whole dataset have been presented in table 7, the total and percentage difference between the datasets has been calculated. The results show that Ni, Cu and Zn have the smallest variation between datasets. Chromium and lead have the largest variation between TXRF and ICP-AES data, both show a difference of over 100%. Gold displays a surprisingly low percentage variance comparing the datasets due to the apparent variation in results, this is considered to be an outlier.

Table 7: A table showing the total values, average elemental composition of each sample and the % difference between average TXRF analysis and ICP-AES analysis across the entire dataset for 11 comparable elements.

	S	**Cr**	**Mn**	**Fe**	**Ni**	**Cu**	**Zn**	**As**	**Sb**	**Au**	**Pb**
Total TXRF	538,192.2	8,235.8	80,246.8	4,351,526.2	9,072.3	5,136.7	2,033.0	247,292.2	1,013.5	132.9	2,628.8
Average TXRF	13,454.8	205.9	2,006.2	108,788.2	226.8	128.4	50.8	6,198.2	27.0	3.3	65.7
Total ICP	1,453,921.0	2,226.0	73,229.0	3,334,460.0	9,091.0	5,540.0	2,303.0	203,656.0	2,446.0	120.7	519.0
Average ICP	33,812.1	51.8	1,703.0	77,545.6	211.4	128.8	53.6	4,736.2	56.9	2.8	12.1
Diff (ICP-TXRF)	20,357.3	-154.1	-303.2	-31,242.6	-15.4	0.4	2.7	-1,462.0	31.6	-0.52	-56.4
% Difference	86.14%	119.64%	16.35%%	33.53%	7.02%	70.33%	5.24%	26.74%	71.14%	16.85%	137.94%

Across the elemental compositions measured by TXRF and ICP-AES within this study, Sulphur (S) displayed the highest R^2 value, 0.945. As Figure 14 shows, sulphur concentration displays a clear correlation which could be used to predict further data points. However, Figure 15 also shows how TXRF analysis has consistently under-estimated Sulphur concentration when compared directly to ICP-AES analysis. Systematic underestimation is due to absorption effects associated with S, Na, Al and P as well as other light elements. Light elements are inaccurately analysed due to the absorption of the distinguishable X-ray fluorescence by the air atmosphere within the machine (Stosnach, 2005).

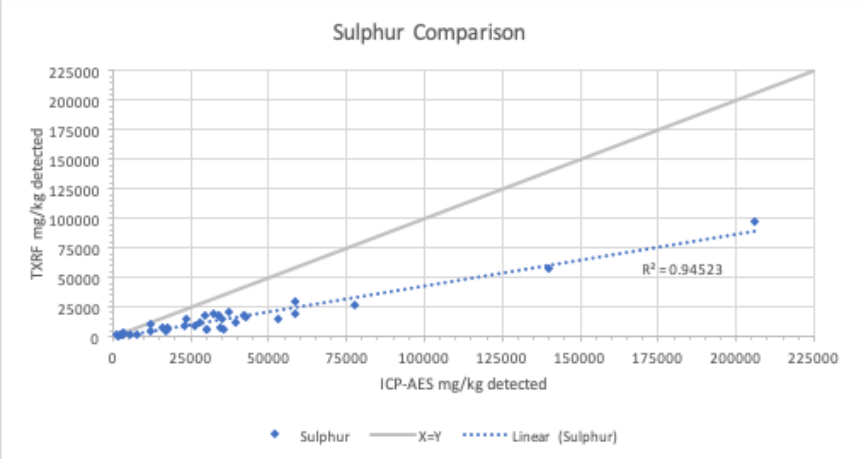

Figure 14: Comparative scatter plot of TXRF quantitative data against the equivalent ICP-AES data for sulphur with the R-squared value labelled.

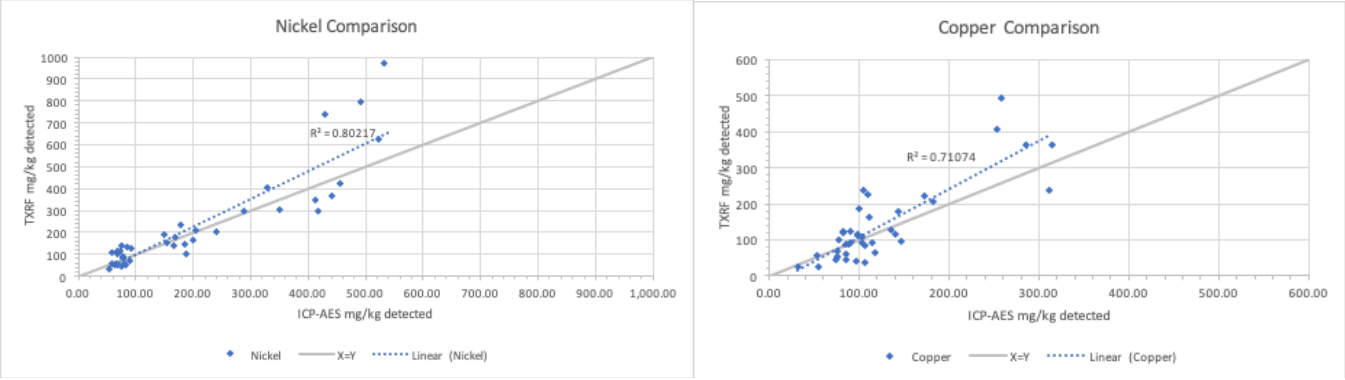

Figure 15: Comparative scatter plots of TXRF quantitative data against the equivalent ICP-AES data for nickel ((a) left) and copper ((b) right) with R-squared values labelled.

Nickel, arsenic, zinc and copper display similar strong correlations of 0.802, 0.783, 0.770 and 0.711 respectively. Figures 15a, 15b, 16a and 16b display the proximity of the trend line to the X=Y line, suggesting little bias between TXRF and ICP-AES when analysing these 4 elements. However, it can be observed that Ni, As and Cu are slightly overestimated with the As average being furthest from the X=Y line. Comparatively, zinc is reported slightly more by ICP-AES in lower concentrations and reported higher by TXRF after a zinc concentration of 50 mg/kg. All 4 figures show strong correlations and proximity to X=Y, suggesting that the TXRF and ICP-AES retrieved data are very similar across the sample range. TXRF analysis of nickel reported a deviation of 4.53% when the TXRF analysis average was compared with the average ICP-AES values. When comparing the average zinc concentration analysed with TXRF and ICP-AES the reported deviation between the two sets was 6.25% and for copper it was 7.17%. Arsenic displayed -31.78% deviation, with the average sample analysed by TXRF being 6,525.74 mg/kg and ICP-AES being 4,736.19 mg/kg.

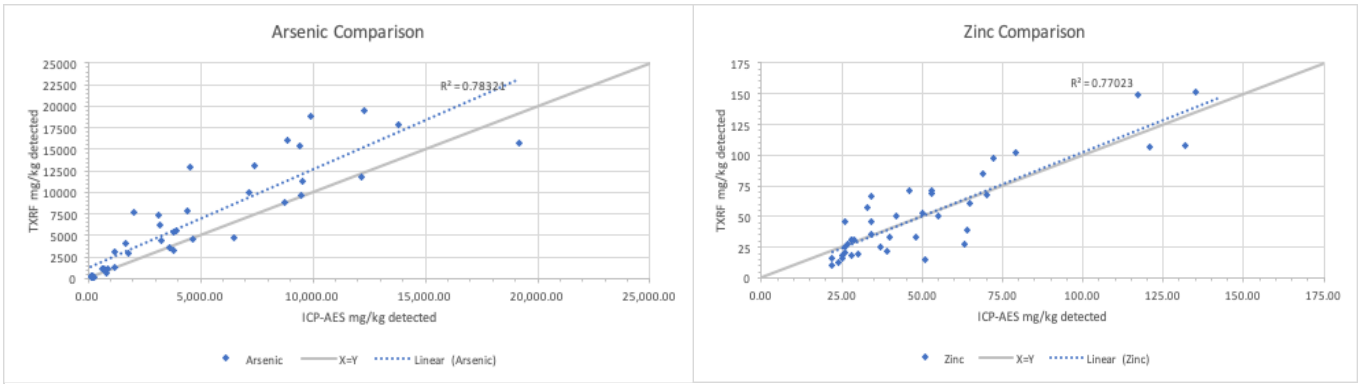

Figure 16: Comparative scatter plots of TXRF quantitative data against the equivalent ICP-AES data for arsenic ((a) left) and zinc ((b) right) with R-squared values labelled.

Of the analysed samples, 50% of TXRF copper concentrations are above those determined by ICP-AES, 47.5% are below and 2.5% are identical, nickel displays the same 50:47.5:2.5 ratio. The spread of copper values suggests that TXRF and ICP-AES measure copper and nickel with

no differential bias. Similarly, with zinc, 52.5% of TXRF values are above the ICP-AES equivalents, 45% are below and 2.5% are identical. In contrast, As shows a clear trend of being reported more highly by TXRF than by ICP-AES with 82.5% of samples registering higher As content and only 17.5% being reported as lower.

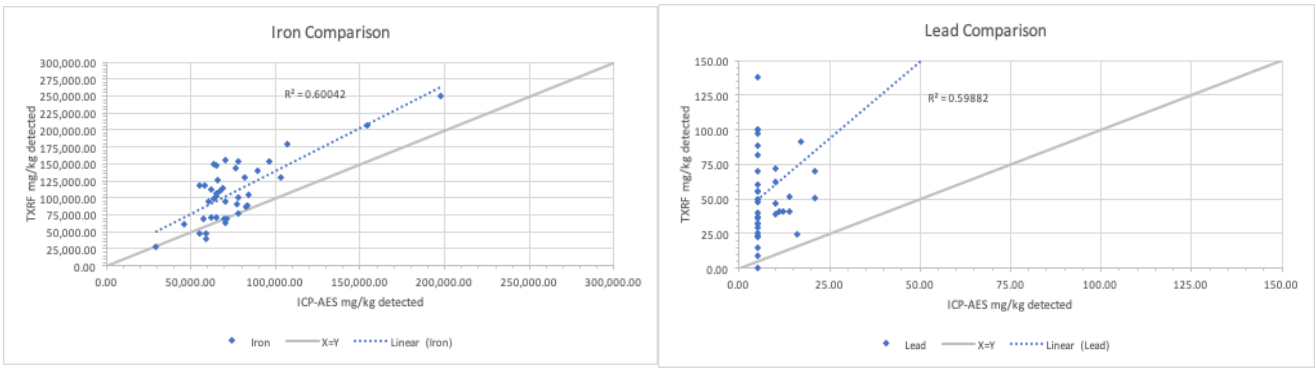

Figure 17: Comparative scatter plots of TXRF quantitative data against the equivalent ICP-AES data for iron ((a) left) and lead ((b) right) with R-squared values labelled.

Comparing iron concentrations (figure 17a) analysed with both methods also revealed a strong correlation of determination of 0.600, though considerably weaker than those of Ni, Cu, As and Zn. Fe data, like Cu, As and Ni, showed a comparative exaggeration by TXRF with the average TXRF concentration diverging by 32.95% compared to the ICP-AES determined value. Only 15% of TXRF iron concentrations fell below the equivalent sample data analysed by ICP-AES.

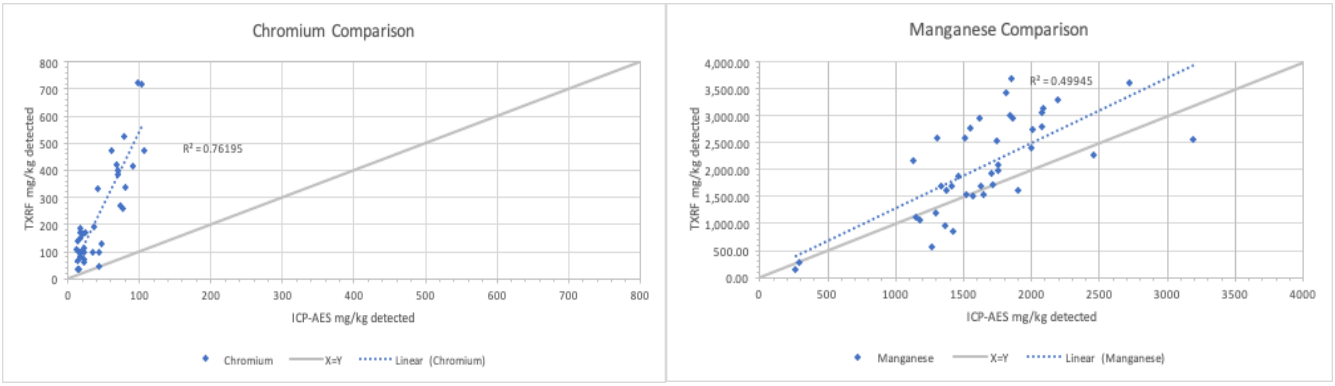

Figure 18: Comparative scatter plots of TXRF quantitative data against the equivalent ICP-AES data for chromium ((a) left) and manganese ((b) right) with R-squared values labelled.

Lead concentrations are displayed in Figure 17b and present an R^2 value of 0.599 suggesting a moderate to strong correlation of determination. However, the high R^2 is likely to have been skewed by the 10 mg/kg detection limit of ICP-AES. All Pb values reported as <10 mg/kg have been set at 5.00 for this analysis which explains the straight line at that value on the X axis. The fitting of this data has reduced the comparability of the two datasets; however, it can be determined that TXRF consistently reports Pb in higher concentrations than ICP-AES. While 63% of ICP-AES Pb measurements registered below the detection limit, only 5% of TXRF measurements fell below the same threshold. The presence of Pb is overestimated by TXRF

due to the concentration being close to the lower limit of detection (LLD) and also due to the immediacy of the high concentration As peak which can cause overestimation (Towett, et al., 2013).

Figure 18a shows how the concentration of Cr is over-reported by TXRF in every sample when compared to ICP-AES data. 95% of samples are reported to have more than double the concentration of chromium compared to the ICP-AES data. However, with the removal of a small number of extreme outliers, a strong correlation of determination of 0.762 is displayed. Despite the connection, Cr is still overestimated; FIKID508147 for example, ICP-AES measured 98 mg/kg of chromium, while TXRF measured 722 mg/kg. The poor estimation of Cr is likely connected to the proximity of its peak with that of Fe, with one of the elements in extremely high concentration and the other in very low concentrations it can lead to the latter being overestimated (Towett, et al., 2013).

Manganese can be explained as having only a weak-to-moderate correlation with an R^2 value of 0.499 in figure 18b. There is an observable positive trend with manganese data are distributed along the X=Y line, showing a bias towards overestimation, however the severity of the exaggeration is lesser than that shown in Cr. These results suggest that Mn cannot reliably be analysed by TXRF in these specific samples, potentially due to the proximity of the large Fe peak.

Of the analysed elements, gold showed the least correlation between the two methods, while the data trend line falls closely to the X=Y line. The gold concentration values for each sample have very little correlation as shown in figure 19. The gold in the Kittilä samples is commonly invisible as it is harnessed within the associated arsenopyrite mineral structure and therefore undetectable by TXRF. Hence, 60% of samples measured by TXRF show 0.00 gold concentration, which is due to the ore type and detection limit of the TXRF.

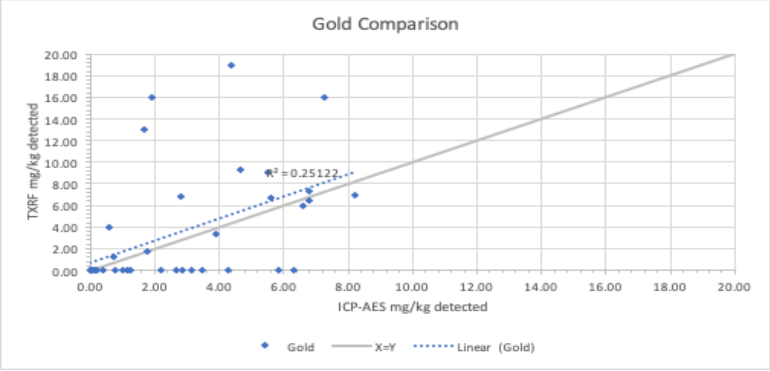

Figure 19: Comparative scatter plot of TXRF quantitative data against the equivalent ICP-AES data for gold with the R-squared value labelled.

In instances where Au is detected by TXRF it is typically over exaggerated with multiple samples registering over 10 mg/kg when a value of below 2 mg/kg was measured by ICP-AES. The concentration of Au according to Pico-Fox software is highly dependent upon the presence of Hg, Os, Re, W and Ta; a number of other elements may also modify the concentration of gold in a sample. Variation from the expected values for Au may be due to the disturbances caused by the overlapping between the low concentration of Au and the very high concentration of As. Similarly, the proximity of Au concentration to the lower limit of detection can also cause the concentrations to be

increasingly unreliable (Towett, et al., 2013). Variation within the dataset associated with specific elements is caused by the low sensitivity of TXRF to light elements (S), elements in concentrations close to their lower limit of detection (Cr, Pb, Au) and overlapping between elemental peaks with high and comparatively low concentrations (Cr/Fe, As/Pb, Ar/Ag) (Towett, et al., 2013).

Table 8: The spectral peaks associated with elements considered important for this project, displaying the spectral peak value, secondary peaks for certain elements and the elements which have overlapping elemental peaks on a spectrum. The overlapping elements explain the reason for low reliability for certain elements including Ag.

Element	Spectral peak	Secondary peaks	Overlapping elemental peaks
S	2.3084 + 2.3095		Mo, Hg, Pb, Nb, Tl
Ar	2.9553 + 2.9575		Ag, Ac, Ra, Pd, Th, Rh
Ag	2.9770 + 2.9827	3.1500 + 3.3470	K, U, In, Cd, Np, Pu, Rh, Th, Pd, Ac, Ar, Ra
Sb	3.5945 + 3.6038		Ca, Sn, Am, Bk, K, Pu, Cd, Cm
Cr	5.4052 + 5.4149	5.9468	V, Pm, La, Ce, Pr, Mn, Gd
Mn	5.8891 + 5.9003	6.4918	Eu, Nd, Pr, Cr, Pm, Fe
Fe	6.3921 + 6.4052	7.0593	Dy, Eu, Mn, Gd, Tm, Tb
Ni	7.4630 + 7.4803	8.2668	Yb, Ho, Er, W
Cu	8.0267 + 8.0463 + 8.0939		Ta, Tm, Os
Zn	8.6141 + 8.6732	9.5704	Re, Lu, Ta, Au
Au	9.6280 + 9.7130		Zn, Ta, W
Pb	10.4490 + 10.5510		As, Os
As	10.5079 + 10.5434		Pb, Os
Mo	17.3750 + 17.4800	2.2889 + 2.2921	S, Pb, Hg, Tl, Nb, Au,

ICP-AES analysis provided information for the concentrations of molybdenum and silver also, however these elements were not considered for analysis during this study due to known analytical errors when analysing using the TXRF. The PicoTAX uses a molybdenum anode for sample excitation and therefore naturally presents a large Mo peak as seen in figures . During this study, TXRF analyses were run in air resulting in the production of a naturally occurring Ar peak in all cases; the Ag peak overlaps with the Ar and Th peaks. Therefore, the reported Ag concentrations were considered unreliable due to extreme over exaggeration because the peak finder assuming the Ar peak to be largely attributed to Ag in many instances. Table 8 shows the spectral peak regions for selected elements which have proven important during TXRF analyses throughout this project. The overlapping elemental peaks explain the poor reliability of certain elements including Ag, Au and Pb. These are very closely associated with other elements that are found within the device or the Kittilä samples.

4.3.1.1 TXRF repeatability

To validate the TXRF measurements, four samples were chosen from the dataset to be analysed three times and be compared for repeatability. Table 9 shows the results for three tests completed on four individual samples. The values for each analysis are shown along with the standard deviation to show the spread of results. ICP-AES data for each sample is also provided as a reference.

Table 9: Repeatability results shown for 4 different Kittilä powder samples individually prepared 3 times and analysed. The results for each individual analysis are shown and the standard deviation has been calculated. The ICP-AES data has been provided as a comparison.

Sample ↓	mg/kg												
Element →	S	Cr	Mn	Fe	Co	Ni	Cu	Zn	As	Ag	Sb	Au	Pb
130 ICP-AES	34,063.00	76.00	1,712.00	83,136.00	40.00	168.00	314.00	121.00	9,492.00	1.00	139.00	5.59	14.00
130 TXRF	13,558	276	1731	90,070		132	144	98	9,796	0	814	10	45
2nd	8,309	198	1354	57,827		84	168	61	4,308	0	0	0	36
3rd	20,843	302	2077	120,680		144	321	98	14,924	0	0	10	73
s.d	5,139	44	295	25,663		26	78	17	4,335	0	384	5	16
152 ICP-AES	12,364.00	95.00	1,815.00	55,101.00	55.00	532.00	111.00	79.00	1,672.00	1.00	29.00	0.76	<10
152 TXRF	11,229	2,467	5634	195,774		1,809	345	122	8,434	0	0	0	40
2nd	5,140	1,052	2492	84,373		690	74	81	2,417	0	0	0	39
3rd	10,019	2,230	4358	151,909		1,257	255	227	5,871	0	0	0	72
s.d	2,632	619	1,290	45,820		457	113	61	2,465	0	0	0	15
185 ICP-AES	5,394.00	20.00	1,521.00	57,854.00	38.00	77.00	106.00	26.00	1,182.00	<1	<20	0.74	<10
185 TXRF	1,805	116	1543	65,499		60	640	27	1,182	0	0	4	28
2nd	1,388	133	1661	73,942		78	74	31	1,366	0	0	0	42
3rd	1,984	249	1425	65,260		120	96	17	2,340	0	0	0	22
s.d	250	59	96	4,038		25	262	6	508	0	0	2	8
200 ICP-AES	23,817.00	90.00	1,741.00	81,846.00	42.00	178.00	182.00	135.00	3,955.00	<1	90.00	1.76	<10
200 TXRF	15,958	393	2639	138,240		274	137	163	8,171	0	0	0	75
2nd	12,902	343	2459	120,971		172	327	159	4,283	0	0	0	83
3rd	14,059	514	2499	128,787		251	157	131	6,843	0	0	5	107
s.d	1,260	72	77	7,061		44	85	14	1,614	0	0	3	14

Repeatability results shown in Table 9 show a significant variation in elemental concentrations across three analyses, despite each sample being prepared from the same initial powder. These results highlight the potential for sample bias which is impossible to completely irradicate using this methodology. Approximately 2-3 µg of sample is being analysed and so a materially minute difference in the sample preparation stage before each analysis can result in significant variations. However, the highest standard deviations shown are often attributed to a single outlier which could potentially be removed should more analyses need to be conducted. For example, sample 185, test 1 determined a Cu concentration of 640 while tests 2 and 3 measured 74 and 96. Analysis of all three values produces an s.d of 262, however, the removal of the outlier reduces the s.d to only 11.

Table 10: Difference displayed between an identical sample and carrier being analysed at a 90° from the previous analysis.

Sample ↓	mg/kg												
Element →	S	Cr	Mn	Fe	Co	Ni	Cu	Zn	As	Ag	Sb	Au	Pb
130 ICP-AES	34,063.00	76.00	1,712.00	83,136.00	40.00	168.00	314.00	121.00	9,492.00	1.00	139.00	5.59	14.00
130 (1)	13,558	276	1731	90,070		132	144	98	9,796	0	814	10	45
130 (2)	27,477	484	3132	170,911		341	816	171	22,584	0	0	23	113
Difference	13,919	208	1,401	80,841		209	672	73	12,788	0	-814	13	68

Analyses 130(1) and 130(2) represent the difference a 90° turn of the sample carrier can make if the sample preparation methodology is not properly completed. The results of 2 analyses on sample 130 are displayed in table 10, the only variable being measured between each test, is the angle at which the sample carrier is entered into the TXRF device. The broad difference observed in values of 130(1) and 130(2) is a result of inhomogeneity in either the sample or in the distribution of the standard within the sample because the excitation beam is divergent. 130(2) displays values for all elements near to or above double the value reported for 130(1) despite the analyses being conducted on the same sample. Therefore, without multiple analyses on each sample, a reliable TXRF dataset cannot be assured.

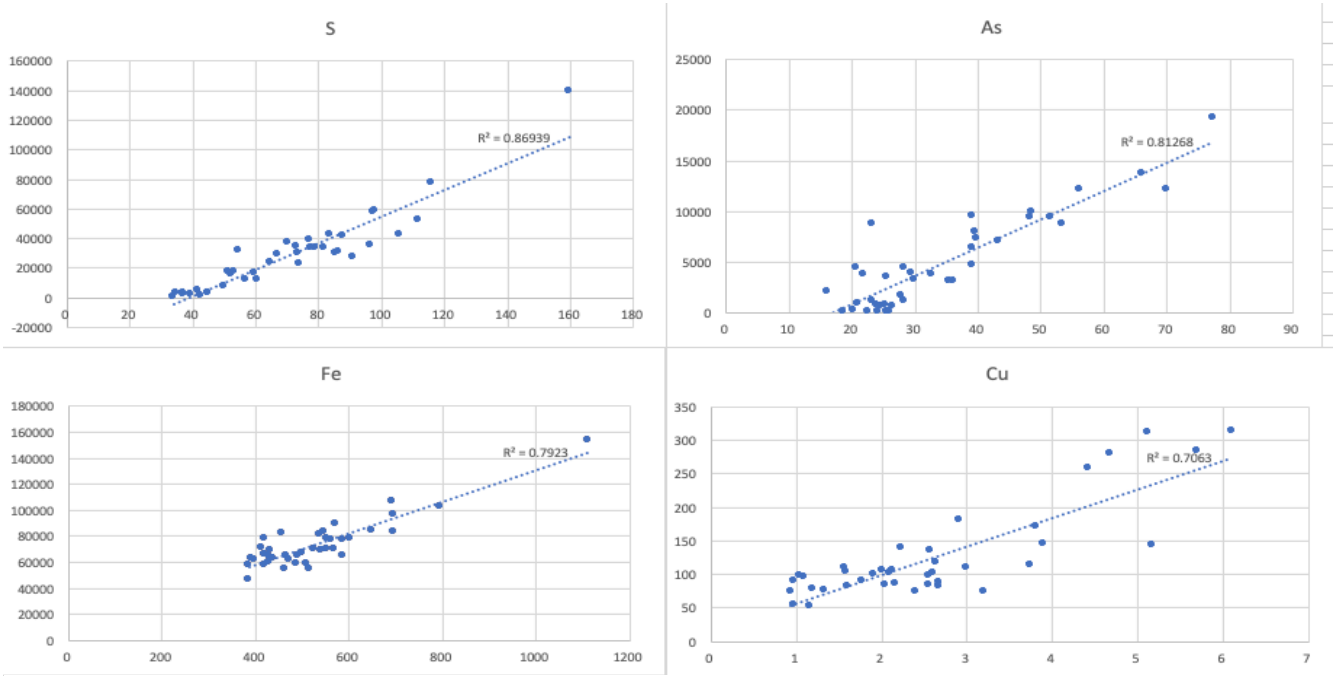

Figure 20: Comparative scatter plots of the LIBS pellet data and the mine laboratory ICP-AES data for the elements with the strongest positive linear correlations. Sulphur ((a) top left), arsenic ((b) top right), iron ((c) bottom left), copper ((d) bottom right).

4.4 LIBS pellet results

LIBS scanned pellets of the Kittilä powder samples revealed a strong similarity with the ICP-AES values provided from the mine laboratory. The LIBS data from these pellets revealed that in 7 out of the 8 tested elements there was a Pearson coefficient of >0.75 suggesting a strong

positive linear correlation. Regarding R^2 values, only 6 of the 8 elements displayed a value over 0.60 with chromium and cobalt being below. The 4 elements with high R^2 values are displayed in figure 20 (a-d), the scatter plots show nickel, manganese and chromium and these can be found in figure 21 (a-c). Scatter plots for lead and cobalt are shown in figure 22 (a-b).

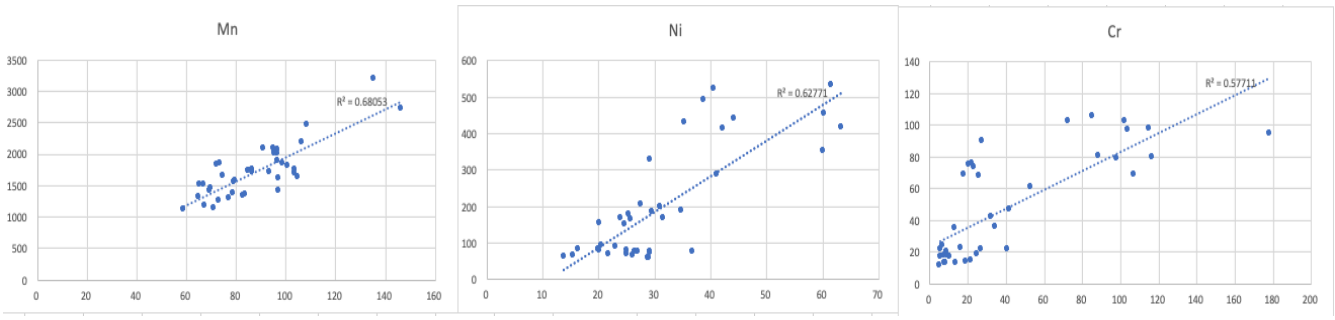

Figure 21: Scatter plots of manganese ((a) left), nickel ((b) centre) and chromium ((c) right). All 3 elements show positive linear correlations however not as strongly as those previously mentioned. Each Y-axis is the LIBS measurement point value in counts, the X-axis displays the mg/kg analysed by ICP-AES.

As shown in figure 20 (a-d), the LIBS data for sulphur (0.869), arsenic (0.813), iron (0.792) and copper (0.706) have the highest R^2 figures when directly compared with the ICP-AES data. Figure 21 (a-c) shows manganese (0.681), nickel (0.628) and chromium (0.577) also indicating a positive linear correlation but to a lesser extent. The three elements shown in Figure 21 produced data which is clearly more scattered than those shown in Figure 20, however the R^2 values still suggest a correlation. Cobalt and lead show a very weak positive correlation with R^2 values of 0.226 (lead) and 0.201 (chromium) see Figure 22 (a-b). Lead and cobalt along with nickel and chromium are either very close to- or below the lower limit of detection of the LIBS device. While there is an apparent correlation, this cannot be considered sufficiently compelling as a conclusion.

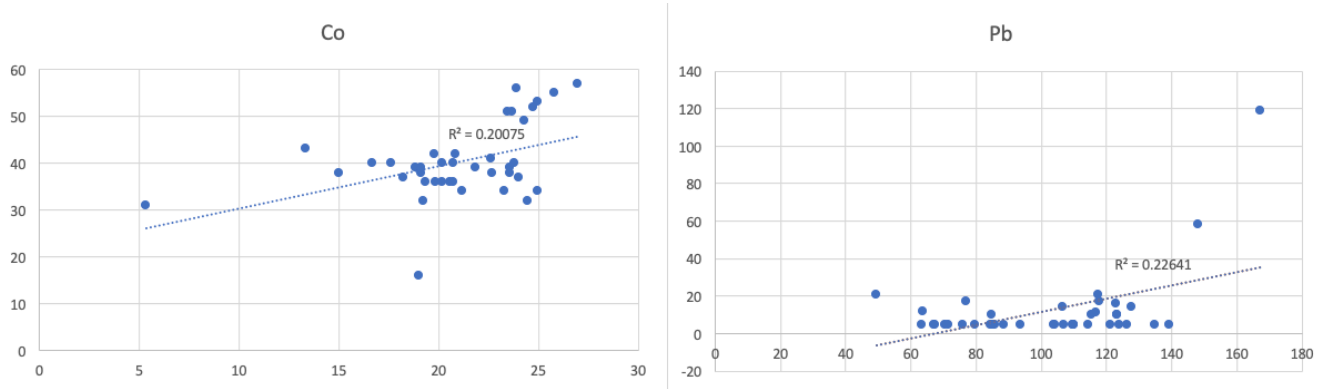

Figure 22: Scatter plots showing cobalt ((a) left) and lead ((b) right) which show very little correlation when comparing LIBS and ICP-AES. Each Y-axis is the LIBS measurement point value in counts, the X-axis is mg/kg as measured during ICP-AES. The R-squared values are labelled on each graph.

4.4.1 LIBS, TXRF and ICP-AES comparison

Comparing TXRF and LIBS data reveals a similarity and positive link between the two analytical techniques. When considering TXRF and LIBS results against ICP-AES, Pearson's correlation coefficient reveals that the correlations of As, S, Fe and Ni are within 0.075 between the two techniques (see table 11). Increased correlation is seen in Pb and Cr in the TXRF v ICP-AES data when compared to the LIBS equivalent, while Cu and Mn are more correlated in the LIBS data.

4.4.1.1 R-Squared and Pearson values

R-squared coefficient of determination (R^2) values are statistical tools used to represent variance within measured values for a dependant variable which is predictable from an independent variable. R^2 values measure the ability of regression predictions to approximate real data points. The R^2 value is calculated by 1- SSres/SStot, or 1- the unexplained variation divided by the total variation. An R^2 value of 1 means that any change in the values of variable 1 are directly linked to the independent variable of interest, contrarily, an R^2 value of 0 is indicative of two variables sharing no measurable connection. Moore, et al., 2013 suggest that R^2 values >0.7 constitute a strong effect size and $0.5 < r < 0.7$ is considered a moderate effect size. Alternatively, Ozili, 2016 declares an R^2 of 0.60 or higher is required for pure science studies such as this, since molecules and concentrations are reasonably predictable, therefore 0.60 will be used as a threshold value to judge the results in this section.

Table 11: Comparison of the Pearson correlation coefficient of LIBS and TXRF data against the mine laboratory ICP-AES results for the selected 8 elements. A value of +1 represents a perfect linear correlation between 2 variables.

	Arsenic	Cobalt	Chromium	Copper	Iron	Manganese	Nickel	Sulphur	Lead
LIBS v ICP-AES	0.901	0.448	0.760	0.840	0.890	0.825	0.792	0.932	0.131
TXRF v ICP-AES	0.882	N/A	0.873	0.751	0.759	0.687	0.859	0.974	0.598

When considering R^2 values, S has the highest correlation in both TXRF and LIBS compared to ICP-AES data and the differences in R^2 values in As and Cu are insignificant (see table 12). The R^2 values for Fe and Mn are higher for LIBS while they are higher for Pb, Cr and Ni in the TXRF dataset. Overall, the TXRF data shows increased correlation with the ICP-AES results 6 elements display R^2 values over 0.7; only 4 elements in the LIBS dataset are above the same mark.

Overall, TXRF has a higher correlation of values with the ICP-AES data, meaning that a model can be produced with increased accuracy based on these results. Despite the underestimation of S and the overestimation of Cr, they are exaggerated in correlation and so correction factors can be produced allowing for the production of a model. The same can be said for a number of elements within the LIBS dataset which present strong correlations.

Table 12: Comparison between the R-squared values calculated for LIBS- and TXRF compared to ICP-AES for 11 minerals.

LIBS v ICP-AES		TXRF v ICP-AES	
S	0.869	S	0.945
As	0.812	Ni	0.802
Fe	0.792	As	0.778
Cu	0.706	Zn	0.770
Mn	0.681	Cr	0.762
Ni	0.628	Cu	0.711
Cr	0.577	Fe	0.600
Pb	0.226	Pb	0.599
Co	0.201	Mn	0.499
Au	N/A	Au	0.251
Zn	N/A	Co	N/A

The ICP-AES technique has drawbacks which could affect the results through systematic over- or underestimation of specific elements due to the technique or the required sample preparation. It is likely that the Kittilä mine laboratory has prepared the ICP-AES samples by acid digestion in aqua regia due to the minimal loss of As and near-total recovery of base metals. However, the use of aqua regia causes underestimation of Cr (Santoro, et al., 2017) which has been shown in the results of this study, therefore it is likely that the Cr values presented by the TXRF are closer to the true value. An alternative sample preparation possibility for ICP-AES is dissolution in HF followed by fusion to allow for analysis of As and other elements. However, a disadvantage of all fusion preparation methods is the introduction of large quantities of total dissolved solids (TDS) to increase dilution, causing the concentration of certain elements to fall below the detection limit. There is an increased potential of loss in more volatile elements including Pb, Zn and others (Lar, n.d).

4.5 Drill core LIBS scanning

Reference library data has subsequently been used in the analysis of Kittilä drill core samples. The development of the reference library and the calibration of the data set has allowed for the drill core scans to be completed with increased reliability and accuracy. By understanding the sample material through a series of alternative laboratory analytical techniques the process as allowed the bulk drill core material to be accurately analysed in a fraction of the time and with a far increased accuracy than could occur without the calibration and reference library.

Kittilä drill core data images are shown in Figure 23. The images show the original drill core box is shown alongside images produced using LIBS data focussing on 8 specified elements. Areas of high elemental concentration are more yellow while areas with lower concentration (or where the element is absent) are shown by grey/dark blue. The higher quality images are shown in the appendix. Post-calibration drill core scanning shows the effectiveness of LIBS in displaying elemental maps. Structures are clearly visible as well as regions of elemental variance which can provide exploration geologists with useful additional data. Using the LIBS data, an average elemental composition can be determined and used as a decision-making tool for mining companies.

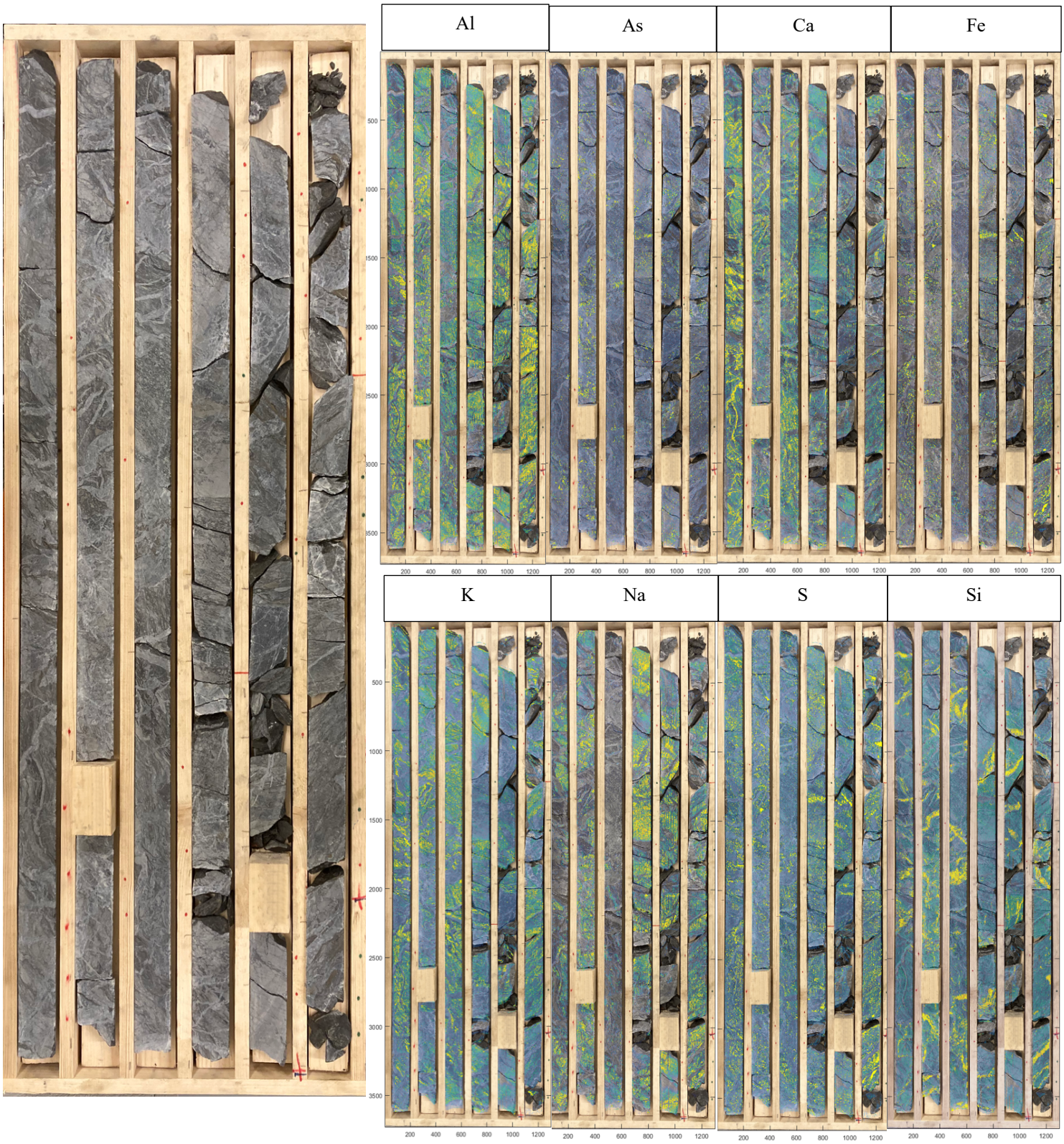

Figure 23:A photo of a Kittilä drill core box which has been scanned by LIBS (far left). 8 images are shown which have been produced using LIBS data, each image shows the same drill core box with a heat map for the labelled element. Yellow denotes the highest concentration of the labelled element while grey/dark blue represents a low concentration or absence of the specified element.

The data reveals a consistently high concentration of Al, K and S throughout the drill core box, with regions of higher or lower concentration levels. Trends can be seen in the spread of Ca and Na, both of which have large areas of elemental absence and specific areas of very high concentrations. As and Fe tend to be seen in low concentrations throughout the drill core, however they both appear in very high concentrations within thin structures throughout. Neither As nor Fe are seen as matrix materials but they are found in enriched regions. The presence and spread of As is particularly important in this case because As rich minerals host the desired gold.

5 Discussion and conclusion

5.1 TXRF analysis discussion

TXRF offers a cheap, fast and effective method of elemental analysis for a range of samples, and the opportunity to compare data with ICP-AES results. Data collected from TXRF analysis has proven useful and allowed for conclusions to be drawn which benefit the project as a whole. However, there are some reliability issues which could be addressed in future research to improve the effectiveness of the technique. Previous studies have been used to verify the results determined in this thesis. Due to drawbacks with the device used, Ag and Mo were not analysed as part of this project despite their concentrations being provided in the ICP-AES dataset. An internal Mo anode causes a large peak when analysis is completed without a sample present, meanwhile the presence of Ar in the atmosphere causes severe disturbances to the Ag peak. Corrective measures may include: the use of a nitrogen atmosphere to remove the Ar peak; lowering the device operating temperature to gain better energy resolution or manual corrections (Juvonen, et al., 2009). However, these methods were considered impractical in reality.

Nickel, zinc and copper display the highest R^2 values of 0.802, 0.770 and 0.711 and are in closest proximity to the expected ICP-AES values. These results align with the findings of Towett, et al., 2013 and Juvonen, et al., 2009 who determined Ni, Zn and Cu to agree with the expected results. Similar comparisons between this study and others can be drawn based on the collected data.

Towett, et al., 2013 reported consistent overestimation of Pb by TXRF when compared with ICP-AES across a range of soil samples. The same Pb concentration exaggeration is shown in the results of this study, the overestimation may be due to a number of causes. Sampling in solution can lead to biases, potentially associated with the high density of Pb. The methodology outlined in section 3.0 outlines that the time between homogenisation and sample extraction should be minimal. However, since sample extraction is not instantaneous, there is opportunity for particles to sink. In addition, when a pipette is then used to extract the sample solution from the base of the sample tube, this can potentially lead to higher concentrations of Pb than are truly representative. Towett, et al., 2013 also reported that peak overlap between an element with a high concentration and one with a low concentration can also lead to overestimation. Juvonen, et al., 2009 concluded a direct link between the abundance ratio of Pb and As and

interferences in their determinations and therefore decided to exclude Pb measurements from the study. In consequence, due to the relatively high concentrations of As within the Kittilä samples, the low concentration of Pb has been overestimated.

Similar issues were reported with gold which displayed either no presence at all or an overestimation. Concentrations of Au reported by ICP-AES all fall below 10 mg/kg and 44% of samples have a gold content of below 1.5 mg/kg. Therefore, small errors, minor contamination or sampling biases can lead to large variations. If a particle of Au is collected in the pipette then a sample may have a comparatively very high Au concentration while if a gold particle isn't collected in the pipette or if the gold is within the arsenopyrite structure then no gold will be reported. Examples include FIKID508167; ICP-AES analysed 1.69 mg/kg while TXRF reported 13.00 mg/kg, a difference which could bankrupt a mining company if a go-ahead decision was made based on TXRF data. Contrarily, FIKID508169 was reported by ICP-AES to have an Au concentration of 6.34 mg/kg, while TXRF determined that Au was not present in the sample. Reproducibility is said to be low when an element is present in a sample close to the lower limit of detection (Towett, et al., 2013). The minor concentrations (<10 mg/kg) of Au within the sample suggests that the variation may have been a result of the proximity of concentrations to the lower limit of detection (LLD).

An R^2 value of 0.762 was determined for Cr, however with an extreme overestimation by TXRF across all samples. Both Juvonen, et al., 2009 reported on the inter-element interferences caused by Fe on Co, Cr and Mn; the overlapping peak regions and high concentration of Fe within the Kittilä samples which explains the exaggeration of Cr concentrations. The peak interferences also explain the variation within the Mn dataset, that despite showing a clear positive trend as expected, did not display clear accuracy. Additional evidence to support the TXRF Cr data is the likely underestimation by ICP-AES; due to the interaction of Cr and aqua regia which has been used in ICP-AES sample preparation. Santoro, et al., 2017 found that only 89% of Cr was dissolved in the solution and it was the worst performing element in the study. Therefore, if the same results occurred during ICP-AES preparation then the Cr concentrations are systematically underestimated.

In addition to known device inconsistencies such as peak overlap and the lower limits of detection, sampling errors may have occurred and caused bias across all elements within the study. Those elements with a higher R^2 across the dataset may have been less impacted by the sample preparation methodology. Multiple series of sample splitting are therefore likely to have resulted in heterogeneous or non-representative TXRF samples to be submitted for analysis. In the future, to combat any heterogeneity in the sample, a larger volume of sample material should be digested in acid and then analysed. Digestion ensures the even spread of material within the liquid without the possibility of gravity driven particle settling. Digesting a larger sample size than the micro-volume used during this study will remove the possibility of any nugget effect impacting specific elements. The digestion removes the possibility of selection bias and the potential particles to settle out of solution.

5.1.1 Pellet data

The Kittilä pellets measured by LIBS and compared to the ICP-AES results showed a similarity to the entrusted mine laboratory data. Problems arose with the detection limits for Ni, Co and Cr, all of which likely fell below or very close to the respective detection limit expected for each element. Therefore, the results for Ni, Co and Cr are not the most accurate when compared to the ICP-AES data. Overall, the strength of the correlations between the majority of elements across both techniques provides strong support for continuing research into LIBS. Though the current LIBS set-up may not be able to compete on analytical capability when compared to the standard reliable laboratory technique, there is strong evidence to suggest that the LIBS data could provide a reliable analytical dataset for sample analysis. The perfect linear correlation between LIBS peak intensity and elemental composition has been assumed for simplicity. However, it is understood that matrix effects and sample self-absorption will have had an effect on the results.

Pellet pressing took only minutes per sample, scanning was equally rapid and so it is demonstrated that there is no need for complex or expensive machinery at any stage in the preparation. Furthermore, pelletization requires no sample digestion or additional chemicals which could react with or impact the sample. In this instance the sample had been previously milled to a sufficient fineness to allow for immediate pelletization, if milling was required then this would be the most time-consuming step. Core samples require milling before ICP-AES also and so assuming the milling to require equal time for both methods, LIBS can provide similar results in a fraction of the time. Therefore, it can be concluded that pelletization and subsequent LIBS analysis offers a rapid, cheap and simple alternative for sample screening. However, until the LIBS technique is developed, ICP-AES and other laboratory analysis techniques will be required where to capture detailed data.

5.2 Evaluation of thin disk preparation

Throughout this thesis the sample preparation for the analysis of thin disks as part of the pioneering Thin Disk Preparation has been completed. In total, 40 thin disk slices have been produced and scanned with LIBS and analysed using TXRF. However, with the proven failings of TXRF demonstrated during this study, it is concluded that the data is not sufficient to use as a comparison to the LIBS data. Therefore, with no comparative data LIBS analysis cannot be validated and so the results have not been published in this thesis.

The thickness of the prepared thin disks results in certain samples being translucent or transparent in certain regions, especially noticeable in samples containing a high volume of quartz or veins of translucent material. The translucency raises issues with the auto-focus system which fails to accurately determine the sample surface. To combat this, a manually set focal point surface had to be enforced. This method was effective as the thin disks are all similar in thickness and have optically very flat surfaces. However, manually determining and inputting a focal surface for translucent and transparent samples is not an ideal or long-term solution.

The 40 thin disk slices were pulverised to a grain size of below 20 μm in preparation for XRD analysis which will go ahead during the project but after the submission of this thesis. The collected thin disk XRD data will confirm or refute the potential of thin disk preparation in future studies. In addition to the 40 thin disk powders, 80 Kittilä powder samples have also been further milled to a suitable size and will be sent to XRD also to be used as a comparison with the TXRF, LIBS pellet and ICP-AES data. With the addition of XRD data for 120 samples, the data produced within this thesis constitutes a very significant volume of information to be used to improve and calibrate the LASO-LIBS algorithms.

In order to optimally calibrate the LIBS device, the reference library of information from which the analysis is drawn should be as comprehensive and as closely related to the bulk sample material as possible. Through optimising the calibration stage, the eventual LIBS analytical data can be produced more quickly and reliably. We believe that the use of Thin Disk Preparation could revolutionise the classification accuracy of LIBS algorithms in the future. Upon the presentation of a new rock type or mineral assemblage, a calibration stage can be performed to enhance the abilities of LIBS and specifically focus the algorithms to improve accuracy in the detection of the specific mineral set in question. By formulating a methodology whereby a single volume of material can be analysed by a wide range of techniques, it allows the LIBS algorithms to learn from highly accurate and reliable training data.

5.3 Conclusions

A total of 227 samples have been produced and analysed by LIBS, TXRF and/or ICP-AES during this thesis for a total of 40 gold ore deposit samples, combined with an additional 67 mineral samples. In total, 80 Kittilä powders, 40 thin disks and 67 mineralogical samples have been analysed by multiple techniques in a range of sample preparation conditions. Analysis by TXRF was completed on 40 pulverised thin disk samples, 40 Kittilä powders corresponding to the thin disk samples, 40 pellets produced from Kittilä powders and 10 mineralogical samples. LIBS analysis has been conducted on 39 pellets produced from Kittilä powders, 40 thin disk slices and 67 mineralogical samples. ICP-AES analysis was completed on 80 Kittilä powders and provided to the project by Agnico Eagle to be used as a comparative dataset.

The data produced from these samples has been analysed and input into the algorithm which the LASO-LIBS device will rely upon when analysing new unknown samples. The addition of known data for the LASO-LIBS algorithm to learn from allows for increased accuracy in future scans. Further data produced by XRD analysis will be released later during the LASO-LIBS project as coronavirus related delays have restrained this thesis to less time-consuming and in-house analysis techniques.

TXRF has displayed the ability of being a useful comparative tool for use in elemental investigation. When compared with ICP-AES data useful trends are shown in S, Ni, As, Fe, Zn and Cu. The use of the produced datasets will go on to improve the reliability of LIBS analysis data by allowing for accurate peak identification during the analysis of LIBS measurement

points. However, TXRF presents a plethora of potential issues which can render a dataset unreliable, inaccurate and unusable as was presented in the reliability study and the differences reported in sample 130(1) and 130(2).

Comparison between the datasets collected during this study has revealed a positive similarity between the LIBS data and that produced by proven methods. The LIBS data shows strong correlations for a number of elements which are validated by similar correlation patterns analysed by TXRF. The LIBS results which vary from the ICP-AES or TXRF data can be explained through known errors in either LIBS or the comparative technique. The strongest correlations between LIBS and ICP-AES are in S, As, Fe, Cu, Ni and Mn, in a number of cases proving to have stronger correlations than the TXRF results. Comparisons in the ICP-AES data for Pb and Co varied in both LIBS and TXRF, with both displaying no substantial trend. However, ICP-AES has a detection limit of 10 mg/kg for Pb and the concentration is likely to have been affected by the sample preparation. As 63% of ICP-AES measured samples registered below the detection limit, it is difficult to draw reliable comparisons for Pb.

A dividing factor between TXRF and LIBS compared with ICP-AES is the possibility of contamination and selection bias. Due to the requirements of ICP-AES the sample preparation involves the dissolution of the sample in a chemical. Therefore, assuming the sample is fully dissolved, the solution which is analysed contains all components of the initial sample, as dissolution removes the impact of gravity, nugget effects and grain size variances in the eventual analyte. Contrarily, producing pellets for LIBS and sample-laden solutions for the quantitative analysis by TXRF presents the opportunity for sample bias to take place. By moving a small volume of powdered sample from one container to another can lead to a non-representative selection. Potential selection bias may arise from; particles with increased size or density that may sink to the base of a container whether in powder or in solution; larger grains may be underestimated as much of the grain will not be optically available therefore reducing the detectability of certain harder or more adhesive particles; the nugget effect may either over- or underestimate the concentration of a particular element depending upon the selection or non-selection of a nugget.

5.4 Project reflection and future

5.4.1 Situational overview

The aim of this thesis has been to produce a wide range of training and calibration data for the optimisation of LIBS algorithms used during LASO-LIBS analyses. However, the coronavirus outbreak caused, not only a severe loss of laboratory time but stringent and unprecedented new protocols while moving back into the working environment. The loss of time and increased volume of remote work has led to minor issues becoming more time consuming and complicated to overcome. Furthermore, for a period of time throughout March, April and May there were significant constraints in ordering equipment and necessary supplies thus prolonging device downtime.

Issues and necessary equipment modifications are expected when working on a pioneering

project such as this. The technology has not yet been perfected and so unforeseen challenges present themselves. Some of the issues we experienced include: the installation of a new set of spectrometers and their necessary modifications; measurement head motor breakdown and forced replacement; coding issues associated with the autofocus system and adjustments to the new hardware.

The global pandemic also made it impossible to send thin disk powder and core powder samples to Synchrotron XRD analysis in Switzerland. Originally the aim was to focus on XRD results which would be used to compare with alternative analytical methods to. Furthermore, the investigation into Thin Disk Preparation was planned to be a large part of this thesis, however, without XRD analysis there are no comparable data sets to validate the results. The samples will be sent for XRD analysis in the future, however not on a time scale suitable for this thesis.

5.4.2 Further study in LASO-LIBS

The LASO-LIBS project will continue and external agencies will no doubt increase their interest in the technology. There remains some challenges and questions which currently remain unanswered. As the project evolves, more questions will be raised and subsequently solved until a time where the technique can be introduced as a saleable product. LASO-LIBS has the potential to increase the throughput of geological core logging, and while it may not completely replace the use of laboratory analyses LASO-LIBS can become a staple of the exploration and mining industry. Research should continue into the production and optimisation of a field-ready analytical device reliant upon LIBS technology. The theory has been proven and LIBS has been used for decades across many industrial fields, difficulties have been demonstrated in the calibration of LIBS devices for use in geological analysis due to the increased sample complexity. The LASO-LIBS project and this thesis has gone some way to aiding the identification and calibration of the LIBS device by providing accurate data from geological samples allowing for the optimisation of peak identification.

To become a saleable product the LASO-LIBS device needs to be able to meet the requirements stipulated by potential customers and stakeholders. Therefore, the environments within which the device will likely be used need to be considered and modifications need to be made to ensure the success of the device. Practical considerations for a saleable product include understanding the impacts of; environmental factors such as airborne dust, air moisture concentration and air temperature. Different customers may require increased durability for field work, while others may desire an automated conveyor system with built in photographical capabilities. In some core sheds with a large concentration of air particulates the cores may first need to be cleaned - a system could be devised to complete this automatically. Furthermore, the health and safety considerations in relation to fumes must be considered. LIBS works by ablating a volume of sample which then enters the local atmosphere, in an enclosed space it may be possible that the sample fumes reach critical limits. Especially with the As-containing Kittilä samples, there is potential for harm. Air particulate concentrations should be studied to

determine whether harmful quantities of toxic elements may potentially develop after, for example, a full day of scanning within a confined area. Should an issue present itself then ventilation and area requirements should be considered and their effectiveness proven before the device can be installed.

The global situation at the time of writing has caused delays and restrictions forcing many original aims to be reworked to the most beneficial alternatives for the project. This thesis has laid the theoretical and practical foundation for further research into site-specific calibration of LIBS analysis for geological samples. The adversity faced throughout the project has led to the investigation of alternative research pathways which have proven effective in benefitting the project. Moving forward, research should continue to focus on the potential benefits of sample preparation for LIBS analysis, rather than relying on the commonly considered benefit of no preparation being required. Sample preparation for LIBS can improve the science to allow for the scope and reliance to increase into the future.

6 Bibliography

Agnico Eagle, 2010. *Technical Report on the December 31, 2009, Mineral Resource and Mineral Reserve Estimate and the Suuri Extension Project, Kittila Mine, Finland,* Vancouver: Agnico Eagle.

Agnico Eagle, 2019. *Mineral reserves and mineral resources,* s.l.: Agnico Eagle.

Agnico Eagle, 2020. *Kittilä, northern Finland.* [Online]
Available at: https://www.agnicoeagle.com/English/operations/operations/kittila/default.aspx

Andrade, D. F., Pereira-Filho, E. R. & Amarasiriwardena, D., 2020. Current trends in laser-induced breakdown spectroscopy: a tutorial review. *Applied Spectroscopy Reviews.*

Avantes, 2020. *AvaSpec-ULS4096CL-EVO (CMOS).* [Online]
Available at: https://www.avantes.com/products/spectrometers/starline/item/1288-avaspec-uls-4096clevo
[Accessed 01 10 2020].

Bolger, J. A., 2000. Semi-Quantitative laser-induced breakdown spectroscopy for analysis of drill core. *Applied Spectroscopy.*

Boliden, 2018. *Kevitsa Mine. Boliden Summary Report. Resources and Reserves,* Kevitsa: Boliden.

Brand, N. W. & Brand, C. J., 2014. Performance comparison of portable XRF instruments. *Geochemistry: Exploration, Environment, Analysis, Vol. 14.*

Brech, F. & Cross, L., 1962. Optical microemission stimulated by a ruby MASER. *Applied Spectroscopy.*

Brouard, D., Gravel, J. F. Y., Viger, M. L. & Boudreau, D., 2007. Use of sol-gels as solid matrixes for laser-induced breakdown spectroscopy. *Spectrochimica Acta Part B,* pp. 1361-1369.

Caporaso, N., Whitworth, M. B. & Fisk, I. D., 2018. Near-Infrared spectroscopy and hyperspectral imaging for non-destructive quality assessment of cereal grains. *Applied Spectroscopy,* 53(8), pp. 667-687.

Cremers, D. A. & Radziemski, L. J., 2013. *Handbook of laser-induced breakdown spectroscopy.* s.l.:John Wiley & Sons, Ltd.

Dalm, M. & Buxton, M. W. N., 2016. *Characterizing the economic value of an epithermal Au-Ag ore with Laser Induced Breakdown Spectroscopy (LIBS): Possibilities and limitations.* s.l.:s.n.

Dalm, M., Buxton, M. W. N., van Ruitenbeek, F. J. A. & Voncken, J. H. L., 2014. Application of near-infrared spectroscopy to sensor based sorting of a porphyry copper ore. *Minerals Engineering,* Volume 58, pp. 7-16.

Death, D. L., Cunningham, A. P. & Pollard, L. J., 2008. Multi-element analysis of iron ore pellets by Laser-induced Breakdown Spectroscopy and Principal Components Regression. *Spectrochimica Acta Part B.*

Death, D. L., Cunningham, A. P. & Pollard, L. J., 2009. Multi-element and mineralogical analysis of mineral ores using laser induced breakdown spectroscopy and chemometric analysis. *Spectrochimica Acta Part B.*

Debras-Guedon, J. & Liodec, N., 1963. De l'utilisation du faisceau d'un amplificateur a ondes lumineuses par émission induite de rayonnement (laser á rubis), comme source énergetique pour l'excitation des spectres d'émission des elements,. *C.R. Acad. Sci. 257,* pp. 3336-3339.

DeLucia, F. C., Gottfried, J., Munson, C. A. & Mizlolek, A. W., 2009. Current Status of Standoff LIBS Security Applications at the United States Army Research Laboratory. *Spectroscopy -Springfield then Eugene then Duluth,* pp. 32-38.

Diaz, D., Hahn, D. & Molina, A., 2017. Quantification of gold and silver in minerals by laser-induced breakdown spectroscopy.. *Spectrochim, Acta Part B,* Volume 136, pp. 106-115.

Diaz, D., Molina, A. & Hahn, D., 2018. Effect of laser irradiance and wavelength on the analysis of gold-and silver-bearing minerals with laser-induced breakdown spectroscopy. *Spectrochim Acta Part B,* Volume 145, pp. 86-95.

Dixit, Y. et al., 2018. Introduction to laser induced breakdown spectroscopy imaging in food: Salt diffusion in meat. *Journal of Food Engineering,* pp. 120-124.

Fabre, C., 2020. Advances in Laser-Induced Breakdown Spectroscopy analysis for geology: A T critical review. *Spectrochimica Acta Part B,* pp. 1-16.

Fortes, F. J. & Laserna, J. J., 2010. The development of fieldable laser-induced breakdown spectrometer: No limits on the horizon. *Spectrochimica Acta Part B,* pp. 975-990.

Gaft, M., Sapir-Sofer, I., Modiano, H. & Stana, R., 2007. Laser induced breakdown spectroscopy for bulk minerals online analyses. *Spectrochimica acta part B,* Volume 62, pp. 1496-1503..

Gondal, M. A., Hussain, T., Ahmed, Z. & Bakry, A. H., 2007. Detection of contaminants in ore samples using laser-induced breakdown spectroscopy. *Journal of Environmental Science and Health, Part A: Toxic/Hazardous Substances and Environmental Engineering,* 42(7), pp. 879-887.

Grant, K. J., Paul, G. L. & O'Neill, J. A., 1991. Quantitative Elemental Analysis of Iron Ore by Laser-Induced Breakdown Spectroscopy. *Applied Spectroscopy,* 45(4), pp. 701-705.

Haavisto, O., Kauppinen, T. & Häkkänen, H., 2013. *Laser-Induced Breakdown Spectroscopy for Rapid Elemental Analysis of Drillcore.* San Diego, s.n.

Hahn, D. W. & Omenetto, N., 2010. Laser-induced breakdown spectroscopy (LIBS), Part I: Review of basic diagnostics and plasma-particle interactions: Still-challenging issues within the analytical plasma community,. *Applied Spectroscopy.*

Han, D. et al., 2018. Application of laser-induced breakdown spectroscopy to Arctic sediments in the Chukchi Sea. *Spectrochimica Acta Part B,* pp. 84-92.

Hanski, E. & Huhma, H., 2005. Chapter 4 Central Lapland greenstone belt. In: M. Lehtinen, P. A. Nurmi & O. T. Rämö, eds. *Precambrian Geology of Finland—Key to Evolution of the Fennoscandian Shield.* 139-194 ed. Amsterdam: Elsevier, pp. 139-193.

Hanski, E. J., Huhma, H., Lehtonen, M. I. & Rastas, P., 1997. *Isotopic (Sm-Nd, U-Pb) and geochemical evidence for an oceanic crust to molasses evolution of the Paleoproterozoic Kittilä greenstone complex, northern Finland.* Trondheim, Geological Survey of Norway.

Harhira, A. et al., 2017. *Advanced laser-induced breakdown spectroscopy (LIBS) sensor for gold mining.* Vancouver: s.n.

Harmon, R. S. et al., 2019. Laser-Induced Breakdown Spectroscopy—An Emerging Analytical Tool for Mineral Exploration. *Minerals.*

Harmon, R. S. et al., 2009. LIBS analysis of geomaterials: Geochemical fingerprinting for the rapid analysis and discrimination of minerals. *Applied Geochemistry,* 24(6), pp. 1125-1141.

Harmon, R. S., Russo, R. E. & Hark, R. R., 2013. Applications of laser-induced breakdown spectroscopy for geochemical and environmental analysis: A comprehensive review. *Spectrochimica Acta Part B,* pp. 11-26.

Ho, S. K., 2012. A Minimally Destructive Multi-Element Sensing Technique for Metal Alloys by Laser-Induced Breakdown Spectroscopy. *Japanese Journal of Applied Physics.*

Hou, X. & Jones, B. T., 2000. Field instrumentation in atomic spectroscopy. *Microchemical Journal 66.*

Jantzi, S. C. et al., 2016. Sample treatment and preparation for laser-induced breakdown spectroscopy. *Spectrochimica Acta Part B.*

Juvonen, R., Parviainen, A. & Loukola-Ruskeeniemi, K., 2009. Evaluation of a total reflection X-ray

fluorescence spectrometer in the determination of arsenic and trace metals in environmental samples. *Geochemistry Exploration Environment Analysis,* 9(2), p. 173.

Khajehzadeh, N., 2018. Analytical techniques for online mineral identification.

Kojonen, K. & Johanson, B., 1999. Determination of refractory gold distribution by microanalysis, diagnostic leaching and image analysis. *Mineralogy and Petrology,* Volume 67, pp. 1-19.

Kuhn, K., Meima, J. A., Rammlmair, D. & Ohlendorf, C., 2016. Chemical mapping of mine waste drill cores with laser-induced breakdown spectroscopy (LIBS) and energy dispersive X-ray fluorescence (EDXRF) for mineral resource exploration. *Journal of Geochemical Exploration,* Volume 161, pp. 72-84.

Lar, U., n.d. *Sediment geochemistry: laboratory analytical tools, procedures and precautions,* Jos, Nigeria: University of Jos Depatment of Geology and Mining.

Lehtonen, M. et al., 1998. SUMMARY: Geology of the PaleoproterozoicKittila greenstone area, northern Finland. In: *The stratigraphy, petrology and geochemistry of the Kittilä green- stone area, northern Finland: a report of the Lapland Volcanite Project.* Espoo, Finland: Geological Survey of Finland, pp. 128-138.

Liu, X. et al., 2019. Rapid Identification of Genetically Modified Maize Using Laser-Induced Breakdown Spectroscopy. *Food and Bioprocess Technology,* Volume 12, pp. 347-357.

Lopez-Claros, M., Fortes, F. J. & Laserna, J. J., 2018. Subsea spectral identification of shipwreck objects using laser-induced breakdown spectroscopy and linear discriminant analysis. *Journal of Cultural Heritage,* Volume 29, pp. 75-81.

Luque Garcia, J. L. & Luque de Castro, M. D., 2002. *Acceleration and Automation of Solid Sample Treatment.* s.l.:Elsevier Science.

Moore, D. S., Notz, W. I. & Flinger, M. A., 2013. *The basic practice of statistics (6th ed.).* 6 ed. New York: W. H. Freeman and Company.

Niiranen, T., 2015. *A 3D structural model of the central and eastern part of the Kittilä terrane,* Rovaniemi, Finland: Geological Survey of Finland.

Niiranen, T., Lahti, I. & Nykänen, V., 2015. The Orogenic Gold Potential of the Central Lapland Greenstone Belt, Northern Fennoscandian Shield. *Mineral Deposits of Finland,* pp. 733-752.

Nikula, R., 1988. Palaeosedimentology of Precambrian tidal Virttiövaara and fluvial Värttiövaara quartzite formations in Sodankylä, Northern Finland..

Nironen, M., Lahtinen, R. & Koistinen, T., 2002. Suomen geologiset aluenimet–yhtenäisempään nimikäytäntöön. Summary: Subdivision of Finnish bedrock–an attempt to harmonize terminology.. *Geologi,* 54(1), pp. 8-14.

Nisar, S., Dastgeer, G., Shafiq, M. & Usman, M., 2018. Qualitative and semi-quantitative analysis of health-care pharmaceutical products using laser-induced breakdown spectroscopy. *Journal of Pharmaceutical Analysis,* Volume 9, pp. 20-24.

O'Nagy, T., Pacher, U., Pöhl, H. & Kautek, W., 2014. Atomic emission stratigraphy by laser-induced plasma spectroscopy: Quantitative depth profiling of metal thin film systems. *Applied surface science,* pp. 189-193.

Ozili, P. K., 2016. *What is the acceptable r-squared value?* [Interview] (07 09 2016).

Pease, P., 2013. Fused glass sample preparation for quantitative laser-induced breakdown spectroscopy of geologic materials.. *Spectrochimica Acta Part B,* pp. 37-49.

Petruk, W., 2000. Chapter 6 - Applied mineralogy related to gold. In: W. Petruk, ed. *Industry, Applied Mineralogy in the Mining.* s.l.:Elsevier, pp. 111-133.

Picon, A., Ghita, O., Whelan, P. F. & Iriondo, P. M., 2009. Fuzzy Spectral and Spatial Feature Integration for Classification of Nonferrous Materials in Hyperspectral Data. *IEEE Transactions on Industries,* 5(4), pp. 483-494.

Porizka, P. et al., 2014. Laser-induced breakdown spectroscopy for in situ qualitative and quantitative analysis of mineral ores. *Spectrochimica Acta Part B: Atomic Spectroscopy ,* Volume 101, pp. 155-163.

PricewaterhouseCoopers, 2018. *Mine Report 2018,* s.l.: PwC.

Radziemski, L. & Cremers, D., 2012. A brief history of laser-induced breakdown spectroscopy: From the concept of atoms to LIBS 2012. *Spectrochimica Acta Part B.*

Rakovsky, J., Cermak, P., Musset, O. & Veis, P., 2014. A review of the development of portable laser induced breakdown spectroscopy and its applications.. *Spectrochimica Acta Part B,* pp. 269-287.

Ran, L., Zhang, Y., Wei, W. & Zhang, O., 2017. A Hyperspectral Image Classification Framework with Spatial Pixel Pair Features. *Sensors (Basel),* 17(10).

Rifai, K., Doucet, F., Özcan, L. & Vidal, F., 2018. LIBS core imaging at kHz speed: Paving the way for real-time geochemical T applications. *Spectrochimica Acta Part B,* pp. 43-48.

Rifai, K. et al., 2017. Analysis of gold in rock samples using laser induced breakdown spectroscopy: Matrix and heterogeneity effects. *Spectrochimica Acta Part B.*

Rinke-Kneapler, C. N. & Sigman, M. E., 2014. *Applications of laser spectroscopy in forensic science.* s.l.:Woodhead Publishing Ltd.

Rohwetter, P. et al., 2005. Filament-induced remote surface ablation for long range laser-induced breakdown spectroscopy operation. *Spectrochim, Acta Part B,* Volume 60, pp. 1025-1033.

Rosenwasser, S. et al., 2001. Development of a method for automated quantitative analysis of ores using LIBS. *Spectrochimica Acta Part B: Atomic Spectroscopy,* 56(6), pp. 707-714.

Santoro, A. et al., 2017. Comparison of total and aqua regia extractability of heavy metals in sewage sludge: The case study of a certified reference material. *TrAC Trends in Analytical Chemistry,* Volume 89, pp. 34-40.

Schodde, R., 2019. *Trends in Exploration.* Melbourne: IMARC Conference.

Senesi, G. S., 2014. Laser-Induced Breakdown Spectroscopy (LIBS) applied to terrestrial and extraterrestrial analogue geomaterials with emphasis to minerals and rocks. *Earth-Science Reviews,* pp. 231-267.

Shi, L., Lin, O. & Duan, Y., 2015. A novel specimen-preparing method using epoxy resin as binding material for LIBS analysis of powder samples.. *Talanta,* p. 1370–1376.

Sorokin, P. P. & Stevenson, M. J., 1960. Stimulated Infrared emission from trivalent uranium. *Phys. Rev. Lett. 5,* pp. 557-559.

Specac, 2017. *Checklist for making XRF pellets | Spectroscopy Guides.* [Online]
Available at: https://www.specac.com/en/news/calendar/2017/06/xrf-pellet-tips
[Accessed 01 10 2020].

Specac, 2017. *XRF pellet preparation for mined mineral analysis.* [Online]
Available at: https://www.specac.com/en/news/calendar/2017/06/xrf-mining
[Accessed 01 10 2020].

Specac, 2020. *Spectroscopy Sample Packs.* [Online]
Available at: https://www.specac.com/en/products/ftir-acc/kits/sample
[Accessed 01 10 2020].

Speranca, M. A., Pomares-Alfonso, M. S. & Pereira-Filho, E. R., 2018. Analysis of Cuban nickeliferous minerals by laser-induced breakdown spectroscopy (LIBS): non-conventional sample preparation of powder samples. *Analytical Methods 5.*

Stosnach, H., 2005. Environmental Trace-Element Analysis Using a Benchtop Total Reflection X-Ray Fluorescence Spectrometer. *The Japan Society for Analytical Chamistry,* Volume 21, pp. 873-876.

Sun, Q., Tran, M., Smith, B. W. & Winefordner, J. D., 2000. Determination of Mn and Si in iron ore by laser-induced plasma spectroscopy.. *Analytica Chimica Acta 413,* pp. 187-195.

The McCrone Group, 2020. *Milling Equipment Instrument Sales.* [Online]
Available at: https://www.mccrone.com/product/xrd-mill-mccrone/
[Accessed 01 10 2020].

TheIPMI, 2015. *Fire Assay Explained - The workhorse of precious metal analysis - Gold, silver and PGMs,* Pensacola: International Precious Metals Institute.

TheIPMI, 2015. *Precious Metal Analysis - Instrumental Methods for Gold, Silver, Platinum, Palladium and other PGMs ,* Pensacola: International Precious Metals Institute.

TheIPMI, 2015. *Precious Metal Analysis by Wet Chemistry and Gravimetric Analysis Explained- Gold, Silver and PGMs ,* Pensacola: International Precious Metals Institute.

Tiwari, P. K. et al., 2019. Atomic and Molecular Laser-Induced Breakdown Spectroscopy of Selected Pharmaceuticals. *Atoms,* 7(71), pp. 1-11.

Towett, E. K., Shepard, K. D. & Cadisch, G., 2013. Quantification of total element concentrations in soils using total X-ray fluorescence spectroscopy (TXRF). *Science of The Total Environment,* Volume 463-464, pp. 374-388.

Van Loon, J. C., 1980. Chapter 3 - Analysis of Geological Materials. In: J. C. Van Loon, ed. *Analytical Atomic Absorption Spectroscopy.* s.l.:Academic Press, pp. 91-157.

Warner, T. A., Nellis, M. D. & Foody, G. M., 2009. *The SAGE Handbook of Remote Sensing.* 1st ed. s.l.:Sage Publications Ltd.

Wiens, R. C., Maurice, S. & Wong-Swanson, B., 2012. The ChemCam Instrument Suite on the Mars Science Laboratory (MSL) Rover: Body Unit and Combined System Tests. *Space Science Reviews 170,* pp. 167-227.

Wilkie, G. & Blouin, A., 2017. *Proof of concept study for development of combined LIBS-Mid-IR QCL as an industrialised elemental and mineralogical analyser for scanning coarse rock streams,* Queensland: CRC ORE.

Wyche, N. L. et al., 2015. *The Suurikuusikko Gold Deposit (Kittilä Mine), Northern Finland.* s.l.:Elsevier.

Xue, E., 2020. A service vision for a laser based scanning method.

7 Appendices

A selection of images collected during the period of study which reveal the depth and breadth of work which has gone into producing the results for this thesis. Many tasks were also completed during the research which could not be discussed or presented within this thesis, however they will go on to become highly useful in the future of the project.

Figure 24: Thin disk sample, approximately 0.2mm thick. Achieved by cutting and grinding. This sample contains quartz veins which have become clearly translucent due to the thickness of the sample. Both sides of the sample display the same structures with the goal of producing LIBS data which is as similar for both sides as possible.

Figure 25: Drill-core box and camera set up to allow for high quality sample images to be made. The images will go into the LIBS software as a comparative feature - photo against LIBS measurement.

Figure 26: Photos produced using the set-up shown previously. Drill-core box photo can be lined up against the LIBS measurement image to allow for visualisation of element-rich regions, veins, mineral variations etc.

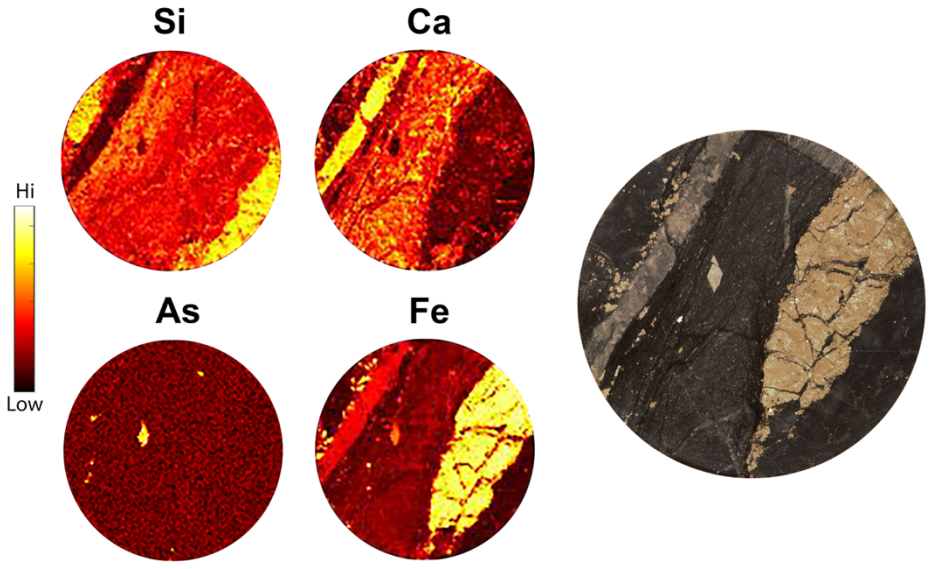

Figure 27: A thin disk sample having undergone LIBS analysis. Comparison between the original sample (right) and 4 elemental maps (left). Showing clearly that the top left vein is Ca rich, the right vein is Fe rich and the rhombus mineral is As rich with higher levels of Fe also. The matrix has regions high in Ca and Si.

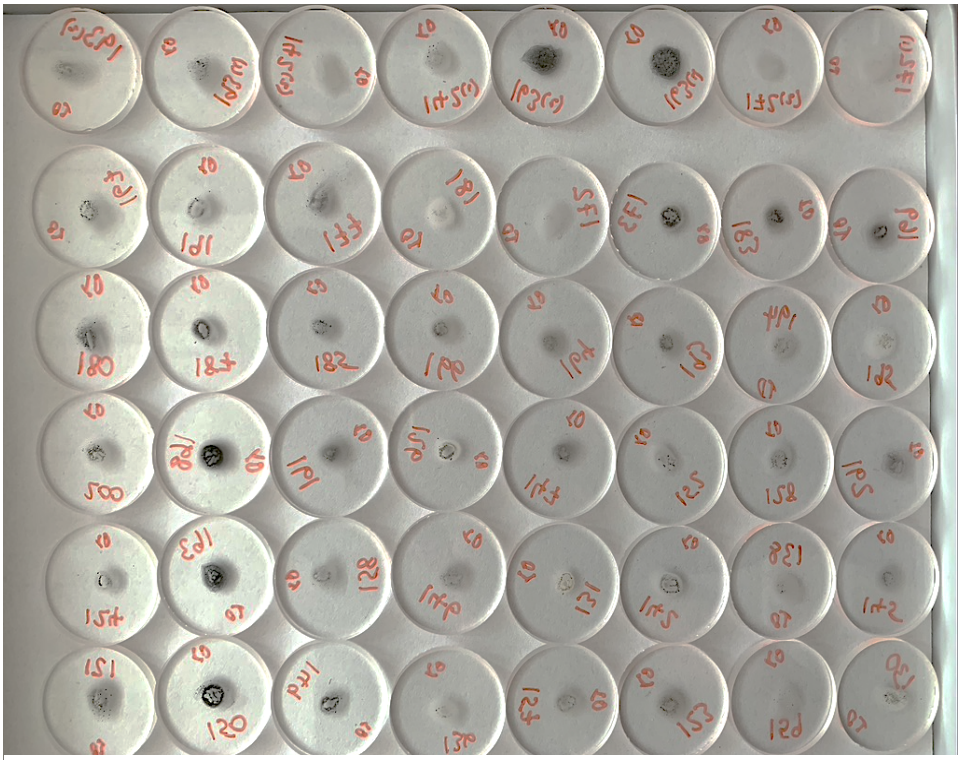

Figure 28: TXRF sample carriers with 10µl of solution containing sample material and Se standard solution. To be analysed in the Bruker PicoTax TXRF device.

Figure 29: Mineralogical sample 44 (aegirine), previously analysed by XRD, being prepared for semi-quantitative analysis. Q-tip used for transferring sample material onto a sample carrier with a thin layer of silicon grease for adhesion.

Figure 30: Janke & Kunkel VF2 sample homogeniser used during the sample preparation of TXRF quantitative samples.

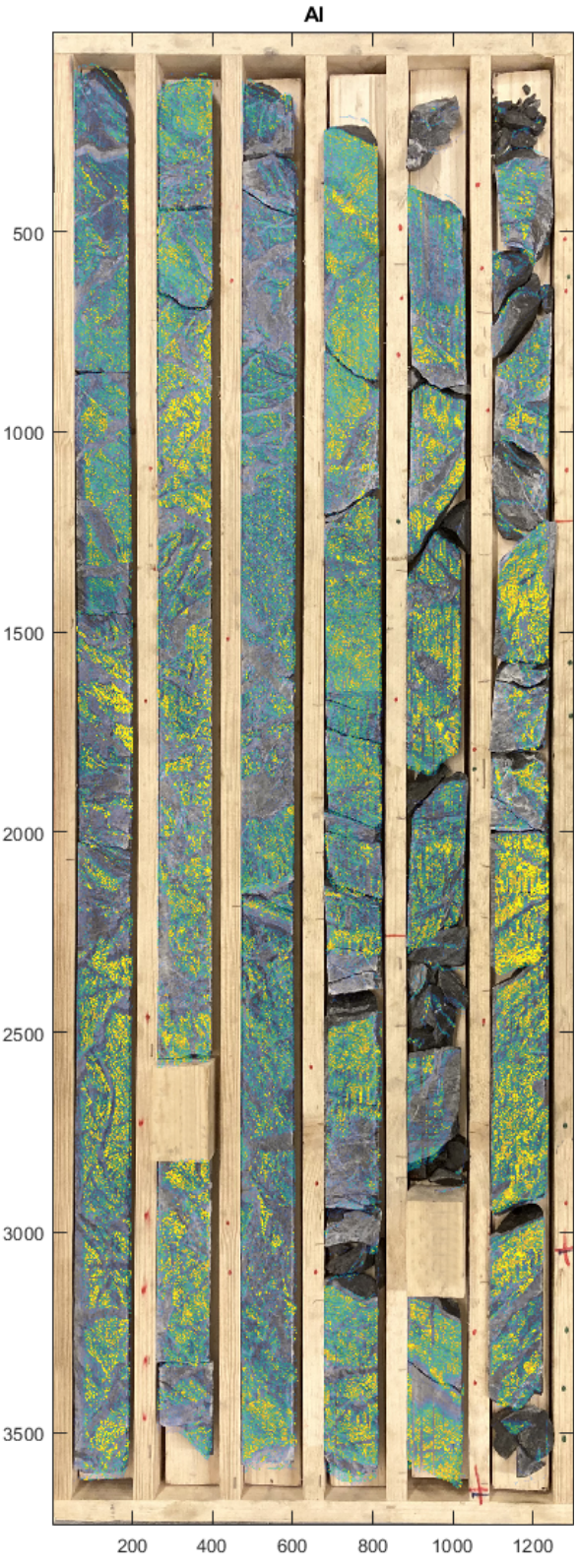

Figure 32: Image produced from LIBS scanning data from Kittilä drill core box, focussing on Al concentration.

Figure 31: McCrone micronising mill used during this study. Used to reduce the particle size of Kittilä samples and thin disk samples to <5µm in preparation for XRD analysis.

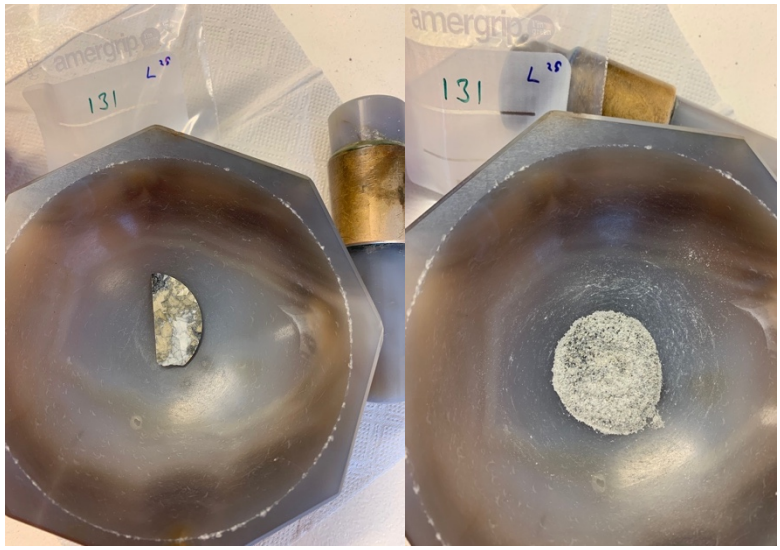

Figure 33: Thin disk sample 131, pre- and post-crushing in preparation for micronising. The McCrone Mill requires a material input of <0.5 mm.

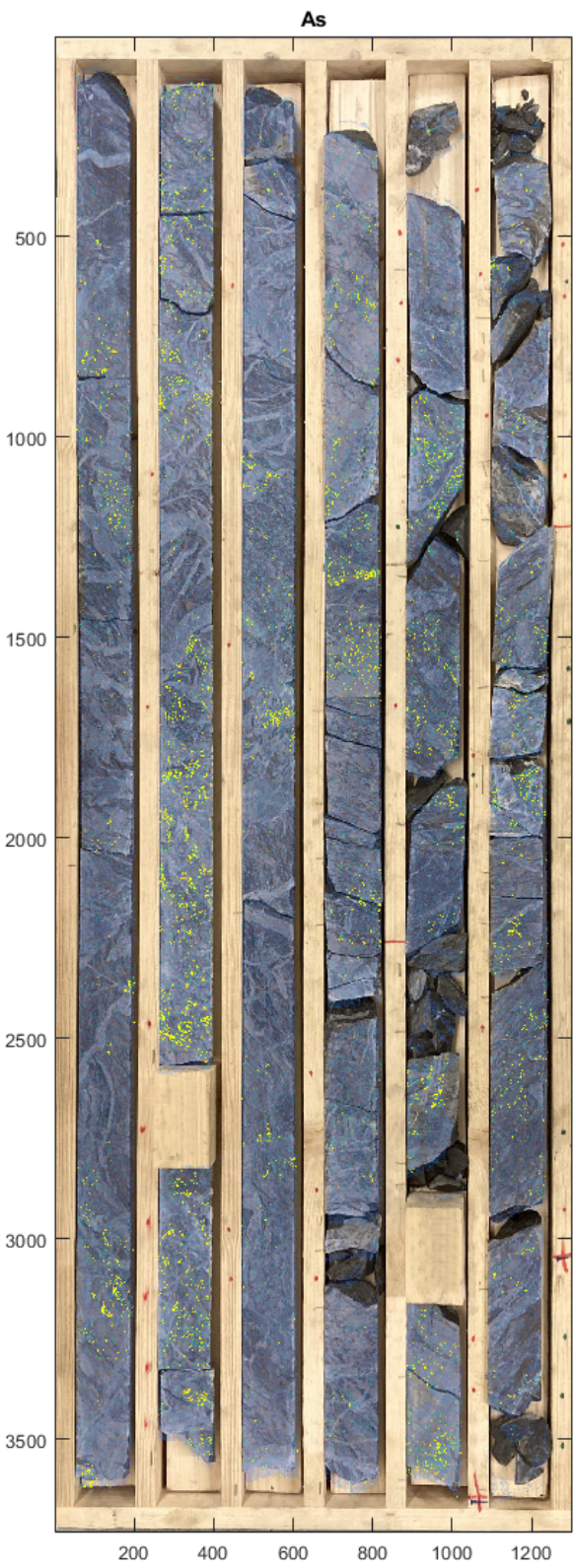

Figure 35: Image produced from LIBS scanning data from Kittilä drill core box, focussing on As concentration.

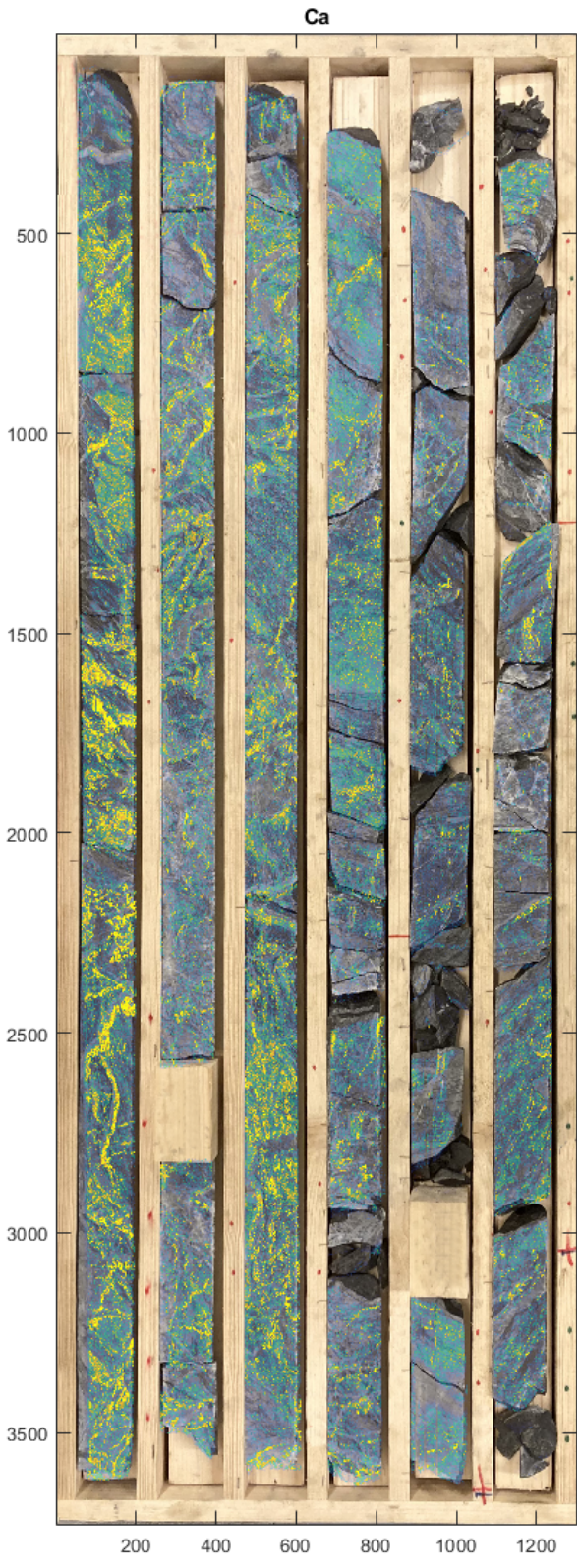

Figure 34:Image produced from LIBS scanning data from Kittilä drill core box, focussing on Ca concentration.

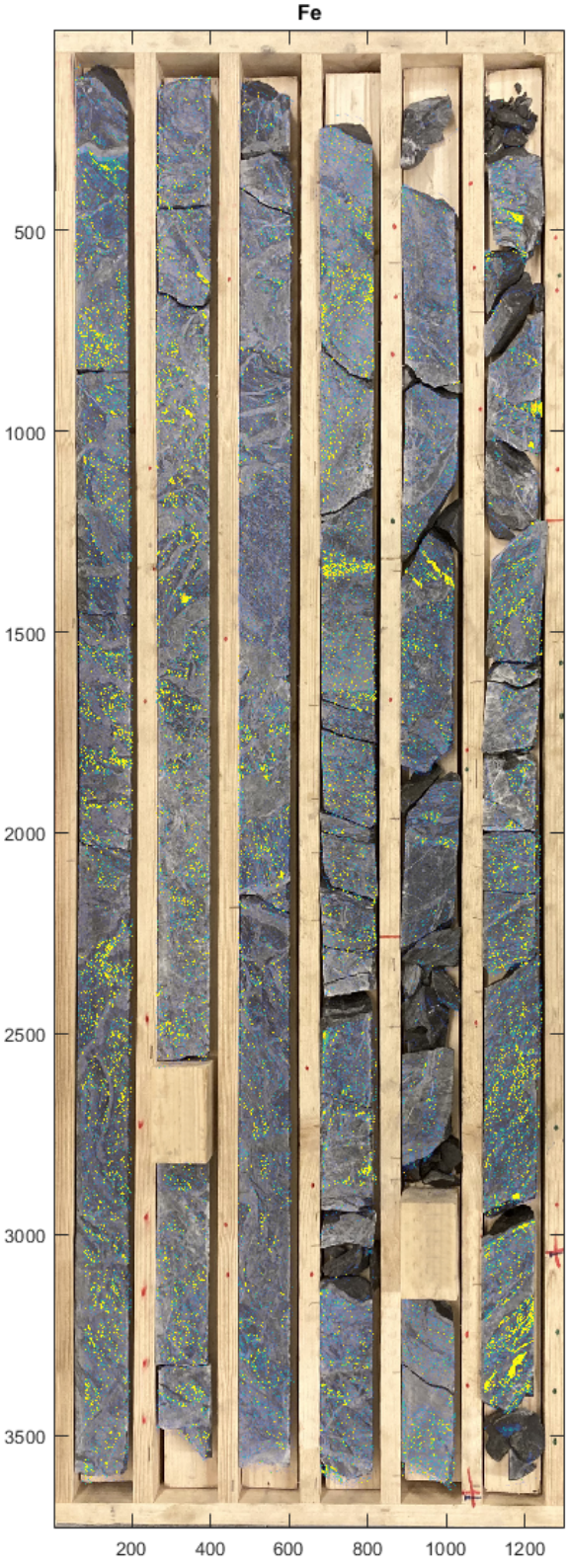

Figure 37:Image produced from LIBS scanning data from Kittilä drill core box, focussing on Fe concentration.

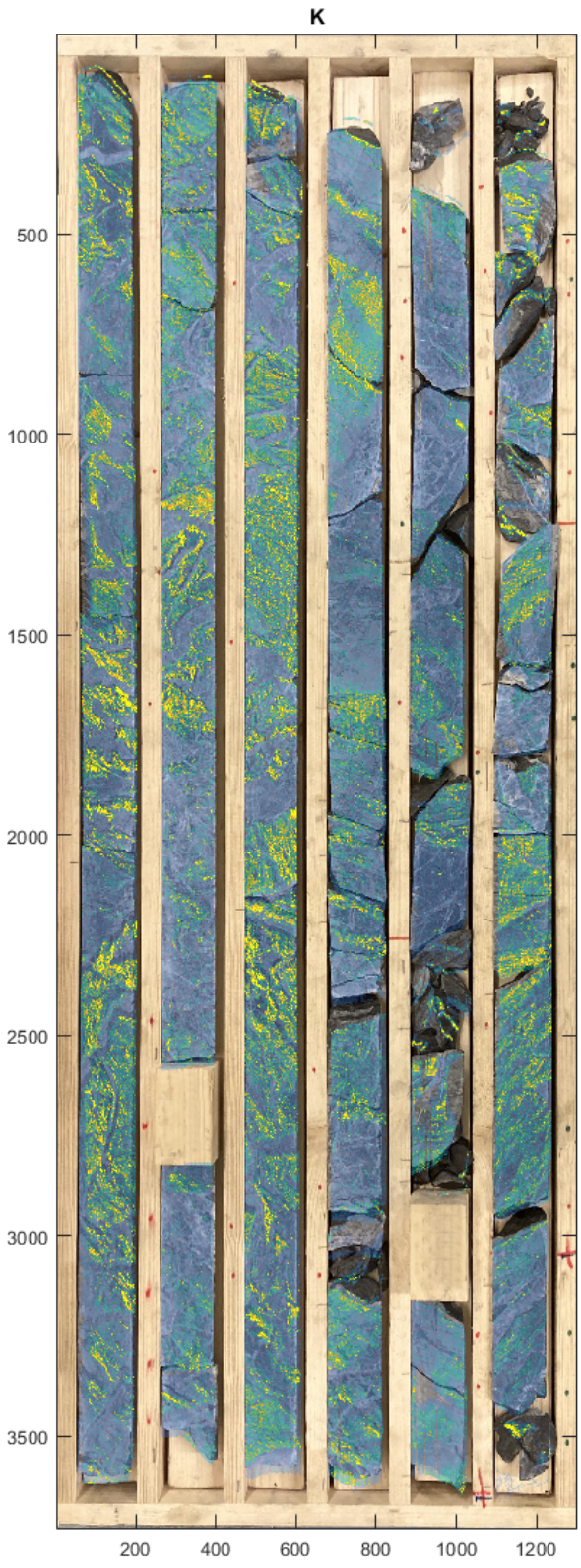

Figure 36: Image produced from LIBS scanning data from Kittilä drill core box, focussing on K concentration.

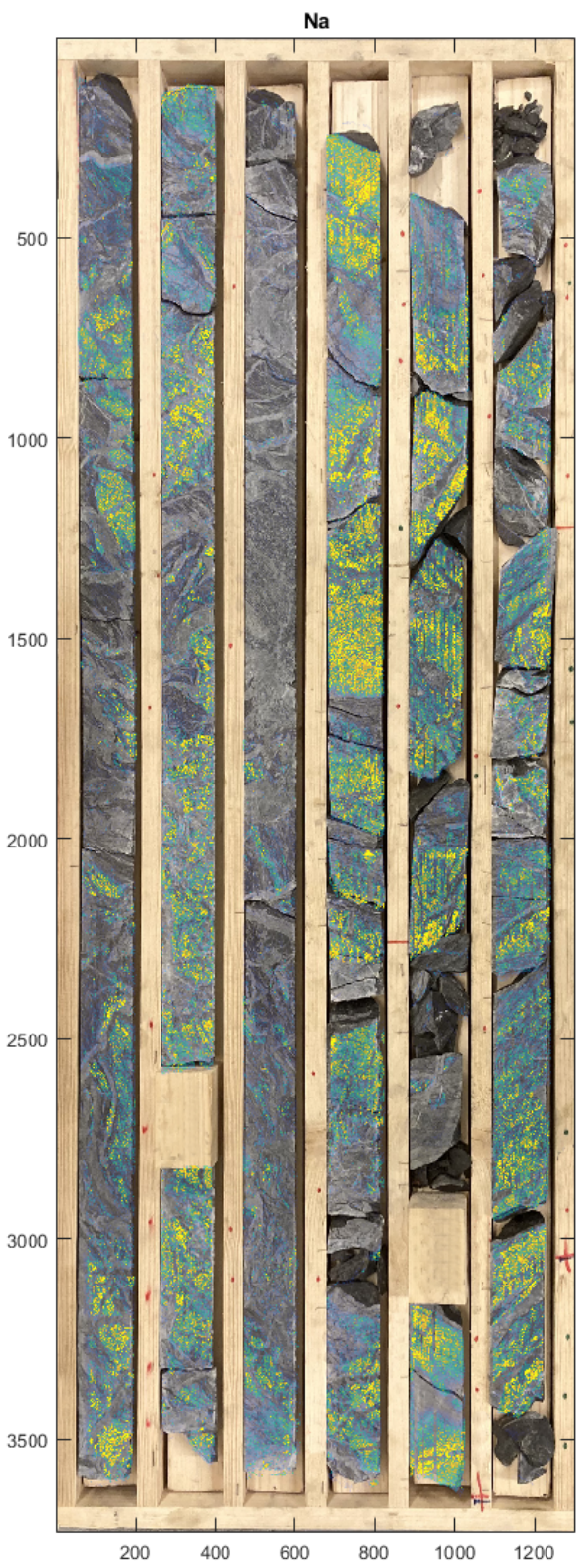

Figure 39:Image produced from LIBS scanning data from Kittilä drill core box, focussing on Na concentration.

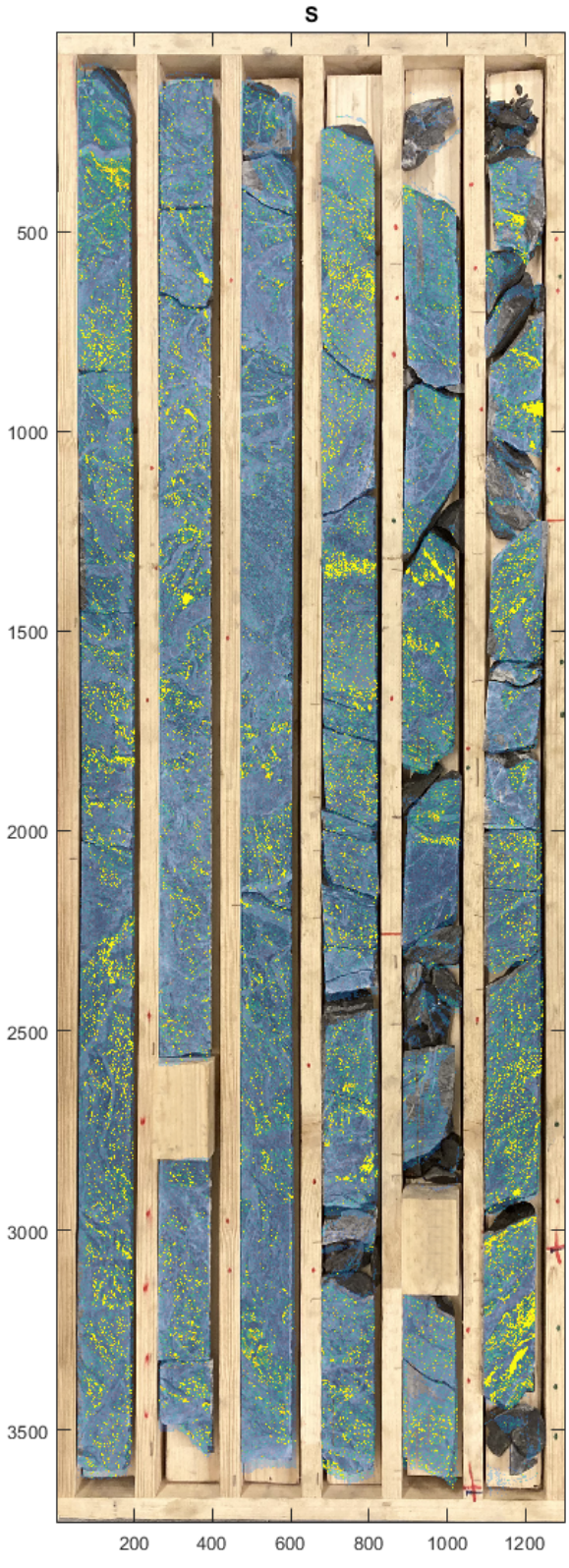

Figure 38: Image produced from LIBS scanning data from Kittilä drill core box, focussing on S concentration.

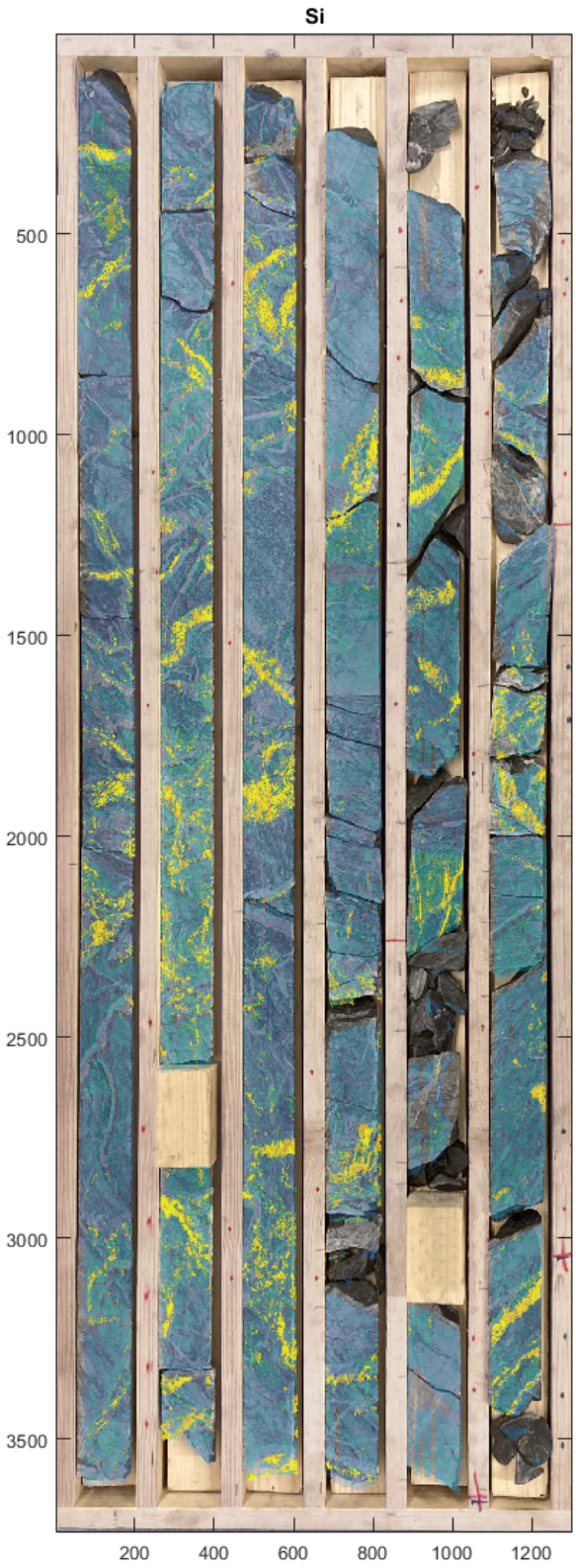

Figure 40: Image produced from LIBS scanning data from Kittilä drill core box, focussing on Si concentration.